PolyPublie
Polytechnique Montréal

POLYTECHNIQUE MONTRÉAL
UNIVERSITÉ D'INGÉNIERIE

Titre: Title:	Contributions to the Performance Analysis of Intervehicular Communications Systems and Schemes
Auteur: Author:	Yahia Alghorani
Date:	2015
Type:	Mémoire ou thèse / Dissertation or Thesis
Référence: Citation:	Alghorani, Y. (2015). Contributions to the Performance Analysis of Intervehicular Communications Systems and Schemes [Thèse de doctorat, École Polytechnique de Montréal]. PolyPublie. https://publications.polymtl.ca/1914/

Document en libre accès dans PolyPublie
Open Access document in PolyPublie

URL de PolyPublie: PolyPublie URL:	https://publications.polymtl.ca/1914/
Directeurs de recherche: Advisors:	Samuel Pierre
Programme: Program:	Génie informatique

Ce fichier a été téléchargé à partir de PolyPublie, le dépôt institutionnel de Polytechnique Montréal
This file has been downloaded from PolyPublie, the institutional repository of Polytechnique Montréal

https://publications.polymtl.ca

UNIVERSITÉ DE MONTRÉAL

CONTRIBUTIONS TO THE PERFORMANCE ANALYSIS OF INTERVEHICULAR COMMUNICATIONS SYSTEMS AND SCHEMES

YAHIA ALGHORANI
DÉPARTEMENT DE GÉNIE INFORMATIQUE ET GÉNIE LOGICIEL
ÉCOLE POLYTECHNIQUE DE MONTRÉAL

THÈSE PRÉSENTÉE EN VUE DE L'OBTENTION
DU DIPLÔME DE PHILOSOPHIÆ DOCTOR
(GÉNIE INFORMATIQUE)
AOÛT 2015

© Yahia Alghorani, 2015.

UNIVERSITÉ DE MONTRÉAL

ÉCOLE POLYTECHNIQUE DE MONTRÉAL

Cette thèse intitulée :

CONTRIBUTIONS TO THE PERFORMANCE ANALYSIS OF INTERVEHICULAR COMMUNICATIONS SYSTEMS AND SCHEMES

présentée par : ALGHORANI Yahia

en vue de l'obtention du diplôme de : Philosophiæ Doctor
a été dûment acceptée par le jury d'examen constitué de :

M. LANGLOIS J.M. Pierre, Ph. D., président

M. PIERRE Samuel, Ph. D., membre et directeur de recherche

M. FRIGON Jean-François, Ph. D., membre

M. AJIB Wessam, Ph. D., membre externe

DEDICATION

To my beloved parents,

brothers and sisters.

ACKNOWLEDGEMENTS

I thank my thesis advisor Prof.Samuel Pierre for his guidance, encouragement, and continuos support during my PhD journey in the Mobile Computing and Networking Research Laboratory of Ecole Polytechnique de Montreal. Most importantly, I thank Prof.Pierre for giving me the freedom to pursue my research interests in the topics I feel more comfortable with. My sincere thankfulness to Prof. Sami Muhaidat and Prof. Naofal Al-Dhahir for their precious guidance and suggestions during this research. Their research collaboration has been very fruitful and greatly appreciated. Finally, I would like to offer a special thanks to Dr.Georges Kaddoum for his research collaboration and partial financial support of this work, many thanks for that.

RÉSUMÉ

Le but des systèmes de communication intervéhicule (Inter-Vehicle Communication – IVC) est d'améliorer la sécurité de conduite en utilisant des capteurs et des techniques de communication sans fil pour être en mesure de communiquer mutuellement sans aucune intervention extérieure. Avec l'utilisation de ces systèmes, les communications véhicule à véhicule (V2V) peuvent être plus efficaces dans la prévention des accidents et la décongestion de la circulation que si chaque véhicule travaillait individuellement.

Une des solutions proposées pour les systèmes IVC est l'utilisation des systèmes de communication coopérative, qui en principe, augmentent l'efficacité spectrale et énergétique, la couverture du réseau, et réduit la probabilité de défaillance. La diversité d'antenne (entrées multiples sorties multiples « Multiple-Input Multiple-Output » ou MIMO) peut également être une alternative pour les systèmes IVC pour améliorer la capacité du canal et la diversité (fiabilité), mais en échange d'une complexité accrue.

Toutefois, l'application de telles solutions est difficile, car les communications sans fil entre les véhicules sont soumises à d'importants effets d'évanouissements des canaux appelés (canaux sujets aux évanouissements de n*Rayleigh, « n*Rayleigh fading channels»), ce qui conduit à la dégradation des performances. Par conséquent, dans cette thèse, nous proposons une analyse de la performance globale des systèmes de transmission coopératifs et MIMO sur des canaux sujets aux évanouissements de n*Rayleigh. Cette analyse permettra d'aider les chercheurs pour la conception et la mise en œuvre de systèmes de communication V2V avec une complexité moindre.

En particulier, nous étudions d'abord la performance de la sélection du relais de coopération avec les systèmes IVC, on suppose que la transmission via « Amplify-and-Forward» (AF) ou bien «Decode-and-Forward» (DF) est assurée par N relais pour transférer le message de la source à la destination. La performance du système est analysée en termes de probabilité de défaillance, la probabilité d'erreur de symbole, et la capacité moyenne du canal. Les résultats numériques démontrent que la sélection de relais réalise une diversité de l'ordre de ($d \approx mN/n$) pour les deux types de relais, où m est un paramètre évanouissement de Rayleigh en cascade.

Nous étudions ensuite la performance des systèmes IVC à sauts multiples avec et sans relais régénératifs. Dans cette étude, nous dérivons des expressions approximatives pour la probabilité

de défaillance et le niveau d'évanouissement lorsque la diversité en réception basée sur le ratio maximum de combinaison (MRC) est employée. En outre, nous analysons la répartition de puissance pour le système sous-jacent afin de minimiser la probabilité globale de défaillance. Nous montrons que la performance des systèmes régénératifs est meilleure que celle des systèmes non régénératifs lorsque l'ordre de cascade n est faible, tandis qu'ils ont des performances similaires lorsque n est élevé.

Ensuite, nous considérons le problème de la détection de puissance des signaux inconnus aux *n** canaux de Rayleigh. Dans ce travail, de nouvelles expressions approximatives sont dérivées de la probabilité de détection moyenne avec et sans diversité en réception MRC. En outre, la performance du système est analysée lorsque la détection de spectre coopérative (CSS) est considérée sous diverses contraintes de canaux (par exemple, les canaux de communication parfaits et imparfaits). Les résultats numériques ont montré que la fiabilité de détection diminue à mesure que l'ordre *n* augmente et s'améliore sensiblement lorsque CSS emploie le schéma MRC.

Il est démontré que CSS avec le schéma MRC maintient la probabilité de fausse alarme minimale dans les canaux d'information imparfaite plutôt que d'augmenter le nombre d'utilisateurs en coopération. Enfin, nous présentons une nouvelle approche pour l'analyse des performances des systèmes IVC sur *n**canaux de Rayleigh, en utilisant n_T antennes d'émission et n_R antennes de réception pour lutter contre l'effet d'évanouissement. Dans ce contexte, nous évaluons la performance des systèmes MIMO-V2V basés sur la sélection des antennes d'émission avec un ratio maximum de combinaison (TAS/MRC) et la sélection combinant (TAS/SC).

Dans cette étude, nous dérivons des expressions analytiques plus précises pour la probabilité de défaillance, la probabilité d'erreur de symbole, et l'évanouissement sur *n**canaux Rayleigh. Il est montré que les deux régimes ont le même ordre de diversité maximale équivalent à ($d \approx \boldsymbol{m} n_T\, n_R\, /n$) . En outre, TAS / MRC offre un gain de performance mieux que TAS/ SC lorsque le nombre d'antennes de réception est plus que celle des antennes d'émission, mais l'amélioration de la performance est limitée lorsque n augmente.

ABSTRACT

The purpose of intervehicular communication (IVC) systems is to enhance driving safety, in which vehicles use sensors and wireless communication techniques to talk to each other without any roadside intervention. Using these systems, vehicle-to-vehicle (V2V) communications can be more effective in avoiding accidents and traffic congestion than if each vehicle works individually.

A potential solution can be implemented in this research area using cooperative communications systems which, in principle, increase spectral and power efficiency, network coverage, and reduce the outage probability. Antenna diversity (i.e., multiple-input multiple output (MIMO) systems) can also be an alternative solution for IVC systems to enhance channel capacity and diversity (reliability) but in exchange of an increased complexity. However, applying such solutions is challenging since wireless communications among vehicles is subject to harsh fading channels called '*n**Rayleigh fading channels', which leads to performance degradation. Therefore, in this thesis we provide a comprehensive performance analysis of cooperative transmission and MIMO systems over *n**Rayleigh fading channels that help researchers for the design and implementation of V2V communication systems with lower complexity.

Specifically, we first investigate the performance of cooperative IVC systems with relay selection over *n**Rayleigh fading channels, assuming that both the decode-and-forward and the amplify-and-forward relaying protocols are achieved by *N* relays to transfer the source message to the destination. System performance is analyzed in terms of outage probability, symbol error probability, and average channel capacity. The numerical results have shown that the best relay selection approach achieves the diversity order of $(d \approx mN/n)$ where m is a cascaded Rayleigh fading parameter.

Second, we investigate the performance of multihop-IVC systems with regenerative and non-regenerative relays. In this study, we derive approximate closed-form expressions for the outage probability and amount of fading when the maximum ratio combining (MRC) diversity reception is employed. Further, we analyze the power allocation for the underlying scheme in order to minimize the overall outage probability. We show that the performance of regenerative systems is better than that of non-regenerative systems when the cascading order *n* is low and they have similar performance when *n* is high.

Third, we consider the problem of energy detection of unknown signals over *n**Rayleigh fading channels. In this work, novel approximate expressions are derived for the average probability of detection with and without MRC diversity reception. Moreover, the system performance is analyzed when cooperative spectrum sensing (CSS) is considered under various channel constraints (e.g, perfect and imperfect reporting channels). The numerical results show that the detection reliability decreases as the cascading order *n* increases and substantially improves when CSS employs MRC schemes. It is demonstrated that CSS with MRC scheme keeps the probability of false alarm minimal under imperfect reporting channels rather than increasing the number of cooperative users.

Finally, we present a new approach for the performance analysis of IVC systems over *n**Rayleigh fading channels, using n_T transmit and n_R receive antennas to combat fading influence. In this context, we evaluate the performance of MIMO-V2V systems based on the transmit antenna selection with maximum ratio combining (TAS/MRC) and selection combining (TAS/SC) schemes. In this study, we derive tight analytical expressions for the outage probability, the symbol error probability, and the amount of fading over *n**Rayleigh fading channels. It is shown that both schemes have the same maximum diversity order equivalent to $(d \approx mn_T\, n_R\, /n)$. In addition, TAS/MRC offers a better performance gain than TAS/SC scheme when the number of receive antennas is more than that of transmit antennas, but the performance improvement is limited as *n* increases.

TABLE OF CONTENTS

LIST OF TABLES

LIST OF FIGURES

LIST OF SYMBOLS AND ABBREVIATIONS

AF	Amplify-and-Forward
AWGN	Additive White Noise Channel
AFD	Average Fade Duration
BER	Bit Error Rate
CRC	Cyclic Redundancy Check
CDF	Cumulative Distribution Function
CSI	Channel State Information
CSS	Cooperative Spectrum Sensing
CR	Cognitive Radio
CG	Coding Gain
DF	Decode-and-Forward
EGC	Equal Gain Combining
EPA	Equal Power Allocation
FC	Fusion Center
GSC	Generalized Selection Combining
IVC	Intervehicular Communications
ITS	Intelligent Transportation System
LCR	Level Crossing Rate

M2M	Mobile-to-Mobile
MIMO	Multiple-Input Multiple-Output
MGF	Moment Generating Function
MRC	Maximum Ratio Combining
OFDM	Orthogonal Frequency Division Multiplexing
PDF	Probability Density Function
PA	Power Allocation
PU	Primary User
PER	Pairwise Error Probability
PSK	Phase Shift Keying
RF	Radio Frequency
RV	Random Variable
ROC	Receiver Operating Characteristic
S-DF	Selective Decode-and-Forward
SNR	Signal-to-Noise Ratio
SC	Selection Combining
STCC	Space-Time Trellis Codes
STBC	Space-Time Block Codes
SER	Symbol Error Rate

SSC	Switch and Stay Combining
TDMA	Time Division Multiple Access
TAS	Transmit Antenna Selection
V2V	Vehicle-to-Vehicle
WSN	Wireless Sensor Networks

LIST OF APPENDICES

CHAPTER 1 INTRODUCTION

Inter-vehicular communications systems (IVCs) have recently attracted much attention in the intelligent transportation system (ITS). These systems are intended to improve safety and traffic congestion by combining information communications technology with road transportation. In general, due to the high mobility of vehicles and non-uniform distribution of vehicles which produce frequent route interruptions [1], the risk of traffic congestion and accidents require the development of a new transportation network technology. This technology is emerging to incorporate the capabilities of wireless communication systems into the vehicles. The idea is to create wireless connections among vehicles, while they are connected to other networks at home or at a workplace. Thus cooperative diversity is considered as a promising solution [2] applied at the physical-layer to simplify routing problems in vehicular ad hoc networks and provide high data rate coverage. The main idea of this technique is to forward a source message to a desired destination through intermediate nodes in case of no direct transmission between the source and the destination.

In the past decade, "cooperative communications" has spurred great interest within the research community, see e.g., [2]-[3]. The basic idea is that, by properly coordinating spatially distributed nodes, virtual multiple-input multiple-output (MIMO) links can be created for reliable end-to-end performance. Cooperative communications can, in principle, increase spectral and power efficiency, network coverage, and reduce the outage probability. The applications of cooperative communications include wireless sensor networks (WSN) and IVC networks. To understand the full potential of cooperative diversity in the context of inter-vehicular communications systems, a n*Rayleigh distribution (also called cascaded-Rayleigh distribution) has been proposed as a realistic propagation model for mobile-to-mobile (M2M) communications that provides two or more independent Rayleigh fading processes around the transmitter and the receiver, which leads to deteriorate the connection quality between two vehicles [11]. For this reason, it is very interesting to study cooperative diversity mechanism over such severe fading channels. Future developments are expected in this field using MIMO systems at transmit and receive sides, which is also considered as a promising candidate for vehicle-to-vehicle (V2V) communications to enhance channel capacity and diversity (reliability) [4,5], since multiple antenna elements can

easily be placed on the large vehicle surface [6]. In addition, the need for efficient utilization of spectrum will, of course, become a fundamental requirement for IVC networks, which is mainly due to spectrum scarcity and the ever-increasing demand for higher data rate applications and internet services. Therefore, using cognitive radio (CR) technology in IVC networks, CR users can monitor the available spectrum bands, capture their information, detect spectrum holes, and then allocate unused portions of the spectrum [7].

1.1 Basic Concepts and Definitions

- **Cooperative Diversity**

In wireless communication systems, *diversity* refers the overall reliability of the link that can be significantly improved by providing more than one signal path between the source and the destination, each of which exhibits a fading process as much independent from the others as possible [3].

Diversity plays a central role in combating fading and co-channel interference. The term *cooperative diversity* indicates a collection of distributed antennas belonging to multiple terminals, each with its own information to transmit [8], in which *cooperative communications* refer to systems or techniques that allow users to help transmit each other's messages to the destination. Most cooperative transmission schemes involve two phases of transmission: a coordination phase, where users exchange their own source data and control messages with each other and/or the destination, and a cooperation phase, where the users cooperatively retransmit their messages to the destination [2]. There are two main relaying schemes utilized by cooperative diversity technology: *Decode-and-Forward* (DF) and *Amplify-and-Forward* (AF). In the former, the relay receives the source message and decodes it with signal noise elimination before re-encoding and retransmitting the source message to its destination, while in the latter, the relay amplifies the analog signal received by the source and forwards it to the destination node [9]. In multi-relay cooperative systems, AF and DF relays can be viewed as distributed transmit beamforming when full instantaneous channel state information (CSI), including the magnitude and phase of all channel coefficients is available at relays, in which the forwarded signals can be aligned in phase to maximize the receive signal to noise ratio (SNR) at the destination [8]. Even though, CSI can be obtained through feedback, it is still difficult in practice to track the changes in phase and co-phase the relays signal towards the destination. Therefore, *multi-node relaying selection* technique has

been proposed in the recent literature to overcome this problem [76], in which the best relay is selected among a set of available relay nodes that has the best link quality with the destination to forward the source message [see Fig.1-1]. Such a technique can provide full diversity order without the excessive demand on bandwidth.

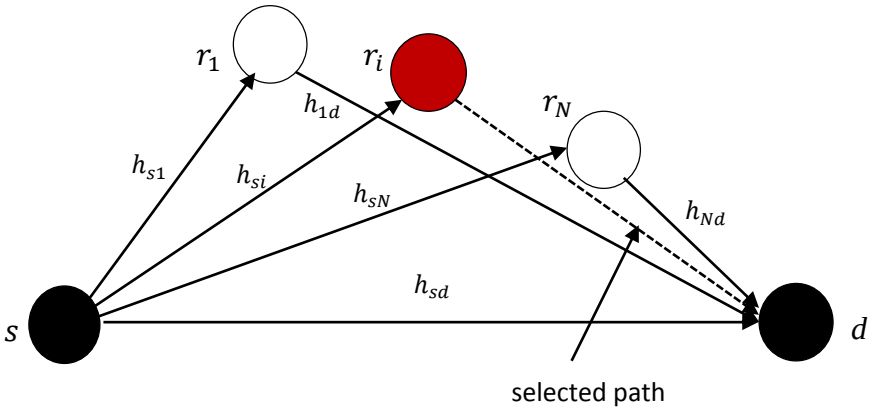

Fig.1-1. Cooperative communication system with relay selection.

In wireless networks, when the distance between the source and destination is large, mutihop transmission with DF/AF relays can be used to reduce the effect of path loss and extend the coverage range of a system without using large transmit power [91, 92]. The main idea of this technique is relaying the source message to the destination via many intermediate nodes in case of no direct path between the source and the destination [see Fig.1-2]. Although multihop relaying systems improve the coverage and offer more energy efficient transmission but in return for this the outage probability increases when the number of hops increases. To mitigate this problem, diversity reception schemes such as maximum ratio combining (MRC) and selection combining (SC) can be employed at each intermediate node to enhance the outage performance, throughput and system capacity.

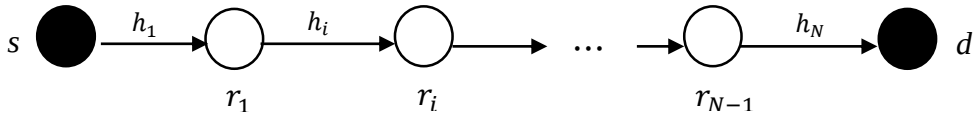

Fig.1-2. Multihop transmission system

- **MIMO Systems**

By using multiple antennas at the transmitter and the receiver, we can exploit diversity in spatial domain which is called spatial diversity (also called antenna diversity) [2, 3]. Both precoding at the transmitter and signal combining at the receiver can be employed to improve the quality and

reliability of a wireless link.. With more than one transmit/receive antenna, a matrix channel **H** consists of different propagation channels is established between the N_t transmit antennas at the transmitter and the N_t receive antennas at the receiver [see Fig.1-3]. Assuming there is a low correlation between channels, the chance of occurrence of destructive interference at the receiver is low. The larger the number of antenna pairs, the higher diversity of the received signals (i.e., the higher the reliability of signal detection). When the transmitter is equiped with a single antenna and the receiver is equiped with multiple antennas, we can get advantage of spatial diversity at the receiver to reduce the complexity associated with MIMO systems, resulting in the so-called single-input multiple-output (SIMO) systems. In a SIMO system, a transmitted signal goes through different channels and signals from each receive antenna are added together, resulting in MRC scheme where the receive SNR is maximized and the outage probability is minimized. Since the knowledge of channel fading amplitudes and channel phases is needed for MRC, this scheme is not practical for coherent and non-coherent detections. Hence, an alternative solution is to adopt the SC scheme where the receiver selects the diversity branch with the highest SNR for detection. In this case, the SC scheme can be used in conjunction with coherent and non-coherent modulation techniques since it does not require knowledge of signal phases on each branch [14].

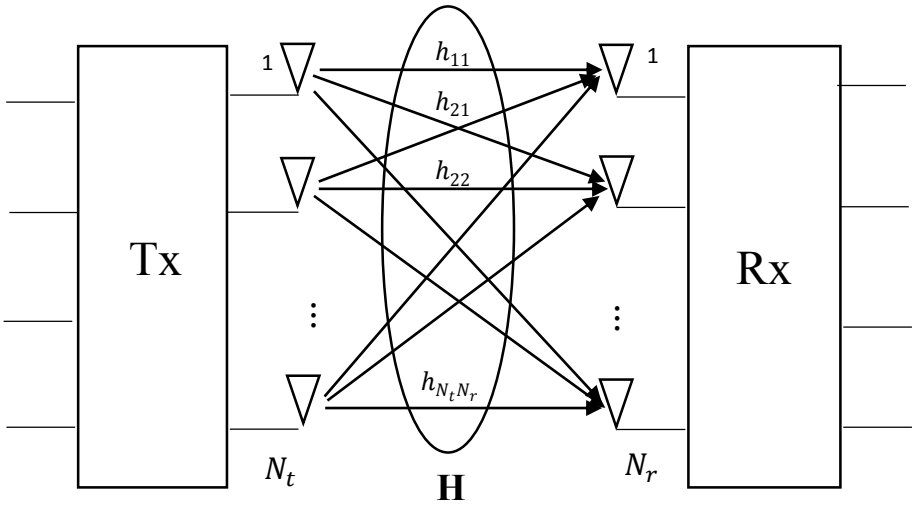

Fig.1-3. MIMO Channel Model [2]

If we assume that the transmitter is only able to obtain knowledge of channel amplitude but not channel phase information (e.g, partial CSI) because of rapid phase changes, *transmit antenna selection* (TAS) scheme is utilized to transmit data only on the antenna with the best channel to avoid destructive interference. In this case, the receiver can estimate the CSI, compute the optimal

channel cofficients and send it to the transmitter through a dedicated feedback channel. To fully exploit the maximum transmit and receive diversity of MIMO systems, the TAS/MRC scheme was proposed by [17] as an effective way to provide low computational complexity and power transmitter requirements, which in turn leads to reducing hardware expenses due to radio frequency (RF) chains required to transmit antennas. By selecting only one transmit antenna that provides the highest post-processing SNR, the feedback overhead of channel state information to the transmitter is effectively minimized compared to conventional MIMO scheme and only a single RF chain can be used at the transmitter regardless of the number of transmit antennas [see Fig.1-4]. To further reduce the number of expensive RF chains at the receive side, the TAS/SC scheme is employed to select a single transmit and receive antenna. By doing so, a single RF chain can be used at both terminals [see Fig.1-5].

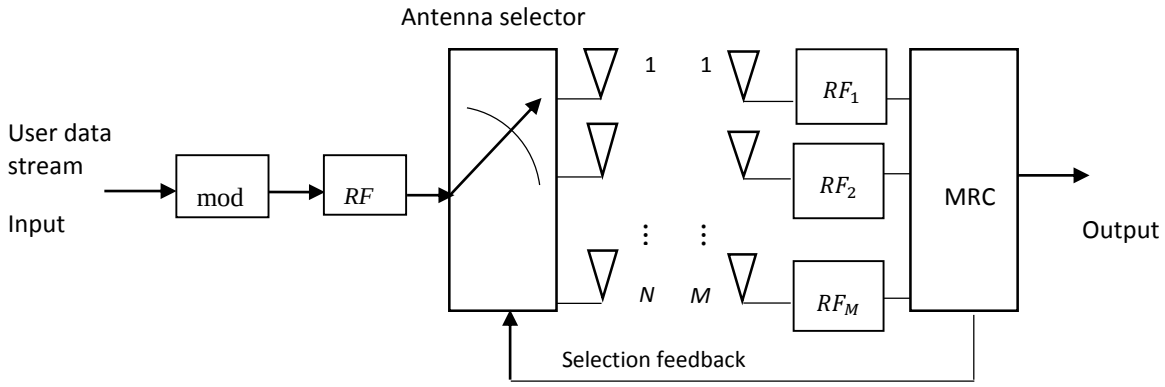

Fig.1-4. Block diagram of TAS/MRC scheme

- **Cooperative Spectrum Sensing**

Over recent years there have been increasing demand for additional bandwidth. Therefore, it is expected that radio spectrum scarcity will also become a critical challenge for wireless communications systems due to the growing number of spectrum uses. In order to solve the spectrum scarcity issue, the use of *cognitive radio* (CR) technology is considered as a promising solution to improve the spectrum utilization because of its ability to change its transmitter parameters based on the interaction with its environment without causing harmful interference to other licensed users [7]. However, one of the most difficult challenges in implementing spectrum sensing is the hidden terminal problem which occurs when the cognitive radio user is shadowed in

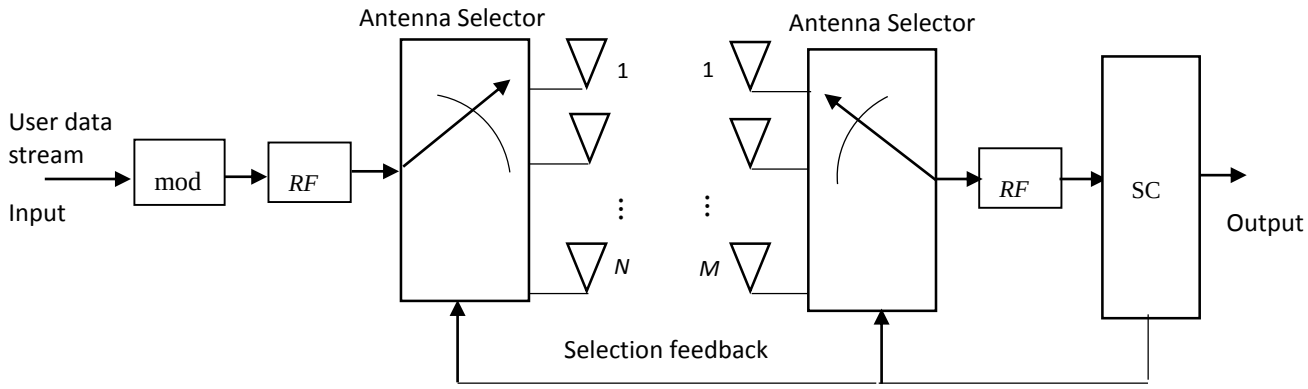

Fig.1-5. Block diagram of TAS/SC scheme

severe multipath fading while the primary user (PU) is operating in the vicinity [18]. Such kinds of problems can cause interference to the licensed users due to the very low SNR environments, which in turn leads to degrade the system performance. Thus *cooperative spectrum sensing* (CSS) can be a powerful solution to combat such effects [19], in which multiple cognitive radio users can cooperate to increase the probability of PU detection [see Fig.1-6]. In general, CSS can be performed as follows:

a) Each CR user (secondary user) sends its binary decision $D_i \in \{0,1\}$, to fusion center (FC).
b) At the FC, all the local decisions are combined according to the OR fusion rule.
c) The global decision is made to infer the presence or the absence of PU after M symbol periods.

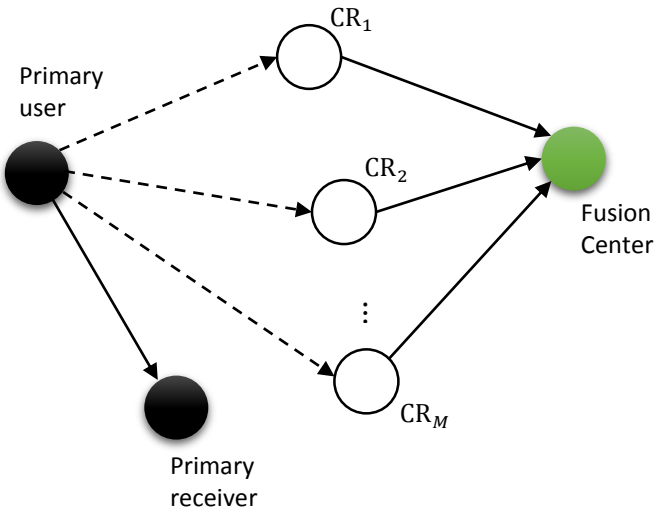

Fig.1-6. Cooperative spectrum sensing in cognitive radio network [95]

- **Vehicle-to-Vehicle Fading Channels**

Vehicle-to-vehicle communications channels often exhibit greater dynamics and more severe fading than fixed-to-mobile (F2M) cellular radio channels, which are mostly limited to classical Rayleigh or Nakagami-*m* distribution (i.e., $n = 1$), where the stationary base stations has high elevation antennas and is relatively free from local scattering [27]. Therefore, it is important to use a proper channel model that characterize the statistical properties of V2V fading channels such as *n*Rayleigh distribution* which has been proposed as an accurate statistical propagation model for V2V communication scenario [10].

In V2V communication, both the transmitter and receiver are in motion, and typically have the same antenna height, resulting in two or more small-scale fading processes generated by independent groups of local scatterers around the two mobile terminals [10] (see Fig.1-7, where two rings of scatterers are separated by a large distance (D) and all propagation paths travel through the same narrow pipe called by a keyhole channel[1]). Generally, such stochastic properties can be encountered in dense urban and forest environments where local scattering objects such as buildings, street corners, bridges, moving vehicles, foliage and mountains, obstruct a direct radio wave path between the transmitter and the receiver giving rise to non line-of-sight propagation (NLOS) [118]. Upon the geometry of obstructing surface, the transmitted signal may undergo reflection, diffraction, and /or scattering. As a result, the received signal consists of different paths, arriving from different directions with random delays resulting in fast or slow fading. Depending on how rapidly the transmitted signal changes with respect to the rate of change in the channel, a channel may be classified either as a fast fading or slow fading channel [119]. If the channel impulse response changes rapidly within one pulse (symbol) duration, it is fast fading, otherwise it is slow fading.

Mathematically speaking, the *n**Rayleigh fading channel model can be classified as a special case of the multiple sctattering channel model [see Fig.1-8], where the narrow-band impulse channel response is expressed as [11, 25]

$$H = k + h_1 + \alpha h_2 h_3 + \beta\, h_4 h_5 h_6 + \cdots \tag{1.1}$$

[1] Keyhole channel can be defined as a multiplier between two fading processes, resulting in a received signal amplitude that is a product of two Rayleigh random variables [11], e.g, double Rayleigh fading ($n = 2$) [113].

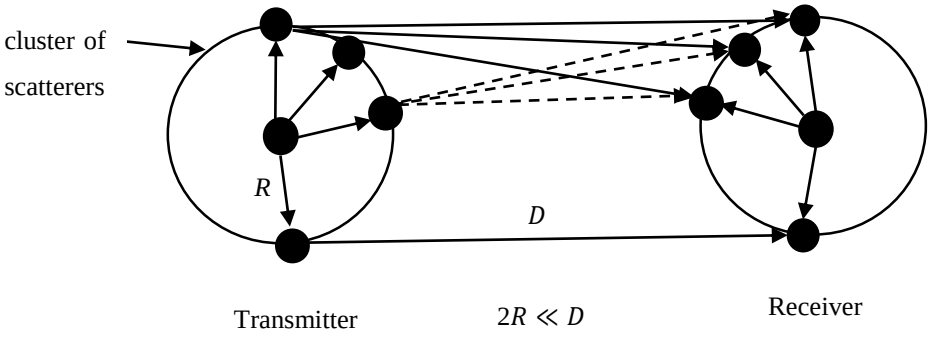

Fig.1-7. Double scattering Model [47]

where k is the Rician factor, h_i are complex, independent Gaussian random variables, α and β are attenuation factors. However, the *n**Rayleigh distribution has been studied by [12], where the probability density function (PDF) of the received fading amplitude $h \triangleq \prod_{i=1}^{n} h_i$, is given by

$$f_h(h) = 2(2^n\sigma^2)^{-\frac{1}{2}} G_{0,n}^{n,0}\left((2^n\sigma^2)^{-1}h^2 \,\middle|\, \overline{\frac{1}{2}, \dots, \frac{1}{2}}\right). \tag{1.2}$$

where $G_{p,q}^{m,n}(.)$ is the Meijer-G function defined in [13, eq.(9.301)]. From (1.2), when $n = 1$ and $n = 2$, the PDF of the received fading amplitude can be reduced to the well-known cases of Rayleigh and double Rayleigh distribution. For example, when $n = 1$ (Rayleigh fading), the Meijer-G function form reduces to $G_{0,1}^{1,0}\left(x \,\middle|\, \overline{a}\right) = x^a \mathrm{e}^{-x}$, resulting PDF as $f_h(h) = \frac{h}{\sigma^2} e^{-\frac{h^2}{2\sigma^2}}$. For $n = 2$ (double Rayleigh), the Meijer-G function reduces to $G_{0,2}^{2,0}\left(x \,\middle|\, \overline{a, b}\right) = 2\, x^{1/2(a+b)} K_{a-b}\left(2\sqrt{x}\right)$, yielding to $f_h(h) = \frac{h}{\sigma^2} K_0(h/\sigma)$, where $K_0(.)$ is the zeroth-order modified Bessel function of the second kind defined in [12, eq. (9.6.21)].

It is clear from (1.2) that the received instantaneous signal power can be defined by h^2. Thus, after the signal is passing through the fading channel, the signal is corrupted by additive white noise channel (AWGN) at the receiver. Consequently, the instantaneous SNR can be defined as $\gamma = |h|^2 P/N_o$, where P is the transmitted signal power and N_o is the power spectral density (W/Hz). In this case, the PDF of γ can be found with the help of [14, eq. (1.2)], as

$$f_\gamma(\gamma) = (\bar{\gamma}\gamma)^{-\frac{1}{2}} G_{0,n}^{n,0}\left(\frac{\gamma}{\bar{\gamma}} \,\middle|\, \overline{\frac{1}{2}, \dots, \frac{1}{2}}\right). \tag{1.3}$$

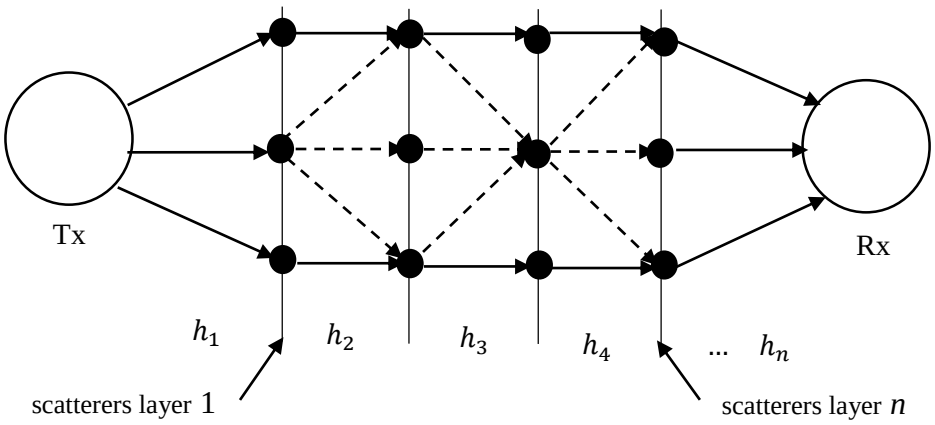

Fig.1-8. Multiple scattering model

where $\bar{\gamma} = \mathbf{E}(|h|^2)P/N_o$ is the average SNR, $\mathbf{E}(.)$ is the expectation operator**.** However, a new accurate approximation for the PDF of *n**Rayleigh distribution has been proposed by [15], which is derived based-on a transformed Nakagami-*m* distribution as

$$f_h(h) \approx 2\left(\frac{m}{\Omega}\right)^m \frac{h^{\frac{2m}{n}-1}}{n\Gamma(m)\sigma^{\frac{2m}{n}}} \mathrm{e}^{-\frac{m}{\Omega\sigma^{2/n}}h^{\frac{2}{n}}}, \quad h \geq 0 \tag{1.4}$$

In this case, the instantaneous SNR per symbol of the channel, γ, is distributed according to

$$f_\gamma(\gamma) \approx \frac{\beta^m \gamma^{\alpha-1}}{n\Gamma(m)} \mathrm{e}^{-\beta\gamma^{\frac{1}{n}}}, \quad \gamma \geq 0 \tag{1.5}$$

where $\alpha = m/n$ and $\beta = 2m/\Omega\bar{\gamma}^{1/n}$. The fading severity parameters (m, Ω) are given by

$$m = 0.6102n + 0.4263, \quad \Omega = 0.8808n^{-0.9661} + 1.12$$

It is important to mention that the approximation for the PDF in (1.4) has been examined in [15], by comparing it to the exact PDF derived in (1.3). The results have shown that the new approximation has high accuracy in most cases considered. Furthermore, the approximate PDF is easy to calculate and to manipulate compared to the exact PDF. As a double check, we verify the accuracy of the PDF in (1.4) using Monte-Carlo simulation, as illustrated in Fig.1-9, the approximate PDF has high accuracy as the cascading order *n* increases.

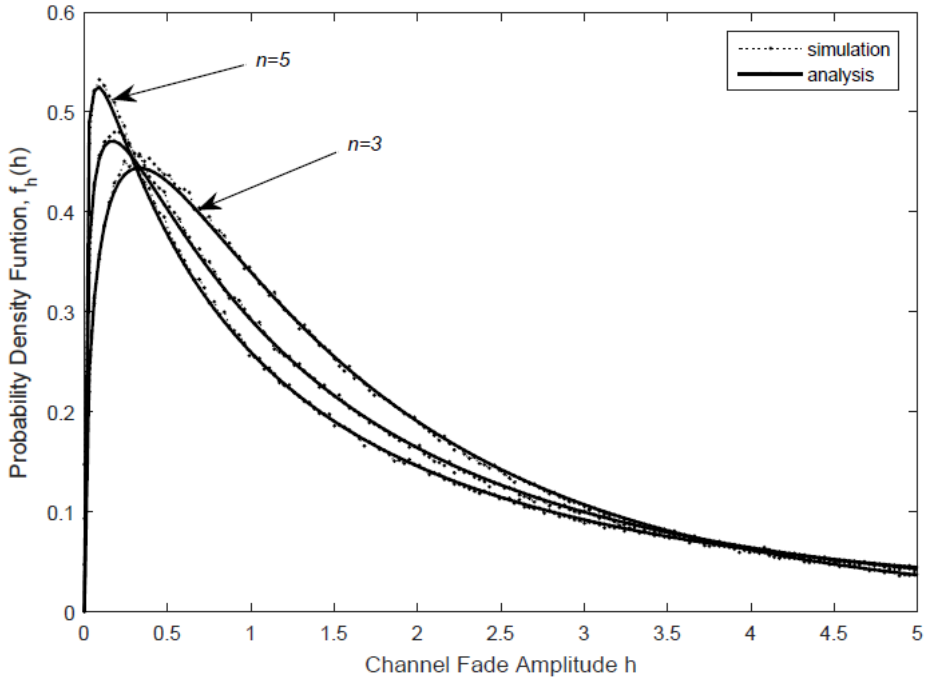

Fig.1-9. Comparison between analytical results and Monte-Carlo simulation for the PDF formulated by (1.4) $(n = 3; m = 2.256, \Omega = 1.424), (n = 4; m = 2.87, \Omega = 1.351), (n = 5; m = 3.477, \Omega = 1.306), \sigma^2 = 1$ and 10^6 iterations

A simple figure characterizing the severity of fading (also called amount of fading (AoF)) is found for n*Rayleigh distribution as $\mathrm{AF} = 2^n - 1$ [12]. The higher the cascading order n is, the larger the amount of fading will be.

1.2 Research Motivation and Problem Statement

Communications in IVC systems are very challenging and existing solutions, for instance, from cellular and ad-hoc networks may not be applicable, which is mainly due to the dynamic nature of wireless links and the mobility patterns. In other words, due to the high speed movement between vehicles, the topology of vehicular networks is always changing compared to cellular networks so that the probability of intermittent connectivity between two vehicles is high, especially when the vehicle density is low. Depending on the scattering environment of mobile radio channels, multipath propagation of cellular radio systems is characterized by the classical Rayleigh fading channel model where the base station is stationary above rooftop level and the mobile station is at street level [34], whereas channel characteristics of V2V communications systems are described by an accurate model called the cascaded Rayleigh fading channel model where the multiple scattering is taken place between the transmitter and the receiver.

Current studies in the field of V2V communications have proven that several small-scale fading processes are multiplied together, resulting in a new product process with worse than Rayleigh statistics between the transmitter and the receiver. Such severe multipath fading can deteriorate link reliability (e.g., high outage probability and low data rate), increase dropped connections and reduce battery life. Therefore, the major challenge in our research is to combat fading effects occurring among vehicles because of *n**Rayleigh fading channels.

Considering the problem and causes, we propose several cooperative schemes and approaches to improve the performance of IVC systems over *n**Rayleigh fading channels. By deploying various cooperative communications systems in IVC networks, one can benefit from increasing the vehicle density. To this end, we develop general mathematical probability models to minimize the end-to-end outage performance using relay selection schemes and multihop systems. In addition, we propose and analyze the performance from the antenna diversity perspective using reduced-complexity MIMO systems such as TAS/SC and TAS/MRC schemes which can easily achieve the spatial diversity gain and are utilized in case there is low traffic density or there are no cooperating nodes available between the source and destination. Moreover, we address the hidden terminal problem which occurs when the CR (secondary user) is hidden in *n**Rayleigh fading channels while the PU is operating in the vicinity. In this case, the CR user fails to observe the presence of the PU and then will access the licensed channel causing interference to the licensed users [120]. Hence, cooperative spectrum sensing has interestingly become a powerful solution to increase the probability of PU detection. In this context, we analyze the energy detection over *n**Rayleigh fading channels when cooperative spectrum sensing is employed in IVC system with and without MRC diversity reception.

To the best of our knowledge, cooperative communications systems, reduced-complexity MIMO systems, and spectrum sensing techniques over *n**Rayleigh fading channels have not been analyzed before. Hence, it is the aim of this work to fill this research gap and study IVC systems under *n**Rayleigh distribution.

1.3 Literature Review

Although wireless network connectivity with multinode relay-selection policy has been extensively studied in the literature, (see, e.g., [20-23] and references therein), most of the current works on cooperative with relay selection is *not* applicable to IVC networks. This is largely due to the

assumption of the underlying fading channel models, i.e., Rayleigh, Nakagami, etc., which are limited to cellular radio systems. It has been demonstrated recently that the so-called *n**Rayleigh fading channel model, which involves the product of two or more independent Rayleigh distributed random variables, provides an accurate statistical description of the IVC channel [10]. However, several papers in the literature discussed the multiple scattering model for Rayleigh distribution, e.g., in [24-26], the authors found that the multiple-Rayleigh channel model can be more appropriate for M2M propagation scenario. In [35], the authors proposed a mathematical reference model for V2V Rayleigh fading channels under NLOS conditions. In [27, 47], simulation methods were proposed for the double-ring model to simulate the two dimensional (2D) local scattering environment. In [28, 29], experimental results in different vehicular communication contexts were reported for the multiple scattering Rayleigh propagation mechanism, in which several small-scale fading processes are multiplied together, leading to a worse-than Rayleigh fading which is used for modeling V2V communication channels.

Recently, a new accurate approximation to the PDF of product of *n* independent Rayleigh random variables has been proposed in [15], which is derived based on a transformed Nakagami-*m* distribution. The authors has examined the accuracy of the new approximation by comparing it to the exact PDF. The results have shown that the new approximation has very high accuracy in most cases considered, which can be utilized for wireless communications applications such as inter-vehicular communications systems. In [30], the authors derive another new approximation for the PDF of the product of independent random variables, which is evaluated based on the previous work of [10]. This new approximate PDF was employed to calculate the outage probability of multihop wireless relaying over cascaded fading channels. The authors proved that the new approximation of the PDF is much simpler than that using the existing methods of infinite series or special functions. A generalized channel model called *n**Nakagami fading was proposed in [31], constructed as the product of *n* Nakagami-*m* distributed random variables. A cascaded Weibull channel model was proposed in [32]. In [33], the authors proposed a new stochastic fading model called *n**generalized *k*-distribution.

In this section, we present the related works to cooperative diversity with DF/AF relaying schemes over cascaded (*generalized)* fading channel models, as well as, we introduce some recent works in the open literature pertaining to MIMO-V2V channel modeling.

1.3.1 Cooperative Diversity Systems

There have been several studies that have investigated the performance of cooperative transmission systems over generalized fading channels when a single-relay scenario is considered. For instance, in [36], the authors studied the symbol error rate (SER) analysis for AF relaying scheme over cascaded Nakagami-*m* fading. In this work, they assumed a single-relay scenario with two source terminals communicate to each other through the same relay, the results showed that the outage performance is diminished by increasing the cascading order *n*. The pairwise error probability (PEP) for AF relaying over a doubly selective fading channel was determined in [37].

In [40], useful exact and asymptotic analytical expressions were derived for the SER for DF relaying scheme under double Nakagami-*m* distribution. In [42], the authors derived SER expressions for AF relaying over *n**Nakagami fading channels. In this study, both instantaneous and average power scaling factors are employed at the relay. The results showed that the instantaneous power scaling factor becomes advantageous over the average power scaling factor when the relay node is close to the source. In [43], an accurate expression for the SER was introduced for single and multi-relay AF systems over imperfect double Rayleigh channel estimates. In [38], an analytical expression for the PEP for distributed space-time trellis codes (STTCs) was derived in AF relaying mode over double Rayleigh fading channels. In [39], closed-form bounds for the outage probability of two-way AF relaying system was presented over double Nakagami-*m* fading channels.

Taking advantage of cooperative diversity systems across generalized fading channels, some studies in the literature have compared the performance of cooperative communications systems with diversity combining schemes. For instance, in [34], both the PEP and bit error rate (BER) of double Nakagami fading channels were analyzed for AF relaying mode and compared with the MRC scheme. Furthermore, a power allocation problem was addressed in this study. The results showed that the considered scheme can extract the full distributed spatial diversity. Additionally, the performance of the cooperative scheme with optimal power allocation can outperform the MRC scheme. In [41], the study investigated the effect of diversity combing reception on relaying systems. In particular, the performance of dual-hop AF relay networks with equal gain combining (EGC) was studied in term of BER over double Rice fading channels. The analytical results showed

that the diversity order can be improved by increasing the number of diversity branches between the source and destination.

Considering the statistical properties of generalized fading channels, analytical expressions for first and second order statistics were provided by [44]-[46]. For instance, in [44], analytical expressions for level crossing rate (LCR) and average fade duration (AFD) of *n**Rayleigh fading channels were presented in AF multihop transmission. In [45], using AF relaying mode, the authors studied the influence of the severity of double Nakagami fading on PDF, cumulative distribution function (CDF), LCR and AFD of the channel capacity. The results showed that an increase of severity of fading in one or both links of double Nakagami-m channels decreases the mean channel capacity while it results in an increase in the AFD of the channel capacity. In [46], statistical characteristics of narrowband AF relay networks fading channels with a single relay scenario was studied over double Hoyt fading, including channel variance, PDF, LCR and AFD.

One the other hand, there have been few contributions that have proposed and discussed the significance of cooperative diversity on routing efficiency over cascaded Rayleigh fading channel, considering the route selection strategy as an efficient solution for the connectivity problem among vehicles, for example, in [16], the authors examine the cooperative diversity transmission with DF relay selection over a double Rayleigh fading model. Upon the performance evaluation, it is observed that the maximum achievable diversity order is equivalent to the number of relays. In [48], cross-layer routing strategies were discussed by using cooperative transmission in IVC systems. The authors proposed a new approach of the path selection to achieve a better trade-off between the transmit power consumption and end-to-end transmission reliability over double Rayleigh fading channels, and proved that a route adopted by the relay selection strategy can improve a quality of wireless link such as lower power consumption or higher reliability.

The effect of the selective DF/AF relaying schemes and multihop systems on *n**Rayleigh fading channels seems sparse in the literature. Therefore, the main target of this research is to give a comprehensive performance analysis for cooperative diversity systems with *n**Rayleigh fading.

1.3.2 MIMO-V2V Systems

Performance analysis of MIMO systems has been extensively studied in the literature (see, e.g., [49],[50] and the references therein), most of these works were focused on classical Rayleigh or

Nakagami distributions. In fact, there a few contributions that conducted MIMO processing over V2V communication channels. For instance, the authors in [51] developed a generic geometry-based stochastic channel model for V2V links built on diffuse and discrete scatterer distributions using MIMO channel measurements performed by 5-GHz band in highways and rural environments. In [52], the authors presented a wide measurement campaign of MIMO-V2V propagation channel model in various environments and non-stationary behaviors such as large-scale and small-scale fading statistics were investigated accordingly. In [53], V2V channel measurements was analyzed based on the placement of multiple antennas on the vehicle and they showed an improvement in diversity gain. The authors in [54] presented MIMO-V2V channel measurements in a highway scenario based on pathloss, power-delay profile and delay-Doppler spectrum.

In [55], the authors reviewed a three-dimensional (3D) reference model for MIMO-V2V channel measurement campaign along with its first and second-order channel statistics in metropolitan area, where a new maximum-likelihood estimator was derived to extract the channel model parameters from the measured data. In [56], a geometrical two-ring scattering model was proposed for MIMO-V2V scheme over frequency-nonselective fading channels, assuming that both the transmitter and the receiver are surrounded by infinite local scatterers. The authors showed that if the distance separation between the transmitter and receiver terminals is much greater than the ring radii around the two mobile terminals, a double-Rayleigh distribution is followed instead of classical (single)-Rayleigh fading channel.

Although the aforementioned geometric models can be used to model the V2V channel characteristics in a wide variety of environments, unfortunately, they are complex and require numerous parameter selections for the specific environment of interest [57]. To get more insight into the characteristics of the V2V propagation channels; we introduce some works that have discussed MIMO systems over the keyhole channels. For example, in [58], the authors analyzed the average SER of MIMO-orthogonal space-time block codes (STBCs) in the presence of the keyhole which is characterized by double Nakagami-*m* fading channels. The results showed that the keyhole significantly degrades the symbol error probability of MIMO-STBC. The authors in [59] investigated the outage capacity distribution of spatially correlated keyhole (double Rayleigh) MIMO channels with perfect CSI knowledge at the receive end and with/or without CSI at the transmit end. The measurements of outage capacity are similarly to full-rank Rayleigh fading

channels, asymptotically Gaussian, when the number of both transmit and receive antennas is large regardless whether or not the CSI is available at the transmitter. In [69], an exact expression for the PEP of STCCs was derived over double Rayleigh fading

In [60], the authors determined exact and approximate expressions for the LCR and AFD of the double Nakagami-*m* random process. In [61], the authors investigated the performance of MIMO-STBC systems over generalized-*K* fading channels. In this study, exact analytical expressions were derived in terms of outage probability, average channel capacity and average SER. In [62], a simple analytical capacity bound was derived for MIMO systems over generalized-*K* fading channels. In [63], the authors introduced closed-forms expressions for outage probability, symbol error probability, amount of fading and egodic capacity for MIMO systems under a double Weibull distribution. In [64], a performance analysis of coded MIMO-orthogonal frequency division multiplexing (OFDM) systems with perfect CSI knowledge at the transmitter and the receiver was tackled under generalized Rician distribution. In [65], the effect of imperfect channel estimation on the performance of STBC-IVC systems was investigated in the BER over cascaded Rayleigh fading channels. In [66], the performance of a single wireless link has been studied over double Rayleigh fading channels, and the results showed that double scattering channels have a severe degradation on the SER.

There have been some works in the literature that have also discussed the effect of diversity combining schemes on generalized fading channels. For instance, in [68], the authors investigated the outage probability and BER for different diversity receivers over cascaded Nakagami-*m* fading, including MRC, SC, EGC and generalized selection combining (GSC) algorithms. The analytical results showed that the MRC algorithm has the best performance over other algorithms. In [70], the author derived a closed-form expression for the SER with receive antenna diversity over double Rayleigh fading channels. The results revealed that the diversity order equal to the number of receive antennas. In [71], the authors analyzed the BER for EGC receiver scheme with non-coherent transmission over generalized-*K* fading channels. The results showed that the diversity order of coherent transmission which relies on the availability of an accurate channel knowledge at the receive side, is the same as in case of non-coherent transmission. In [67], the authors derived analytical expression for the average BER of *M*-PSK modulation when the MRC diversity receiver is considered over double Rician fading channels.

Since the generalized fading channel models for MIMO systems with transmit antenna selection are absent in the literature, we examine the performance of TAS/MRC and TAS/SC schemes over *n**Rayleigh fading channels when partial CSI knowledge is available at the transmitter.

1.4 Thesis Objectives

The main objective of our research is to propose and evaluate the performance of various efficient schemes and approaches that can be used in intervehicular communications networks to avoid poor connections among vehicles because of *n**Rayleigh fading channels. New efforts at different levels are needed, including at the physical layer level, which is the aim of this work. The specific objectives are:

1. Evaluate the performance of DF/AF cooperative communications systems based on both relay selection and multihop strategies over *n**Rayleigh fading channels. In this regard, the main goal is to provide easy-to-compute analytical expressions for the outage probability, the maximum diversity order, the amount of fading, the symbol error rate, and the average channel capacity under *n**Rayleigh distribution.
2. Propose an efficient power allocation scheme to optimize the overall transmit power between the source and the relay nodes when perfect channel state information is available, in which one can reduce the interference for the entire IVC network and consequently, obtain less outage probability.
3. Address and solve the hidden terminal problem over *n**Rayleigh fading channels, using the cooperative spectrum sensing approach with MRC diversity reception.
4. Propose and examine low-complexity MIMO systems with *n**Rayleigh fading such as TAS/MRC and TAS/SC schemes, which allow a system designer to perform comparison between the performance and complexity. To this end, general analytical expressions for the outage and error probabilities should be derived to assess and compare the performance of both schemes.

1.5 Thesis Outline

The thesis outline is as follows:

Chapter 2 analyzes the performance of IVC systems with relay selection over *n**Rayleigh fading channels. In particular, we consider the selective DF relaying protocol in dual-hop inter-vehicular

transmission scenario when there is no direct transmission between the source and the destination. In this chapter, we derive approximate closed-form expressions for the outage probability, the symbol error probability, and the average channel capacity. Furthermore, we address and solve the power allocation problem for the underlying scheme. In Chapter 3, we study the performance of IVC systems when selective AF relaying scheme is considered. In this chapter, approximate closed-form expressions are derived for the outage probability and the symbol error rate. In Chapter 4, we investigate the performance of IVC systems with the multihop transmission approach, assuming regenerative or non-regenerative relays to forward the source message to the destination. We derive approximate and bounds expressions for outage probability and amount of fading. We further propose a power allocation scheme to minimize the outage performance. In chapter 5, we address the problem of energy detection of unknown signals over *n**Rayleigh fading channels, using CSS approach with/without MRC diversity reception. In this chapter, approximate closed-form expressions of the probability of detection for both no-diversity and diversity reception are presented. Chapter 6 presents the performance analysis of IVC systems with TAS/MRC and TAS/SC schemes over *n**Rayleigh fading channels. In this chapter, we derive approximate closed-form expressions for the outage probability, the amount of fading, and the symbol error rate. In chapter 7, general discussion is provided. Finally, we conclude the research with future work in Chapter 8.

CHAPTER 2

ARTICLE 1: RELAY SELECTION IN DUAL-HOP INTER-VEHICULAR COMMUNICATIONS SYSTEMS OVER CASCADED RAYLEIGH FADING CHANNELS

Yahia Alghorani and Samuel Pierre
yahia.alghorani@polymtl.ca; samuel.pierre@polymtl.ca
Mobile Computing and Networking Research Laboratory (LARIM)
Ecole Polytechnique de Montreal
Montreal, Quebec, H3C 3A7, Canada

Sami Muhaidat
sami.muhaidat@uwo.ca
Electrical and Computer Engineering Department
University of Western Ontario
London, Ontario, N6A 5B9, Canada

Naofal Al-Dhahir
aldhahir@utdallas.edu
Department of Electrical Engineering
University of Texas at Dallas
Richardson, TX 75083 USA

Submitted to IEEE Transactions on Vehicular Technology, September 2014

Abstract

In this paper, we investigate the performance of a dual-hop inter-vehicular communications system assuming the selective decode-and-forward relaying protocol. We focus on cascaded Rayleigh (also called *n**Rayleigh) fading channels, which have been recently proposed as realistic propagation channel models for vehicle-to-vehicle communications. We propose and analyze new approximate closed-form expressions for the outage probability, the symbol error probability, and

the average channel capacity, which are derived using a simple and reliable approximation to the probability density function of a product of *n* arbitrary independent cascaded Rayleigh fading channels ($\boldsymbol{n \geq 2}$). Furthermore, we propose a power allocation scheme when the statistical channel state information is available at the source and the relay nodes. Numerical results show that the best relay selection technique achieves an asymptotic diversity order of (mN/n) where N is the number of relays and *m* is a cascaded Rayleigh fading parameter.

Index Terms: Cooperative diversity, inter-vehicular networks, cascaded Rayleigh fading channels, relay selection, outage probability.

2.1 Introduction

Dual-hop vehicle-to-vehicle communications systems have recently received considerable attention in the research community. Such systems are intended to improve safety and reduce traffic congestion by efficient integration of communications technologies in road transportation. In general, due to the high mobility and the non-uniform distribution of vehicles, which can cause frequent route interruptions [1], the risks of traffic congestion and accidents necessitate the development of a new transportation network technology. This emerging technology exploits the capabilities of wireless communication to advance the research in intelligent transportation systems (ITS). The key idea is to create wireless connections among vehicles while they are connected to other networks at home or at a workplace. Thus, cooperative diversity is a promising communication technology [2] to simplify routing problems in inter-vehicular communications (IVC) and provide high data rate coverage. The main idea behind this technique is to forward a source message to a desirable destination with the help of intermediate nodes. However, the need for transmitting data in multi-relay networks over orthogonal (time or frequency) channels reduces spectral efficiency and increases overhead. Additionally, due to power allocation constraints, using multiple relay cooperation is not economical and this motivates the use of relay selection techniques. The most common approach is to select the relay with highest signal-to-noise ratio (SNR) at the destination terminal. In this case, the diversity gain can be improved without the need for multiple antenna deployment at each node [75]. There are two main relaying schemes utilized by cooperative networks, namely, the decode-and-forward (DF) and the amplify-and-forward (AF). In the former, the relay decodes and then retransmits the received source signal to the destination.

In the latter, the relay amplifies the analog signal received from the source and forwards it to the destination node [9].

In fact, wireless network connectivity with relay selection in multi-node cooperation has been extensively studied in the literature, (see, e.g., [20, 21, 23] and references therein). Most of these studies were in the context of ad hoc wireless networks and assumed the classical Rayleigh distribution, which is limited to fixed-to-mobile cellular radio channels. Recently, the cascaded *n**Rayleigh distribution was proposed as an accurate statistical propagation model for mobile-to-mobile scenario. In vehicle-to-vehicle (V2V) communications, both the transmitter and receiver are in motion and typically use the same antenna height, resulting in two or more independent Rayleigh fading processes, generated by independent groups of scatterers around the two mobile terminals [10]. Several papers in the literature have argued that the cascaded Rayleigh distribution accurately characterizes for mobile-to-mobile communication scenarios [24]-[26]. In [12], the authors derive exact probability density function (PDF) and distribution function (CDF) expressions for *n**Rayleigh distribution. A generalized channel model called *n**Nakagami has been proposed by [31], based on the product of *n* Nakagami-m distributed random variables. In [56], multiple-input multiple-output (MIMO) techniques were studied for mobile-to-mobile communications systems. The authors concluded that if the distance separation between the transmitter and receiver terminals is much greater than the ring radii around the two terminals, a double-Rayleigh distribution model should be considered instead of classical (single)-Rayleigh fading channels. In [28],[29], experimental results in different vehicular communication environments have shown that in vehicular networks, several small-scale fading processes are multiplied together, leading to a worse-than Rayleigh fading. More recently, a new accurate approximation of the PDF of the product of *n* independent Rayleigh random variables was proposed by [15], which was derived based on a transformed Nakagami-*m* distribution. The authors examined the accuracy of the new approximation by comparing it to the exact PDF derived in [12]. Their results have shown that the new approximation is highly accurate in most considered cases, hence; it can be utilized for wireless communications applications such as IVC systems. In [30], the authors derived another new approximation for the PDF of the product of independent random variables, which was evaluated based on the earlier work of [15]. This new approximate PDF was employed to calculate the outage probability of multi-hop wireless relaying over cascaded fading channels and the authors proved that the new PDF approximation is much simpler than that

obtained using the existing methods of infinite series or special functions. Few recent works have discussed the significance of cooperative diversity over cascaded Rayleigh fading channels. In [34], the performance of an inter-vehicular cooperative scheme with amplify-and-forward relaying over cascaded Nakagami-*m* fading channel was analyzed where the authors assumed a single-relay scenario operating in half-duplex mode. They have shown that the inter-vehicular cooperative scheme can exploit full spatial diversity. In [16], the authors examined cooperative diversity transmissions with the selective-DF (S-DF) relaying over a double Rayleigh fading model ($n = 2$). They have demonstrated that the maximum achievable diversity gain is equivalent to the number of relays. The authors in [36] studied the symbol error rate (SER) performance of a two-way relay network over cascaded Nakagami fading. The results showed that the improvement in outage performance is diminished by increasing the cascading order (n). In [37], the authors derived a pairwise error probability (PEP) for an amplify-and-forward cooperative systems over a doubly selective fading channel.

To the best of our knowledge, S-DF relaying schemes in inter-vehicular cooperative networks over cascaded Rayleigh (*n**Rayleigh) fading channels have not been studied before. Hence, it is the main goal of this paper to provide a comprehensive performance analysis for IVC systems with relay selection. Specifically, our contributions are summarized as follows:

1. We derive an approximate closed-from expression for the outage probability for the S-DF scheme over *n**Rayleigh fading channels.
2. We derive a new lower-bound expression for the moment generating function (MGF), which is used to compute the symbol error probability of *M*-ary phase shift keying (*M*-PSK) modulation. We further derive an asymptotic expression for the average channel capacity.
3. We propose a power allocation scheme to optimize the overall transmit power between the source and the best relay when statistical channel state information is available at the source. In particular, we study the outage performance over highly unbalanced channel links between the source and the selected relay and the destination.
4. We demonstrate that the maximum achievable diversity order for *n**Rayleigh fading channels is reduced by increasing the cascading order n.

The rest of this paper is organized as follows. Section 2.2 introduces the system and channel model of dual-hop inter-vehicular cooperative transmission. In Section 2.3, we derive the approximate

closed-form expressions for the outage probability, the symbol error probability, and the average channel capacity. In Section 2.4, the numerical results are presented. Finally, Section 2.5 concludes the paper.

2.2 System Model and Assumptions

2.2.1 Channel Model

We consider an IVC transmission system where a source terminal (***s***) transmits information to a destination terminal (***d***) with the assistance of N relays r_i $(i = 1, \ldots, N)$; see Fig. 2-1. We assume that each node is equipped with a single antenna and operates in half-duplex mode.

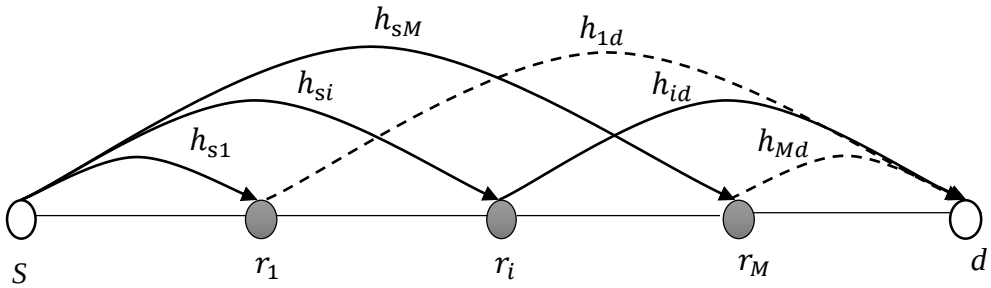

Fig.2-1. Dual-hop inter-vehicular cooperative transmission system

Under this scenario, in the first time slot, the source node broadcasts its message to all potential relaying nodes. In the second time slot, the relays decode the source message and the relay with the maximum SNR at the destination node is selected from the decoding set to forward the source message. The channel coefficients of the links between $s \to r_i$ (h_{si}) and $r_i \to d$ (h_{id}) are modeled as a product of *n* independent circularly complex Gaussian random variables, each of which can be defined as $h_{si} \triangleq \prod_{j=1}^{n} h_{si,j}$, $h_{id} \triangleq \prod_{j=1}^{n} h_{id,j}$ with zero mean and channel variance equivalent to (λ_{si}) and (λ_{id}), respectively, for $i = 1, 2, \ldots, N$. Therefore, $|h_{si}|$ and $|h_{id}|$ follow a cascaded Rayleigh distribution. We assume that all underlying channels are quasi-static which can be justified for vehicular communications scenarios in rush-hour traffic [77]. Due to the broadcast nature of the wireless medium, both the relays and the destination receive a noisy signal. Therefore, the signal received by the relay node from the source $y_{si}(t)$, and that received by the destination node from the best relay $y_{rd}(t)$, are given respectively by [8]

$$y_{si}(t) = h_{si}\sqrt{P}x(t) + w_i(t)$$

$$y_{rd}(t) = h_{rd}\sqrt{P}x_r(t) + w_d(t) \tag{2.1}$$

where $x(t)$ is a transmitted symbol signal from the source, $x_r(t)$ is the transmitted symbol signal forwarded by the best relay to the destination node, P is the transmitted signal power, $w_i(t) \sim \mathcal{CN}(0, N_o)$ and $w_d(t) \sim \mathcal{CN}(0, N_o)$ are additive white Gaussian noise (AWGN) at the relay and destination nodes respectively, assuming that all links have zero mean and variance (N_o).

2.2.2 Cooperative Protocol

In the S-DF relaying scheme, the source transmits its message to a set of relay nodes and the destination. In this stage, the S-DF relaying policy is applied in choosing the i^{th} reliable path between $(s \to r_i)$ and $(r_i \to d)$ links. We define the decoding set $(\mathcal{D})$ as a set of relays that decode the source message successfully when the channel quality between the source and relay node is sufficiently good. We assume that each relay can determine whether the source message is decoded correctly or not through a cyclic redundancy check (CRC). In the second time slot, only one relay from the decoding set $(\mathcal{D})$, having the best link quality with the destination will be able to forward the source message. In this case, two orthogonal time slots are utilized to perform the cooperative transmission, and the transmitted signal on the $(s \to r_i)$ link must be coded with rate $(2R)$ in order to achieve an average end-to-end rate of R, otherwise the $(s \to r_i)$ link is in outage case. Mathematically speaking, the decoding set is given by

$$\mathcal{D} = \{i: \log_2(1 + \gamma_{si}) \geq 2R\} \tag{2.2}$$

where $\gamma_{si} = |h_{si}|^2 P/N_o$, is the instantaneous SNR over $(s \to r_i)$ link. Therefore, the effective SNR, γ_{DF}, received at the destination node can be expressed as

$$\gamma_{DF} = \max_{i \in \mathcal{D}} \{\gamma_{id}\} \tag{2.3}$$

where $\gamma_{id} = |h_{id}|^2 P/N_o$, is the instantaneous SNR over $(r_i \to d)$ link. By introducing the random variable γ_i as an equivalent instantaneous SNR over $s \to r_i \to d$ link, one can rewrite (2.3) to be more analytically tractable as [78]

$$\gamma_{DF} = \max_{i \in N} \{\gamma_i\} \tag{2.4}$$

2.2.3 Deriving the CDF of Received SNR

Both links between $(s \to r_i)$ and $(r_i \to d)$ are modeled by the approximate PDF of n*Rayleigh random variables [15]. This approximation, which is based on a transformed Nakagami-m distribution, is expressed as

$$f_h(h) \approx 2\left(\frac{m}{\Omega}\right)^m \frac{1}{n\Gamma(m)\sigma^{\frac{2m}{n}}}\, h^{\frac{2m}{n}-1} \exp\left(-\frac{m}{\Omega\sigma^{\frac{2}{n}}}\, h^{\frac{2}{n}}\right),\ h \geq 0 \tag{2.5}$$

where m and Ω are the cascaded Rayleigh fading parameters given by

$$m = 0.6102n + 0.4263, \quad \Omega = 0.8808n^{-0.9661} + 1.12 \tag{2.6}$$

To obtain the PDF for the SNR, using the change of variable, we get

$$f_\gamma(\gamma) = \frac{f_h\left(\sqrt{2^n\sigma^2\,\gamma/\bar{\gamma}}\right)}{2\sqrt{\gamma\bar{\gamma}/2^n\sigma^2}} \tag{2.7}$$

By substituting (2.5) into (2.7), we can obtain closed-form expressions for the approximate the instantaneous SNR PDF $(s \to r_i)$ and $(r_i \to d)$ links, respectively as

$$f_{\gamma_{si}}(\gamma) \approx \frac{{\alpha_i}^{m_{si}}}{n_{si}\Gamma(m_{si})}\gamma^{a_i-1}\exp\left(-\alpha_i\gamma^{\frac{1}{n_{si}}}\right), \quad \gamma \geq 0 \tag{2.8}$$

$$f_{\gamma_{id}}(\gamma) \approx \frac{{\beta_i}^{m_{id}}}{n_{id}\Gamma(m_{id})}\gamma^{b_i-1}\exp\left(-\beta_i\gamma^{\frac{1}{n_{id}}}\right), \quad \gamma \geq 0 \tag{2.9}$$

where $\alpha_i = 2\,m_{si}/\Omega_{si}\bar{\gamma}_{si}^{\frac{1}{n_{si}}}$, $\beta_i = 2m_{id}/\Omega_{id}\bar{\gamma}_{id}^{\frac{1}{n_{id}}}$, $a_i = m_{si}/n_{si}$, and $b_i = m_{id}/n_{id}$. The average links SNR of γ_{si} and γ_{id} are independent, but not necessarily identically distributed (i.n.i.d) random variables with means defined as $\bar{\gamma}_{si} = \mathbf{E}(|h_{si}|^2)\,P/N_o$ and $\bar{\gamma}_{id} = \mathbf{E}(|h_{si}|^2)\,P/N_o$, respectively, where $\mathbf{E}(.)$ is the statistical expectation operator.

To derive an approximate PDF for the received SNR at the destination node via the i-th dual-hop $(s \to r_i \to d)$ link, we invoke the technique described in [79]. Consequently, the conditional PDF

of the received SNR indicating that r_i is idle when the instantaneous SNR of $(s \to r_i)$ link is below a predetermined threshold value $(\gamma_o = 2^{2R} - 1)$; is expressed as $f_{\gamma_i|r_i\ is\ off}(\gamma) = \delta(\gamma)$. Hence, the probability that the *i*-th relay will not be in the decoding set $\mathcal{D}$ can be found as follows

$$A_i = \Pr(\gamma_{si} \le \gamma_o) = \int_0^{\gamma_o} f_{\gamma_{si}}(\gamma)\, d\gamma \tag{2.10}$$

By substituting (2.8) into (2.10), and with the help of the fact that [13,eq.(3.381.1) and eq.(8.356.3)]

$$\int_0^u x^{v-1} \exp(-\mu x)\, dx = \mu^{-v}\gamma(v, \mu u)$$

and
$$\gamma(\alpha, x) + \Gamma(\alpha, x) = \Gamma(\alpha) \tag{2.11}$$

we calculate the probability of the $(s \to r_i)$ link under the outage case as

$$A_i = 1 - \frac{\Gamma\left(m_{si}, \alpha_i \gamma_o^{\frac{1}{n_{si}}}\right)}{\Gamma(m_{si})} \tag{2.12}$$

where $\gamma(\alpha, x) = \int_0^x e^{-t} t^{\alpha-1}\, dt$ and $\Gamma(\alpha, x) = \int_x^\infty e^{-t} t^{\alpha-1}\, dt$ represent the lower and the upper incomplete gamma function, respectively, as defined in [80].

On the other hand, the probability that the *i*-th relay is in the decoding set is $(1 - A_i)$, and the conditional PDF given r_i is active is $f_{\gamma_i|r_i\ is\ on}(\gamma) = f_{\gamma_{id}}(\gamma)$. Therefore, the unconditional approximate PDF of the instantaneous SNR (γ_i) over the *i*-th cascaded $(s \to r_i \to d)$ link from the source to the destination can be expressed as

$$f_{\gamma_i}(\gamma) \approx A_i \delta(\gamma) + \frac{{\beta_i}^{m_{id}} (1 - A_i) \gamma^{b_i - 1}}{n_{id}\Gamma(m_{id})} \exp\left(-\beta_i \gamma^{\frac{1}{n_{id}}}\right), \quad \gamma \ge 0 \tag{2.13}$$

Using the facts in (2.11), the approximate CDF of γ_i can be derived from (2.13) as

$$F_{\gamma_i}(\gamma) \approx 1 - (1 - A_i) \frac{\Gamma\left(m_{id}, \beta_i \gamma^{\frac{1}{n_{id}}}\right)}{\Gamma(m_{id})} \tag{2.14}$$

Consequently, the approximate CDF of γ_{DF} can be derived as follows

$$F_{\gamma_{DF}}(\gamma) = \Pr\left(\max_{i\in N}(\gamma_i) \le \gamma\right) = \prod_{i=1}^{N} F_{\gamma_i}(\gamma) \tag{2.15}$$

2.3 Performance Analysis

2.3.1 Outage Probability

The outage probability $P_{out} \triangleq F_{\gamma_{DF}}(\gamma_o)$ of a communication channel can be defined as the probability that the maximum instantaneous SNR (γ_i) falls below a certain threshold (γ_o). In this section, we derive a closed-form expression for the outage probability and determine the achievable diversity order of the S-DF scheme over *n* independent cascaded Rayleigh fading channels. To simplify the notations, we define $\lambda_{si} = \mathbf{E}(|h_{si}|^2), \lambda_{id} = \mathbf{E}(|h_{id}|^2)$, and $\text{SNR} = P/N_o$.

Using (2.15), the outage probability of the S-DF relaying scheme over i.n.i.d cascaded Rayleigh random variables can be found as

$$P_{out} = \prod_{i=1}^{N}\left[F_{\gamma_i}(\gamma_o)\right] \tag{2.16}$$

In the case of i.i.d cascaded Rayleigh random variables, where $(m_{si} = m_{id} = m,\ \Omega_{si} = \Omega_{id} = \Omega,\ n_{si} = n_{id} = n, \lambda_{si} = \lambda_{id} = \lambda,\ \forall\ i = 1,2,\dots,N)$, (2.16) can be upper bounded as

$$P_{out} \le \left[2\frac{\gamma\left(m, \beta\gamma_o^{\frac{1}{n}}\right)}{\Gamma(m)}\right]^N \tag{2.17}$$

Then, at high SNR (i.e., when $\text{SNR} \gg 0$), with the help of the facts that [80, eq.(6.5.12) and eq.(13.5.5)]

$$\gamma(\alpha, x) = \frac{x^\alpha}{\alpha} M(\alpha, \alpha+1, -x)$$

and $$M(a, b, x) = 1 \text{ as } |x| \to 0 \tag{2.18}$$

where $M(.,.,.)$ is the Kummer's confluent hypergeometric function, defined in [80, eq.(13.1.2)], (2.17) can be written as

$$P_{out} \leq \left(\frac{2\left(2m/\Omega\right)^{m}}{m\,\Gamma(m)\lambda^{\frac{m}{n}}} \right)^{N} \left(\frac{\gamma_o}{\mathrm{SNR}} \right)^{\frac{mN}{n}} + \mathcal{O}\left(\left(\frac{\gamma_o}{\mathrm{SNR}} \right)^{\frac{mN}{n}+1} \right) \tag{2.19}$$

Now, it can be easily seen that the achievable diversity order of an IVC system over cascaded Rayleigh fading channels is $d \approx mN/n$. This is due to the fact that the maximum achievable diversity order is defined as the slope of the outage probability as a function of the average SNR in log-log scale, i.e., [81]

$$d = \lim_{\mathrm{SNR}\to\infty} (-\log P_{out} / \log \mathrm{SNR}) = \frac{mN}{n} \tag{2.20}$$

From (2.19), we can also deduce that the effective coding gain (CG) is given by the following expression

$$\mathrm{CG} = \left[\frac{2\left(2m/\Omega\right)^{m}}{m\,\Gamma(m)\lambda^{m/n}} \right]^{-\frac{n}{m}} \tag{2.21}$$

Note that the coding gain in (2.21) depends only on the severity fading parameters and channel variance which are assumed to be fixed during the whole transmission time, regardless of the value of the parameter N.

2.3.2 Average Symbol Error Rate

For simplicity, we analyze the SER performance of *M*-PSK modulation with the S-DF relaying scheme over i.i.d cascaded Rayleigh random variables. The symbol error probability can be calculated through the so-called MGF approach [14]

$$P(e) = \frac{1}{\pi} \int_{0}^{\pi - \frac{\pi}{\mathrm{M}}} \Phi_{\gamma_{DF}} \left(\frac{\sin^2(\pi/M)}{\sin^2\theta} \right) d\theta \tag{2.22}$$

where $\Phi_{\gamma_{DF}}(\cdot)$ is the MGF of effective SNR received by the destination, given by $\Phi_{\gamma_{DF}}(s) = s\mathcal{L}\{F_{\gamma_{DF}}(\gamma); s\}$, where $\mathcal{L}(.;.)$ denotes the Laplace Transform. Since the fading severity parameter m in (2.15) is a real-valued parameter, it is challenging to derive a closed-form expression for the MGF of γ_{DF} with a finite-sum representation. Therefore, using the bounds for

the incomplete gamma function given in [83, eq.(4.1)], the CDF of γ_{DF} can be further simplified to

$$F_{\gamma_{DF}}(\gamma) \approx \left[1-(1-A)\left(1-\frac{\beta^m \gamma^{\frac{m}{n}}}{m\Gamma(m)} e^{-\frac{m}{m+1}\beta\gamma^{\frac{1}{n}}}\right)\right]^N \tag{2.23}$$

Now, using the fact that $\exp(-x) = G_{0,1}^{1,0}\left(x\middle|\begin{matrix}-\\0\end{matrix}\right),\ \forall x$ and the identity in [84, eq.(07.34.21.0088.01)], we get the MGF lower-bound given as

$$\Phi_{\gamma_{DF}}(s) \approx \frac{\sqrt{n}}{(2\pi)^{\frac{n-1}{2}}} \sum_{k=0}^{N}\sum_{l=0}^{k} (-1)^{k+l}\binom{N}{k}\binom{k}{l}(1-A)^k \left(\frac{\beta^m}{m\Gamma(m)}\right)^l$$

$$\times s^{-\frac{ml}{n}} G_{1,n}^{n,1}\left(\left(\frac{ml\beta}{n(m+1)}\right)^n s^{-1}\middle|\begin{matrix}-\frac{ml}{n}\\0,\ldots,\frac{n-1}{n}\end{matrix}\right) \tag{2.24}$$

Special Case: From (2.24) with the help of [84], we can reduce the G-function form to the case of double-Rayleigh $(n=2)$ distribution, as

$$G_{1,2}^{2,1}\left(z\middle|\begin{matrix}1-a\\0,\ \frac{1}{2}\end{matrix}\right) = \Gamma(a)\Gamma\left(a+\tfrac{1}{2}\right)U\left(a,\tfrac{1}{2},z\right)$$

where $U(.,.,.)$ is Tricomi confluent hypergeometric function defined in [80, eq. (13.2.5)]. Substituting (24) into (2.22), replacing $\theta = \pi/2$ to evaluate the upper-bound symbol error rate for the S-DF relaying scheme, which can be expressed as

$$P(e) \le \frac{M-1}{M}\Phi_{\gamma_{DF}}(\sin^2(\pi/M)) \tag{2.25}$$

Asymptotic Analysis: From (2.23), we derive an asymptotic expression for the symbol error rate in the high SNR regime (i.e., $\bar{\gamma} \gg 0$), using the zeroth-order Taylor approximation (where $e^{-x} \approx 1$ for x sufficiently small), and after some algebraic manipulations, the SER of binary phase shift keying (BPSK) modulation is obtained as

$$P(e) \leq \frac{1}{2}\sum_{k=0}^{N}\binom{N}{k}A^{N-k}\left(\frac{\left(m/\Omega\bar{\gamma}^{\frac{1}{n}}\right)^{m}}{m\Gamma(m)}\right)^{k}\Gamma\left(1+\frac{km}{n}\right) \tag{2.26}$$

Notice that the diversity order can also be deduced from (2.26) as $d \approx mN/n$ when $k = N$.

2.3.3 Channel Capacity

In this section, we investigate the asymptotic average channel capacity for the S-DF relaying scheme over i.i.d cascaded Rayleigh random variables. The average channel capacity for the S-DF relaying scheme is given as

$$\bar{C} = \frac{BW}{2}\int_{0}^{\infty}\log_2(1+\gamma_{DF})\,f_{\gamma_{DF}}(\gamma_{DF})\,d\gamma_{DF} \tag{2.27}$$

where *BW* [Hz] is the transmitted signal bandwidth. From (2.15), the PDF of γ_{DF} over i.i.d n*Raleigh random variables can be expressed as

$$f_{\gamma_{DF}}(\gamma_{DF}) \approx N(1-A)\frac{\beta^{m}\gamma^{\frac{m}{n}-1}e^{-\beta\gamma^{\frac{1}{n}}}}{n\Gamma(m)}\left[1-(1-A)\frac{\Gamma\left(m,\beta\gamma^{\frac{1}{n}}\right)}{\Gamma(m)}\right]^{N-1} \tag{2.28}$$

To the best of our knowledge, the integral in (2.27) is intractable due to the complexity of finding a closed-form expression for the PDF (2.28) using a finite series since the fading parameter m takes real values. Therefore, we derive the average channel capacity for the underlying scheme in the high-SNR regime (i.e, when $\bar{\gamma} \to \infty$). Using (2.28) with the help of the facts that $\Gamma(a,z) = z^{a}e^{-z}\,U(1,1+a,z)$ [85, eq. (8.5.3)], [80, eq. (13.5.6)], and [84, eq.(01.04.26.0003.01), eq.(07.34.21.0088.01)], the average channel capacity can be approximated as

$$\bar{C} \approx \frac{Nn^{m-\frac{1}{2}}}{2\ln 2\,(2\pi)^{\frac{n-1}{2}}\Gamma(m)}\sum_{k=0}^{N-1}(-1)^{k}\binom{N-1}{k}\frac{(1-A)^{k+1}}{(k+1)^{m}}$$

$$\times G_{2+n,2}^{1,2+n}\left(\left(\frac{n}{(k+1)\beta}\right)^{n}\middle|\begin{matrix}\frac{1-m}{n},\ldots,\frac{n-m}{n},1,1\\ 1,0\end{matrix}\right) \tag{2.29}$$

Using the asymptotic expansion for the Meijer's G-function presented in [84, eq. (07.34.06.0006.01)], an accurate simple approximation for (2.29) is obtained.

2.3.4 Transmit Power Allocation Optimization

In the context of IVC transmission, optimizing the power allocation among the source and the relays is critical to reduce the total transmit energy. Hence, in this section, we analyze the power allocation (PA) for the S-DF relaying scheme over cascaded Rayleigh fading channels when the links statistics $(\lambda_{si}, \lambda_{id})$ are available at the source and relay nodes instead of the instantaneous channel state information. By doing so, we can minimize the outage probability under the following total power constraint $P_s + P_r \leq P_T$, where $P_s \triangleq E_s/N_o$ is the transmitted signal power from the source, $P_r \triangleq E_r/N_o$ is the received signal power at the selected relay, and $P_T \triangleq E_T/N_o$ is the total transmit power, where $E_T = E_s + E_r$ is the total transmitted energy per symbol from the source and the selected relay. Here, we assume that each relay has a signal power equivalent to $P_i = P_r,\ \forall\, i = 1, 2, .., N$; hence, the optimization problem can be formulated as follows

$$\min_{P_s,P_r} \prod_{i=1}^{N}\left[1 - \frac{\Gamma\left(m_{si}, \alpha_i\gamma_o^{\frac{1}{n_{si}}}\right)\Gamma\left(m_{id}, \beta_i\gamma_o^{\frac{1}{n_{id}}}\right)}{\Gamma(m_{si})\Gamma(m_{id})}\right]$$

$$\text{subject to}\quad P_s + P_r \leq P_T \text{ and } \quad P_s, P_r \geq 0 \tag{2.30}$$

where $\bar{\gamma}_{si} = P_s\,\lambda_{si},\ \bar{\gamma}_{id} = P_r\lambda_{id}$. The convex problem above can be expressed as

$$\mathcal{L}(P_s, P_r, \xi) = \prod_{i=1}^{N}\left[1 - \frac{\Gamma\left(m_{si}, \alpha_i\gamma_o^{\frac{1}{n_{si}}}\right)\Gamma\left(m_{id}, \beta_i\gamma_o^{\frac{1}{n_{id}}}\right)}{\Gamma(m_{si})\Gamma(m_{id})}\right] + \xi(P_s + P_r - P_T) \tag{2.31}$$

where ξ is a Lagrange multiplier. Taking the derivative of (2.31) with respect to P_s and P_r and

setting both $\frac{\partial \mathcal{L}}{\partial P_s}$ and $\frac{\partial \mathcal{L}}{\partial P_r}$ to zero, we obtain

$$P_s \approx \sum_{i=1}^{N} \frac{P_{out}\mu_i \left(\alpha_i {\gamma_o}^{\frac{1}{n_{si}}}\right)^{m_{si}} e^{-\alpha_i {\gamma_o}^{\frac{1}{n_{si}}}}}{n_{si}\Gamma(m_{si})(1-\mu_i\omega_i)\xi} \tag{2.32}$$

$$P_r \approx \sum_{i=1}^{N} \frac{P_{out}\omega_i \left(\beta_i {\gamma_o}^{\frac{1}{n_{id}}}\right)^{m_{id}} e^{-\beta_i {\gamma_o}^{\frac{1}{n_{id}}}}}{n_{id}\Gamma(m_{id})(1-\mu_i\omega_i)\xi} \tag{2.33}$$

where

$\omega_i = \Gamma(m_{id}, \beta_i {\gamma_o}^{\frac{1}{n_{id}}})/\Gamma(m_{si})$, $\mu_i = \Gamma(m_{id}, \beta_i {\gamma_o}^{\frac{1}{n_{id}}})/\Gamma(m_{id})$. Replacing (2.33) into (2.32), and setting $P_r = P_T - P_s$, the approximate power allocation for P_s can be written in the following form

$$P_s \approx P_T \left[\frac{\sum_{i=1}^{N} \omega_i \eta_i \left(\beta_i {\gamma_o}^{\frac{1}{n_{id}}}\right)^{m_{id}} e^{-\beta_i {\gamma_o}^{\frac{1}{n_{id}}}}}{\sum_{i=1}^{N} \mu_i \theta_i \left(\alpha_i {\gamma_o}^{\frac{1}{n_{si}}}\right)^{m_{si}} e^{-\alpha_i {\gamma_o}^{\frac{1}{n_{si}}}}} + 1 \right]^{-1} \tag{2.34}$$

where

$$\eta_i = 1/n_{id}\Gamma(m_{id})(1-\omega_i\mu_i),\ \theta_i = 1/n_{si}\Gamma(m_{si})(1-\omega_i\mu_i).$$

Note that (2.34) is a transcendental function and it is challenging to find a closed-form for the source power. Thus, we calculate it numerically using a root-finding algorithm such as Bisection, Newton or successive numeric approximation methods. At this stage, given the total power constraint, the source and the selected relay power can be set as $P_s = \rho P_T$ and $P_r = (1-\rho)P_T$, respectively, where ρ is referred as the power allocation ratio ($\rho \in (0,1)$), which is calculated from (2.34) using the following successive approximation algorithm [86, section 14.1]

$$\rho^{(t+1)} \approx \left[\frac{\sum_{i=1}^{N} \omega_i \eta_i \left({X_{id}}^{(t)}\right)^{m_{id}} e^{-{X_{id}}^{(t)}}}{\sum_{i=1}^{N} \mu_i\, \theta_i \left({X_{si}}^{(t)}\right)^{m_{si}} e^{-{X_{si}}^{(t)}}} + 1 \right]^{-1} \tag{2.35}$$

where

$${X_{si}}^{(t)} = \frac{m_{si}}{\Omega_{si}} \left(\frac{\gamma_o}{\lambda_{si}\rho^{(t)}P_T}\right)^{\frac{1}{n_{si}}},\ {X_{id}}^{(t)} = \frac{m_{id}}{\Omega_{id}} \left(\frac{\gamma_o}{\lambda_{id}\left(1-\rho^{(t)}\right)P_T}\right)^{\frac{1}{n_{id}}}$$

As a result, the minimum outage probability can be expressed in terms of the total transmitted power P_T as

$$P_{out} \approx \prod_{i=1}^{N}\left[1 - \frac{\Gamma\left(m_{si}, \frac{m_{si}}{\Omega_{si}}\left(\frac{\gamma_o}{\lambda_{si}\rho\, P_T}\right)^{1/n_{si}}\right)}{\Gamma(m_{si})}\frac{\Gamma\left(m_{id}, \frac{m_{id}}{\Omega_{id}}\left(\frac{\gamma_o}{\lambda_{id}\,(1-\rho)P_T}\right)^{1/n_{id}}\right)}{\Gamma(m_{id})}\right] \tag{2.36}$$

Asymptotic Solution: a simple asymptotic solution for (2.34) can be found by using the fact that [13, eq.(8.356.2]

$$x^{\alpha}e^{-x} = \Gamma(\alpha+1, x) - \alpha\Gamma(\alpha, x)$$

and by noting that $\Gamma(\alpha+1, x) \leq \alpha\Gamma(\alpha)$, which is a tight bound for x sufficiently small. In this case, the optimization problem can be rewritten in a simple compact form as

$$P_s \approx P_T\left[\frac{\sum_{i=1}^{N}(m_{id}/n_{id})}{\sum_{i=1}^{N}(m_{si}/n_{si})} + 1\right]^{-1} \tag{2.37}$$

From (2.37), it can be seen that the power allocation for the source depends only on the fading severity parameters, regardless of the channel statistics $(\lambda_{si}, \lambda_{id})$.

2.4 Numerical Results

In this section, we present numerical and simulation results for the investigated S-DF relaying scheme. In particular, we evaluate the outage probability P_{out} given by (2.16), for $\gamma_o = 3$, and study the achievable diversity order (d), the average SER (2.25) for 16-PSK, and the average channel capacity (2.29). Furthermore, we analyze the outage probability with power allocation.

Fig.2-2 shows the approximate outage probability over cascaded Rayleigh fading channels ($n = 2, 3, 4, 5$) with different values of cooperating nodes N. From Fig.2-2, there is an excellent match between the analytical and simulation results. In addition, we observe that P_{out} for the S-DF relaying scheme degrades for larger (n) in comparison to double Rayleigh fading. Specifically, at $P_{out} = 0.02$ and $N = 3$, a performance loss of 4.65, 8.80, 12.50 dB is observed for $n = 3, 4,$ and 5, respectively. Moreover, it is noticed that increasing the number of cooperating nodes (N)

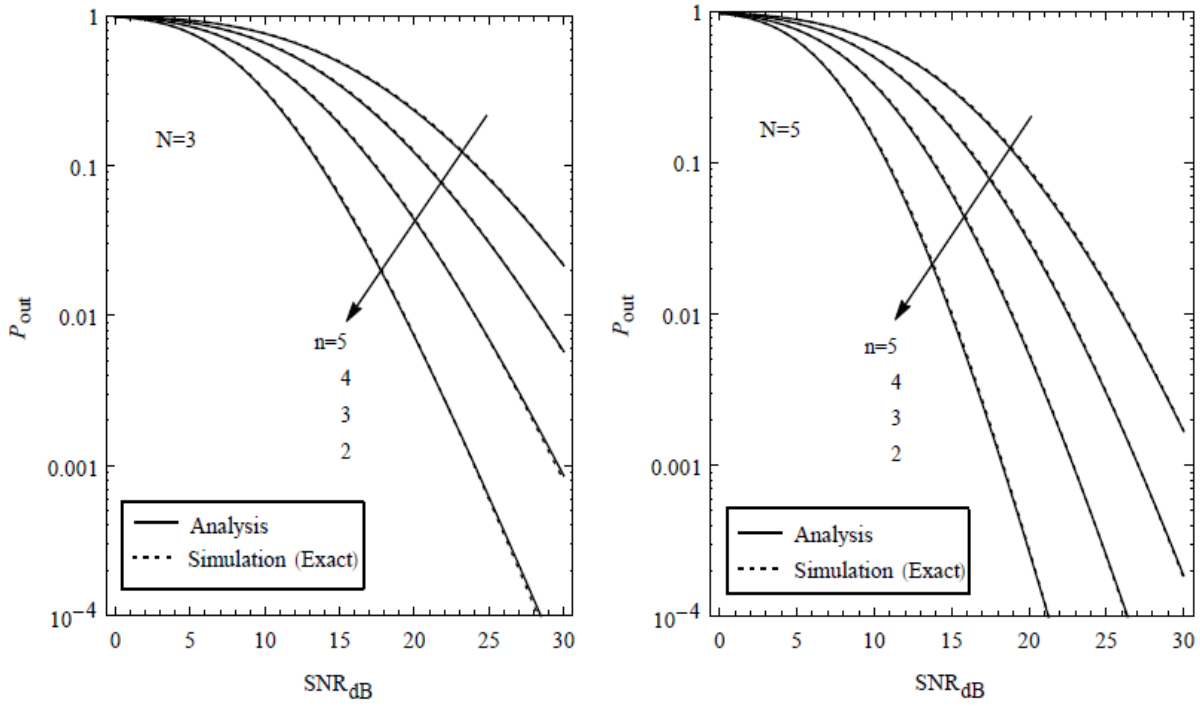

Fig.2-2. Outage probability for the S-DF relaying scheme over cascaded Rayleigh fading channels

improves the system performance for cascaded Rayleigh fading channels, in which the outage probability is minimized by increasing the number of cooperating partners.

Fig.2-3. depicts the diversity order over Rayleigh and cascaded Rayleigh fading channels, assuming $N = 2$ and 4. As it can be observed, the full diversity order for the Rayleigh fading channel model approaches N as SNR tends to infinity, while the diversity order for cascaded Rayleigh fading channels decreases linearly with increasing (n) to reach an asymptotic value equivalent to mN/n, confirming our analytical results.

Fig.2-4. shows the average SER for 16-PSK modulation type over cascaded Rayleigh fading channels, and compares the analytical results (i.e., (2.15)) with the proposed bound counterpart (2.23). Fig.2-4. demonstrates that the SER improves as n decreases, since the diversity gain ($d \approx mN/n$) increases as n decreases. Moreover, the slopes of the analytical SER performance curves match very well with the lower bound curves over all SNR values and the tightness is improved in the high SNR regime, which confirms that our proposed bound is tight. Moreover, the lower the value of n is, the tighter the proposed bound will be.

In Fig.2-5, the average channel capacity over cascaded Rayleigh distribution is investigated in the high SNR regime. We observe that the double Rayleigh channel outperforms the cascaded

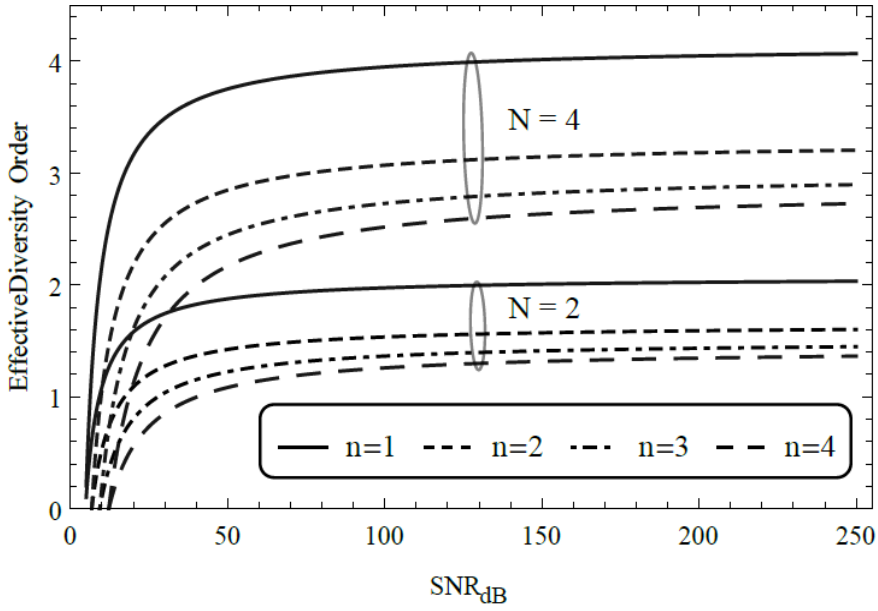

Fig.2-3. Effective diversity order for the S-DF relaying scheme over Rayleigh and cascaded Rayleigh fading channels.

Rayleigh fading channels due to the fact that the maximum data rate of communication over $n = 2$ can be attained with a smaller error probability compared to $n = 3, 4$, and 5. Additionally, there is a comparable decrease in channel capacity among n*Rayleigh fading channels. For instance, at $P/N_o = 15$ dB, the underlying scheme with double Rayleigh fading achieves about 3bps/Hz, whereas a power loss of 20, 25, 30 dB is observed for $n = 3, 4$, and 5 respectively to achieve the same capacity gain, so double Rayleigh fading channels save about four orders of magnitude of power compared to $n = 5$.

In Fig.2-6, we evaluate the impact of power allocation mode on the S-DF relaying scheme over cascaded Rayleigh fading channels. Two transmission modes are compared: the PA is our proposed mode under statistical CSI, and the equal power allocation (EPA) where the total transmitted power P_T is divided equally between the source and the selected relay ($P_s = P_r = P_T/2$). We assume that the channel quality between the selected relay and the destination is much better than that between the source and the selected relay (i.e, $\lambda_{sr} = 1$, $\lambda_{rd} = 10$). As observed from Fig.2-6, the PA mode has an advantage over the EPA mode by reducing the outage probability. This is mainly because approximation algorithm the PA mode devotes larger power to the weaker link to reduce the overall outage probability. In this case, the power allocation ratio $\rho = P_s/P_T$ is evaluated from (2.35) using the successive, which turns out to be, $\rho \approx 0.757,\ 0.629,\ 0.534$ and 0.462 for $n = 1, 2, 3$

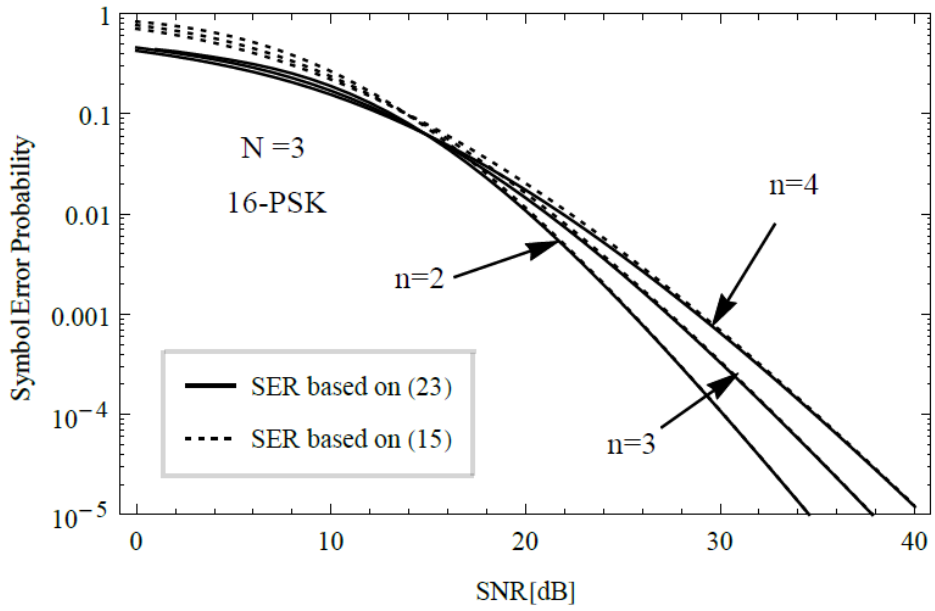

Fig.2-4. SER for the S-DF relaying scheme over cascaded Rayleigh fading channels

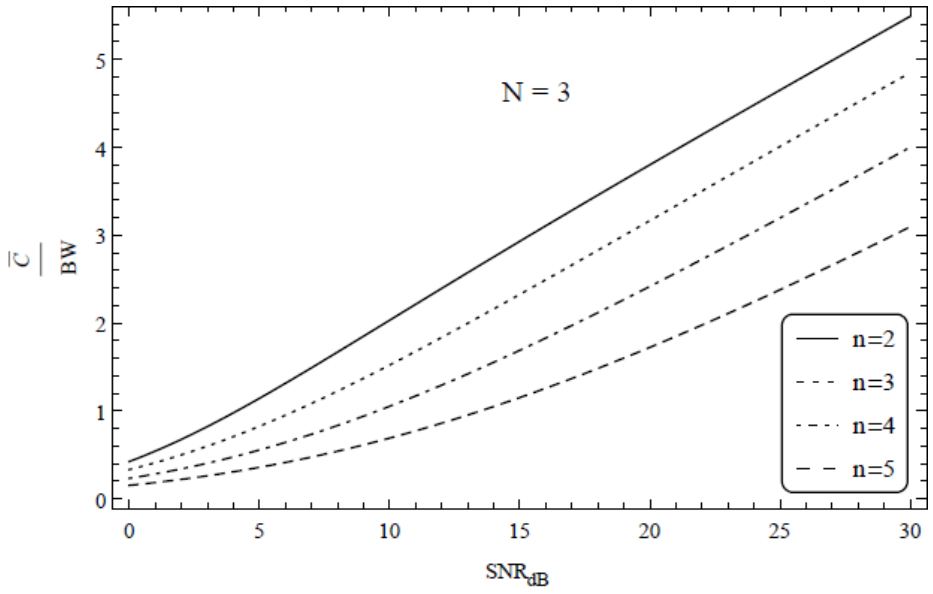

Fig.2-5. Average channel capacity for the S-DF relaying scheme over cascaded Rayleigh fading channels

and 4 respectively. It should be noted here that the power allocation ratio converges to 0.5 when n increases, which means that no optimization is required for power when $n \geq 4$. In this case, the EPA mode is used instead of the PA mode to achieve the minimum outage probability.

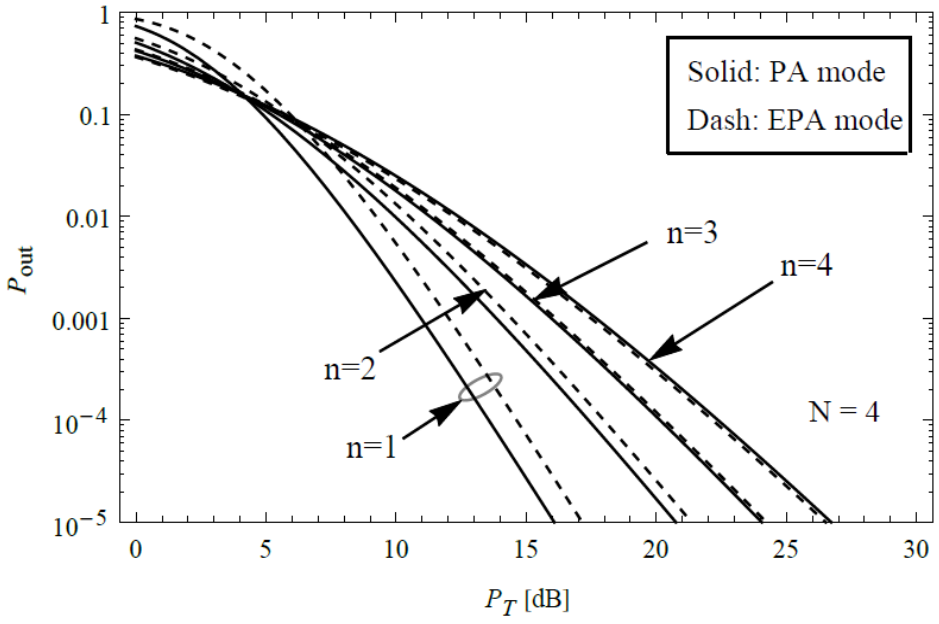

Fig.2-6. Effect of the PA and EPA modes on the outage performance of the S-DF relaying scheme over Rayleigh and cascaded Rayleigh fading

2.5 Conclusion

In this paper, we derived an end-to-end performance analysis of the selective-DF relaying scheme over cascaded Rayleigh fading channels. Specifically, we derived novel closed-form expressions for the outage probability, the symbol error probability, and the average channel capacity. Our analysis and numerical results have shown that the maximum achievable diversity order is $(\approx mN/n)$. Furthermore, our results confirm that transmit power allocation optimization is required for IVC systems when the cascading order $n < 4$.

CHAPTER 3

ARTICLE 2: AMPLIFY-AND-FORWARD RELAY SELECTION IN INTER-VEHICULAR COMMUNICATIONS SYSTEMS OVER CASCADED RAYLEIGH FADING CHANNELS

Yahia Alghorani and Samuel Pierre
yahia.alghorani@polymtl.ca; samuel.pierre@polymtl.ca
Mobile Computing and Networking Research Laboratory (LARIM)
Ecole Polytechnique de Montreal
Montreal, Quebec, H3C 3A7, Canada

Sami Muhaidat
sami.muhaidat@uwo.ca
Electrical and Computer Engineering Department
University of Western Ontario
London, Ontario, N6A 5B9, Canada

Naofal Al-Dhahir
aldhahir@utdallas.edu
Department of Electrical Engineering
University of Texas at Dallas
Richardson, TX 75083 USA

Submitted to IEEE Wireless Communications Letters, April 2015

Abstract

We investigate the performance of an amplify-and-forward dual-hop cooperative vehicular network with relay selection. We assume a generalized fading channel model, known as cascaded Rayleigh (*n**Rayleigh), which involves the product of *n* independent Rayleigh random variables. This channel model provides a realistic description of intervehicular communications, in contrast

to the conventional Rayleigh fading assumption, which is more suitable for cellular systems. We derive a closed-form expression for the end-to-end outage probability with best relay selection over identical and non-identical n*Rayleigh fading channels. In addition, we analyze the investigated symbol error rate for the scenario. Numerical results demonstrate that our best relay selection strategy achieves an asymptotic diversity order of (mN/n), where N is the number of relays and m is a cascaded Rayleigh fading parameter.

Index Terms: Cooperative diversity, intervehicular networks, outage performance, cascaded Rayleigh fading channels, relay selection.

3.1 Introduction

The design of intervehicular communications (IVC) systems is very challenging and existing solutions, for example, from cellular and ad-hoc networks may not be applicable, which is mainly due to the dynamic nature of wireless links and the involved mobility patterns. New research efforts at different levels are needed, including at the physical layer level, which is the aim of this Letter.

In IVC systems, both the transmitter and receiver are in motion and typically use the same antenna height, resulting in two or more independent Rayleigh fading processes, generated by independent groups of scatterers around the two mobile terminals [10]. A generalized channel model called n*Nakagami was proposed in [31], based on the product of n Nakagami-m random variables, which provided a realistic description for the IVC channel model.

To understand the full potential of cooperative diversity in IVC, an in-depth analysis of the system performance under a realistic channel model is required. Towards this end, unlike the earlier works in this area, we consider the *generalized* fading channel model, i.e., the "n*Rayleigh" model [28].

There have been some recent works on cooperative diversity in the context of IVC networks. However, all reported results have mainly focused on double-Rayleigh/Nakagami fading channels (i.e., $n = 2$). For example, in [16], the authors investigated a cooperative diversity system with relay selection over double Rayleigh fading channels. They demonstrated that the maximum achievable diversity order is equal to the number of relays. The authors in [36] studied the symbol error rate (SER) performance of a two-way relay network over cascaded Nakagami fading. The

results showed that the improvement in outage performance is diminished by increasing the cascading order (n).

To the best of our knowledge, cooperative IVC systems with relay selection over cascaded Rayleigh distribution (i. e, $n > 2$) have not been studied yet. Hence, it is the aim of this work to fill this research gap. Specifically, we derive approximate closed-form expressions for the outage probability over identical and non-identical *n**Rayleigh fading channels. Moreover, we derive a lower-bound expression for the moment generating function (MGF), which is used for computing the SER of *M*-ary phase shift keying (*M*-PSK) modulation type.

3.2 System Model

In this letter, we consider a dual-hop cooperative IVC system with multiple relays, in which a source (s), relays r_i $(i = 1, 2, \dots, N)$ and a destination (d) operate in half-duplex mode and are equipped with a single pair of transmit and receive antennas. For each time instant, only one vehicle acts as a source, while the other vehicles serve as relays that help forward the source's message to its destination node. All underlying channels between $s \to r_i$ and $r_i \to d$ links are modeled by a product of n independent circularly-symmetric complex Gaussian random variables, each of which can be defined as $h_{si} \triangleq \prod_{k=1}^{n} h_{si,k}$, $h_{id} \triangleq \prod_{k=1}^{n} h_{id,k}$ with zero mean and channel variance of (λ_{si}) and (λ_{id}) respectively, for $i = 1, 2, \dots, N$ and $k = 1, 2, \dots, n$. Therefore, $|h_{si}|$ and $|h_{id}|$ follow a cascaded Rayleigh distribution. In this system model, we assume that all underlying channels are quasi-static which can be justified for IVC scenarios in rush-hour traffic. We further assume that the additive white Gaussian noise (AWGN) at all relays and the destination node have zero mean and variance (N_o). Both links between $(s \to r_i)$ and $(r_i \to d)$ are subject to *n**Rayleigh fading and are represented by accurate approximations for the probability density function (PDF) of instantaneous SNR $(\gamma_{si}, \gamma_{id})$ given by [15] with the help of [14, eq.(2.3)]

$$f_{\gamma_{si}}(\gamma) \approx \frac{{\beta_{si}}^{m_{si}}}{n_{si}\Gamma(m_{si})}\gamma^{\alpha_{si}-1}\exp\left(-\beta_{si}\gamma^{\frac{1}{n_{si}}}\right), \quad \gamma \geq 0 \tag{3.1}$$

$$f_{\gamma_{id}}(\gamma) \approx \frac{{\beta_{id}}^{m_{id}}}{n_{id}\Gamma(m_{id})}\gamma^{\alpha_{id}-1}\exp\left(-\beta_{id}\gamma^{\frac{1}{n_{id}}}\right), \quad \gamma \geq 0 \tag{3.2}$$

where $\beta_{si} = 2\,m_{si}/(\,\Omega_{si}\bar{\gamma}_{si}^{\frac{1}{n_{si}}})$, $\beta_{id} = 2m_{id}/(\,\Omega_{id}\bar{\gamma}_{id}^{\frac{1}{n_{id}}})$, $\alpha_{si} = m_{si}/n_{si}$ and $\alpha_{id} = m_{id}/n_{id}$. The n*Rayleigh fading parameters $(m_{si}, m_{id}, \Omega_{si}, \Omega_{id})$ are given in [15], and the instantaneous SNRs of γ_{si} and γ_{id} are independent (but not necessarily identically distributed) random variables with means defined, respectively, as $\bar{\gamma}_{si} = \mathbf{E}(|h_{si}|^2)\,P/N_o$ and $\bar{\gamma}_{id} = \mathbf{E}(|h_{id}|^2)\,P/N_o$, where $\mathbf{E}(.)$ is the statistical expectation operator, and P is the transmitted signal power.

In our selection scheme, two transmission phases are implemented, assuming the amplify-and-forward (AF) protocol. In the first phase, the source sends its codeword $x(t)$ to the relays and the received signal can be expressed as $y_{si}(t) = h_{si}\sqrt{P}x(t) + w_i(t)$, where $w_i(t)$ is the AWGN at the relay node. In the second phase, only the selected relay with the maximum effective SNR is chosen to forward the amplified received signal $x_r(t)$ to the destination with a normalized channel gain $G = \sqrt{P/(P|h_{sr}|^2 + N_o)}$. In this case, the received signal at the destination node can be expressed as $y_{rd}(t) = h_{rd}\sqrt{P}x_r(t) + w_d(t)$, where $x_r(t) = Gy_{sr}(t)$ and $w_d(t)$ is the AWGN at the destination. Therefore, the effective end-to-end instantaneous SNR for the selected relay, can be written as [115]

$$\gamma_{AF} = \max_{i\in N} \frac{\gamma_{si}\,\gamma_{id}}{\gamma_{si}+\gamma_{id}} \tag{3.3}$$

Using the definition of the harmonic mean of two random variables, which is given as $\mu_H(X_1, X_2) = 2X_1X_2/(X_1 + X_2)$, (3.3) can be rewritten as

$$\gamma_{AF} = \max_{i\in N}\{\gamma_{ti}\} \tag{3.4}$$

where $\gamma_{ti} = \mu_H(\gamma_{si}, \gamma_{id})/2$, is the harmonic mean of two random variables. However, it is worthwhile to note that the derivation of the outage probability over n*Rayleigh fading which is based on (3.3) does not lend itself to a closed-form solution. Thus, to simplify the analysis, the instantaneous end-to-end SNR can be upper bounded as follows [88]

$$\gamma_{AF} \leq \gamma_{ub} = \max_{i\in N} \min\{\gamma_{si}\,, \gamma_{id}\} \tag{3.5}$$

It can be shown that the SNR upper-bound given by (3.5) is analytically tractable, and has been shown to be quite tight at medium-high SNR levels.

3.3 Derivation of PDF and CDF for the Harmonic SNR

To find the approximate PDF and the cumulative distribution function (CDF) of the harmonic SNR $\gamma_t = \gamma_{sr}\gamma_{rd}/(\gamma_{sr} + \gamma_{rd})$ when the average links SNR $(\gamma_{si}, \gamma_{id})$ are i.i.d random variables, we first introduce the following proposition:

Proposition: Suppose Y_1 and Y_2 are two i.i.d. gamma RVs, defined as $Y_1 = X_1^{\frac{1}{n}}$ and $Y_2 = X_2^{\frac{1}{n}}$ with parameters $n\alpha > 0$ and $\beta > 0$ (i.e., $Y_i \sim \mathcal{G}(n\alpha, \beta),\ i = 1, 2$ and $n \in \mathbb{N}^+$), the PDF and CDF of the harmonic mean of two gamma RVs, $Y = \mu_H(Y_1, Y_2)$, can be respectively expressed as

$$f_Y(y) = \frac{\sqrt{\pi}\beta^{n\alpha}}{\Gamma^2(n\alpha)}\left(\frac{y}{2}\right)^{n\alpha-1} e^{-2\beta y} U\left(\frac{1}{2} - n\alpha, 1 - n\alpha; 2\beta y\right) \tag{3.6}$$

and

$$F_Y(y) = \frac{\sqrt{\pi}\beta\ \ y}{2^{2(n\alpha-1)}\Gamma^2(n\alpha)} G_{2,3}^{2,1}\left(2\beta y \,\middle|\, \begin{matrix} 0, n\alpha - \frac{1}{2} \\ n\alpha - 1, 2n\alpha - 1, -1 \end{matrix}\right) \tag{3.7}$$

where $U(\cdot,\cdot;\cdot)$ is the confluent hypergeometric function defined in [80, eq. (13.2.5)], and $G_{p,q}^{m,n}(\cdot)$ is the Meijer-G function defined in [13, eq. (9.301)].

Proof: Following a procedure similar to that in [89], (3.6) and (3.7) can be proven.
Using (3.6) with the help of the fact that [13, eq. (7.621.6)],

$$\int_0^\infty t^{b-1} U(a, c; t)\, e^{-st} dt = \frac{\Gamma(b)\Gamma(b - c + 1)}{\Gamma(a + b - c + 1)} s^{-b} \times\ {}_2F_1(a, b; a + b - c + 1; 1 - s^{-1}) \tag{3.8}$$

where ${}_2F_1(.,.;.;.)$ is Gauss hypergeometric function defined in [80, eq. (15.1.1)], the *n*-th moment of Y can be evaluated as

$$\mathbf{E}(Y^n) = \frac{\sqrt{\pi}\ \beta^{n\alpha-1}\ \Gamma(n\alpha + n)\Gamma(2n\alpha + n)}{2^{n\alpha}\ \Gamma^2(n\alpha)\Gamma\left(n\alpha + n + \frac{1}{2}\right)} \tag{3.9}$$

Notice that the Gauss hypergeometric function of (3.8) reduces to one when the last argument is equal to zero. Using the transformation of variables $f_U(u) = 2f_Y(2y)$ and $F_U(u) = F_Y(2y)$, where

$U = \gamma^{1/n}$, and since the RV γ is a one-to-one continuous monotonically increasing function, from (6) and (7), with $\alpha = m/n$, and $\beta = 2\,m/(\,\Omega\bar{\gamma}^{1/n})$, the PDF and CDF of the harmonic SNR γ_t can easily be found with the help of [90, Sec. 5.1, Sec. 5.2], yielding

$$f_{\gamma_t}(\gamma) \approx \frac{2\sqrt{\pi}\left(\frac{m}{\Omega\bar{\gamma}^{\frac{1}{n}}}\right)^{m}}{n\Gamma^2(m)}\gamma^{\frac{m}{n}-1}e^{-4\frac{m}{\Omega}\left(\frac{\gamma}{\bar{\gamma}}\right)^{1/n}}U\left(\frac{1}{2}-m,1-m,4\frac{m}{\Omega}\left(\frac{\gamma}{\bar{\gamma}}\right)^{1/n}\right) \tag{3.10}$$

and

$$F_{\gamma_t}(\gamma) \approx \frac{\sqrt{\pi}\frac{m}{\Omega}(\gamma/\bar{\gamma})^{1/n}}{2^{2m-3}\Gamma^2(m)}G_{2,3}^{2,1}\left(4\frac{m}{\Omega}\left(\frac{\gamma}{\bar{\gamma}}\right)^{1/n}\middle|\begin{matrix}0, m-\frac{1}{2}\\ m-1, 2m-1, -1\end{matrix}\right) \tag{3.11}$$

where $\bar{\gamma} = \mathbf{E}(|h|^2)\,P/N_o$, $\lambda = \mathbf{E}(|h|^2)$, $\mathrm{SNR} = P/N_o$. Using (3.9) with $\alpha = m/n$ and $\beta = 2\,m/(\,\Omega\bar{\gamma}^{1/n})$, in addition to the fact that $\Gamma(2\alpha) = 2^{2\alpha-\frac{1}{2}}\Gamma(\alpha)\Gamma\left(\alpha+\frac{1}{2}\right)$ [80, eq. (6.1.18)], and [90, Sec.5.3], we obtain the approximate average SNR $\bar{\gamma}_t$ as

$$\bar{\gamma}_t \approx \frac{2^{2m-1}(m/\Omega)^{m-1}(m)_n(2m)_n}{\left(m+\frac{1}{2}\right)_n}\,\bar{\gamma}^{\frac{1-m}{n}} \tag{3.12}$$

where $(x)_n = \Gamma(x+n)/\Gamma(x)$

3.4 Performance Analysis

3.4.1 Outage Probability

The outage probability of $P_{out} \triangleq F_{\gamma_{AF}}(\gamma_o)$ channel is defined as the probability that the maximum SNR (γ_{ti}) falls below a certain threshold $(\gamma_o = 2^{2R}-1)$, namely

$$P_{out} = \Pr\left(\max_{i\in N}\{\gamma_{ti}\} \le \gamma_o\right) \tag{3.13}$$

Therefore, in case of i.i.d random variables (i.e., $\gamma_{ti} = \gamma_t$), the approximate expression for the outage probability can be obtained using (3.11) as

$$P_{out} = \left[F_{\gamma_t}(\gamma_o)\right]^N \tag{3.14}$$

In addition, at high SNR levels (i.e., when $\bar{\gamma} \gg 0$), we can apply (3.10) instead of (3.11) to simplify the analysis of the maximum diversity order (d) achievable over cascaded Rayleigh fading channels, using the facts that [80, eq. (13.5.12)]

$$U(a,b,x) = \frac{\Gamma(1-b)}{\Gamma(1+a-b)} + \mathcal{O}(|x|), \qquad |x| \to 0$$

and $\int_0^u x^{v-1} \exp(-\mu x)\, dx = \mu^{-v}\gamma(v,\mu u)$ [13, eq.(3.381.1)],where $\gamma(\alpha,x) = \int_0^x e^{-t}t^{\alpha-1}\, dt$ is defined as the lower incomplete gamma function [9]. This leads us to rewrite the outage probability in an asymptotic form as

$$P_{out} \approx \left[\frac{1}{2^{2m-1}}\left(\frac{\gamma\left(m, 4\frac{m}{\Omega}\left(\frac{\gamma_o}{\bar{\gamma}}\right)^{1/n}\right)}{\Gamma(m)}\right)\right]^N \tag{3.15}$$

As a result, we rewrite (3.15) in the asymptotic form based-on the facts [80, eq.(6.5.12) and (13.5.5)], as follows

$$P_{out} \approx \left(\frac{2^{2m-1}(8\,m/\Omega)^m}{m\,\Gamma(m)\lambda^{\frac{m}{n}}}\right)^N \left(\frac{\gamma_o}{\mathrm{SNR}}\right)^{\frac{mN}{n}} + \mathcal{O}\left(\left(\frac{\gamma_o}{\mathrm{SNR}}\right)^{\frac{mN}{n}+1}\right) \tag{3.16}$$

Now, it can be deduced from (3.16) that the maximum achievable diversity order for the cascaded Rayleigh distribution is $d \approx mN/n$.

For the case of i.n.i.d random variables, we use (3.5) to derive an approximate outage probability expression as follows

$$P_{out} = \Pr\left(\max_{i\in N}\{\min\{\gamma_{si}, \gamma_{id}\} \le \gamma_o\right)$$

$$= \prod_{i=1}^{N} [1 - \Pr(\gamma_{si} > \gamma_o) \Pr(\gamma_{id} > \gamma_o)]$$

Finally, the approximate outage probability of the selective AF-relaying scheme can be expressed as

$$P_{out} \approx \prod_{i=1}^{N} \left[1 - \Gamma\left(m_{si}, \frac{m_{si}}{\Omega_{si}} \left(\frac{\gamma_o}{\lambda_{si} \mathrm{SNR}} \right)^{1/n_{si}} \right) \Gamma\left(m_{id}, \frac{m_{id}}{\Omega_{id}} \left(\frac{\gamma_o}{\lambda_{id} \mathrm{SNR}} \right)^{1/n_{id}} \right) / \left(\Gamma(m_{si}) \Gamma(m_{id}) \right) \right] \quad (3.17)$$

where $\lambda_{si} = \mathbf{E}(|h_{si}|^2), \lambda_{id} = \mathbf{E}(|h_{id}|^2)$.

3.4.2 Average Symbol Error Rate

In this subsection, we derive the average SER expression for *M*-PSK modulation using the MGF approach. Due to (3.5), the average SER expression is indeed a lower bound on the average SER given by [14]

$$P(e) = \frac{1}{\pi} \int_0^{\pi - \frac{\pi}{\mathrm{M}}} \Phi_{\gamma_{AF}} \left(\frac{\sin^2(\pi/M)}{\sin^2 \theta} \right) d\theta \quad (3.18)$$

where $\Phi_{\gamma_{AF}}(\cdot)$ is the MGF of the effective SNR received by the where $\Phi_{\gamma_{AF}}(\cdot)$ is the MGF of the effective SNR received by the destination, given by $\Phi_{\gamma_{AF}}(s) = s\mathcal{L}\{P_{out}|_{\gamma_o = \gamma}; s\}$, where $\mathcal{L}(.;.)$ denotes the Laplace Transform. To the best of our knowledge, finding a closed-form expression for the SER-based (3.14) is highly complex due to the Meijer G-function. For this reason, we invoke (3.17) to evaluate the SER over i.i.d *n**Rayleigh random variables. Since the fading severity parameter m in (3.17) is real-valued, it is challenging to find a closed-form expression for the MGF of γ_{AF} with a finite-sum representation. Therefore, for simplicity we use the bounds for the incomplete gamma function given in [84, eq.(4.1)] and the fact that $\gamma(\alpha, x) + \Gamma(\alpha, x) = \Gamma(\alpha)$, to approximate (3.17) as

$$P_{out} \approx \left[1 - \left(1 - \frac{\beta^m {\gamma_o}^{\alpha}}{m\Gamma(m)} e^{-\frac{m}{m+1} \beta {\gamma_o}^{\frac{1}{n}}} \right)^2 \right]^N \quad (3.19)$$

Now, using the fact that $e^{-x} = G_{0,1}^{1,0}\left(x\middle|\begin{matrix}-\\0\end{matrix}\right)$, $\forall x$ and the useful identity defined in [85, eq.(07.34.21.0088.01)], the MGF lower-bound can be derived as

$$\Phi_{\gamma_{AF}}(s) \approx \sum_{i=0}^{N}(-1)^i\binom{N}{i}\left(\frac{\beta^m}{m\Gamma(m)}\right)^{i+N}\frac{2^{N-i}\sqrt{n}s^{-\alpha(i+N)}}{(2\pi)^{\frac{n-1}{2}}}$$

$$\times G_{1,n}^{n,1}\left(\left(\frac{m(i+N)\beta}{n(m+1)}\right)^n s^{-1}\middle|\begin{matrix}-\alpha(i+N)\\0,\dots,\frac{n-1}{n}\end{matrix}\right) \tag{3.20}$$

Substituting (3.20) into (3.18), and replacing $\theta = \pi/2$, we can bound the average SER as $P(e) \leq \frac{M-1}{M}\Phi_{\gamma_{AF}}(\sin^2(\pi/M))$.

Asymptotic Analysis: To gain further insight into the performance over cascaded Rayleigh fading channels, we present an asymptotic analysis for the symbol error rate which provides the achievable diversity order of the underlying scheme. Thus, in the high-SNR regime (i.e., $\bar{\gamma} \gg 0$), we apply the zeroth-order Taylor approximation to (3.19) (where $e^{-x} \approx 1$ for x sufficiently small), and after some algebraic manipulations, the SER of binary phase shift keying (BPSK) modulation can be obtained in a simple compact form as

$$P(e) \leq 2^{N-1}\left(\frac{\left(m/\Omega\bar{\gamma}^{\frac{1}{n}}\right)^m}{m\Gamma(m)}\right)^N\Gamma\left(1+\frac{mN}{n}\right) \tag{3.21}$$

Notice that the maximum diversity order can also be deduced from (3.21) as $d = mN/n$.

3.5 Numerical Results

In this section, we present numerical results for the approximate outage probability P_{out} with $\gamma_o = 3$, for the selective AF-relaying scheme over *n**Rayleigh fading channels.

Fig.3-1. shows the approximate outage probability for the selective AF-relaying scheme based on (3.3) and (3.5) over Rayleigh ($n = 1$) and cascaded Rayleigh fading channels ($n = 2, 3, 4$) at a fixed number of cooperating nodes ($N = 4$). It is clear from Fig.3-1 that the classical Rayleigh fading channel outperforms the cascaded fading channel model, confirming our earlier observations that the diversity order decreases when increasing the fading severity parameter (n).

It can also be observed from Fig.3-1 that the approximate outage probability based on (3.5) is tight for small n values in the high-SNR regime, although it degrades as n increases. Based on these observations, it is important to take into account the dynamic range of the measurement devices for detecting such severe fading channels. For example, when the outage probability based on (3.3) is assumed at $P_{out} = 10^{-3}$, the required minimum SNR levels for receiving undistorted signal are 12.30, 16.67, 20.36, and 23.77 dB for $n = 1, 2, 3, 4$, respectively. A radio receiver with limited dynamic range will lead to amplitude distortion. Therefore, cooperative diversity systems can play a major role in enhancing the dynamic range of the measurement devices.

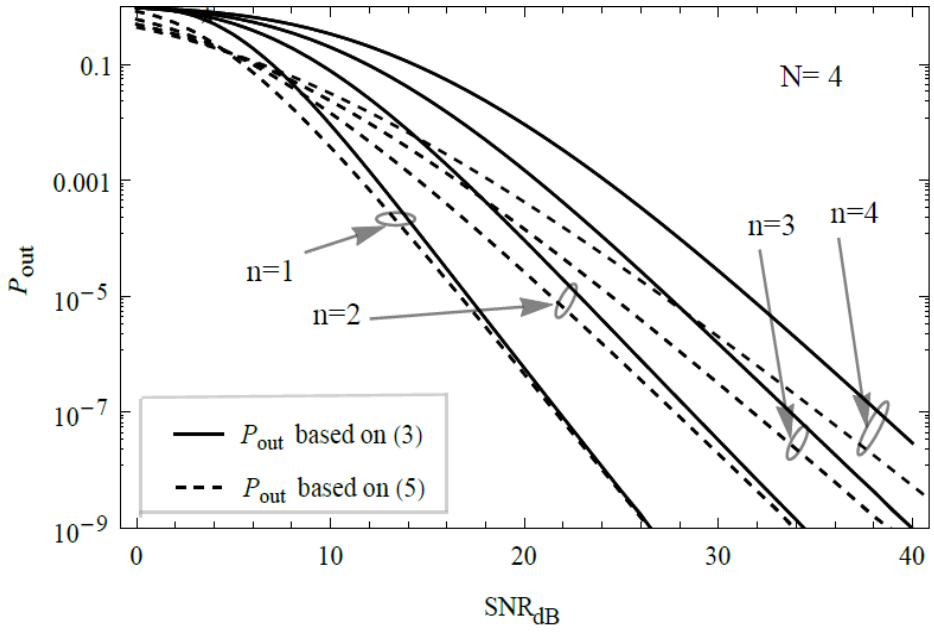

Fig.3-1. Outage probability of the selective AF-relaying scheme over Rayleigh and cascaded Rayleigh fading channels.

Fig.3-2 illustrates the SER performance of (3.17) and (3.19) with quadrature phase shift keying (QPSK) modulation. It can be clearly seen that the performance of the proposed bound in (3.19) converges to that of (3.17), over all SNR values and the tightness is improved in the high-SNR regime. Further, it can be deduced from Fig.3-2 that the diversity order of the considered scheme, i.e., $d \approx mN/n$ is improved when the fading severity parameter n is reduced. In addition, the lower the value of n is, the tighter the proposed bound will be.

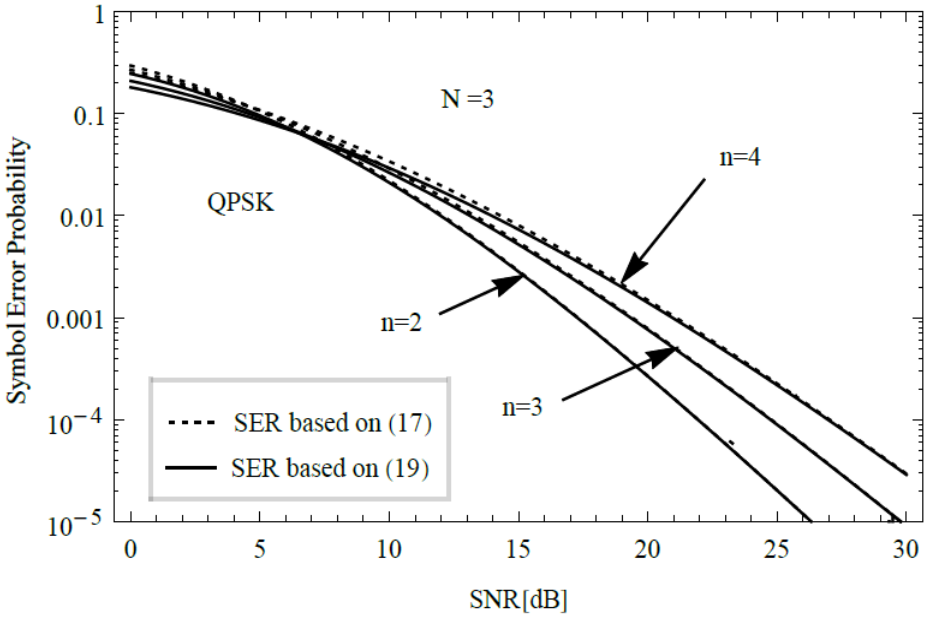

Fig.3-2. SER for the selective AF-relaying scheme over cascaded Rayleigh fading channels.

3.6 Conclusion

We derived approximate closed-form expressions for the PDF, CDF, and MGF for the selective-AF relaying scheme over *n**Rayleigh fading channels. The outage probability and the symbol error rate have been analyzed. Numerical results show that the diversity order is inversely proportional to n, which is considered a valuable guidelines for engineers working on the design of the measurement devices for inter-vehicular cooperative transmission systems over cascaded Rayleigh fading channels. For instance, the dynamic range of the received signal affected by cascaded Rayleigh fading channels can calibrate the performance characteristics of the measurement device. The higher the dynamic range of the measurement device is, the better its achievable performance will be.

CHAPTER 4

ARTICLE 3: ON THE PERFORMANCE OF MULTIHOP INTER-VEHICULAR COMMUNICATIONS SYSTEMS OVER N*RAYLEIGH FADING CHANNELS

Yahia Alghorani and Samuel Pierre
yahia.alghorani@polymtl.ca; samuel.pierre@polymtl.ca
Mobile Computing and Networking Research Laboratory (LARIM)
Ecole Polytechnique de Montreal
Montreal, Quebec, H3C 3A7, Canada

Sami Muhaidat
sami.muhaidat@uwo.ca
Electrical and Computer Engineering Department
University of Western Ontario
London, Ontario, N6A 5B9, Canada

Naofal Al-Dhahir
aldhahir@utdallas.edu
Department of Electrical Engineering
University of Texas at Dallas
Richardson, TX 75083 USA

Submitted to IEEE Wireless Communications Letters, June 2015

Abstract

We investigate the performance of multihop-intervehicular communication systems with regenerative and nonregenerative relay. We consider the so-called "*n**Rayleigh distribution" as an adequate multipath fading channel model for vehicle-to-vehicle communication scenarios. We derive a novel approximation for the outage probability of maximum ratio combining diversity

reception. In addition, we analyze the amount of fading and optimize the power allocation for the investigated scheme. Numerical results show that regenerative systems are more efficient than nonregenerative systems when the cascading order ($\boldsymbol{n}$) is low, and they have similar performance when $\boldsymbol{n}$ is high.

Index Terms: Multihop, *n**Rayleigh fading, MRC, diversity, intervehicular communications.

4.1 Introduction

Multihop transmission is advantageous when the distance between the source and destination is large, as it can be used to extend the coverage without using large transmit power [91, 92].

In intervehicular communication (IVC) systems, both the transmitter and receiver are in motion and typically use the same antenna height, resulting in two or more independent Rayleigh fading processes, generated by independent groups of scatterers around the two mobile terminals [10]. Such kind of keyhole propagation scenarios is possible when two rings of scatterers separated by a large distance and all propagation paths travel through the same narrow pipe called ‘‘*n**Rayleigh fading channels’’[12]. A special case of this fading model was studied in [113] when double Rayleigh fading is considered (i.e., $n = 2$). The multiple-input multiple-output (MIMO) case was also discussed in [116]. In [28], experimental results in different vehicular communication environments have shown that in vehicular networks, several small-scale fading processes are multiplied together, leading to a worse-than Rayleigh fading.

There have been some recent studies that have investigated dual hop IVC systems with relay selection strategy, e.g., [16, 117]. However, all results have been reported over double-Rayleigh/Nakagami fading channels. To the best of the authors’ knowledge, multihop systems with maximum ratio combining (MRC) schemes over *n**Rayleigh fading channels (i. e, $n \geq 2$) have not been analyzed yet. Therefore, it is the aim of this work to fill this research gap and investigate the performance of multihop-IVC systems with MRC diversity reception under *n**Rayleigh distribution.

4.2 System Model

We consider a *N*-hop intervehicular communications system where the source (s) transmits information to its destination (d) through intermediate nodes r_i ($i = 1, 2, \ldots, N-1$), acting as

regenerative or nonregenerative relays. All underlying N channels/hops are modeled as a product of n independent circularly-symmetric complex Gaussian random variables, each of which can be defined as $h_i \triangleq \prod_{j=1}^{n} h_{i,j}$ with zero mean and channel variance λ_i. Thus, $|h_i|$ follows the n*Rayleigh distribution. We assume that the received signal undergoes slow fading (i.e., the symbol period of the received signal is smaller than the coherence time of the channel), which can be justified for rush-hour traffic. We further assume that the additive white Gaussian noise (AWGN) random processes at all relays and the destination node have zero mean and variance (N_o). In this case, the instantaneous signal-to-noise ratio (SNR) of the ith hop is given by $\gamma_i = |h_i|^2 P/N_o$, where P is the transmitted signal power. An accurate approximation for the probability density function (PDF) of the instantaneous SNR γ_i is given by [15] with the help of [14, eq.(2.3)]

$$f_{\gamma_i}(\gamma) \approx \frac{{b_i}^{m_i}\gamma^{a_i-1}}{n_i\Gamma(m_i)} \exp\left(-b_i\gamma^{\frac{1}{n_i}}\right), \quad \gamma \geq 0 \quad . \tag{4.1}$$

where $\Gamma(.)$ represents the Gamma function, defined in [13, eq.(8.310.1)], $a_i = \frac{m_i}{n_i}$, and $b_i = 2\,m_i/\Omega_i{\bar{\gamma}_i}^{1/n_i}$ where $\bar{\gamma}_i = \lambda_i P/N_o$ is the average SNR of the i-th hop, $\lambda_i = \mathbf{E}(|h_i|^2)$ with $\mathbf{E}(.)$ denoting expectation. The fading severity parameters (m_i, Ω_i) are positive real numbers given by [15]

$$m_i = 0.6102n_i + 0.4263, \;\; \Omega_i = 0.8808{n_i}^{-0.9661} + 1.12$$

It is important to note that the novel approximation for the PDF in (1) was examined in [15], by comparing it to the exact PDF derived in [92, eq.(8)] and showing that the new approximation has high accuracy in most cases considered. Furthermore, the approximate PDF is easy to calculate and to manipulate compared to the exact PDF.

Assume that each node in the considered multihop scheme is equipped with L diversity branches, then the total SNR at the output of the MRC combiner is given by $\gamma_{ti} = \sum_{l=1}^{L}\gamma_{i,l}$. Normalizing (4.1) by the PDF of the SNR at the MRC output with Nakagami fading [92, eq.(7)] and replacing the factor m_i/Ω_i by $2Lm_i/\Omega_i$, and $\bar{\gamma}_i$ by $L\bar{\gamma}_i$, the approximate PDF of the combined SNR γ_{ti} for the ith hop over independent and identically distributed (i.i.d) n*Rayleigh fading random variables, can be derived as

$$f_{\gamma_{ti}}(\gamma_t) \approx \frac{{\beta_i}^{Lm_i}{\gamma_t}^{\alpha_i-1}}{n_i\Gamma(Lm_i)} \exp\left(-\beta_i{\gamma_t}^{\frac{1}{n_i}}\right). \tag{4.2}$$

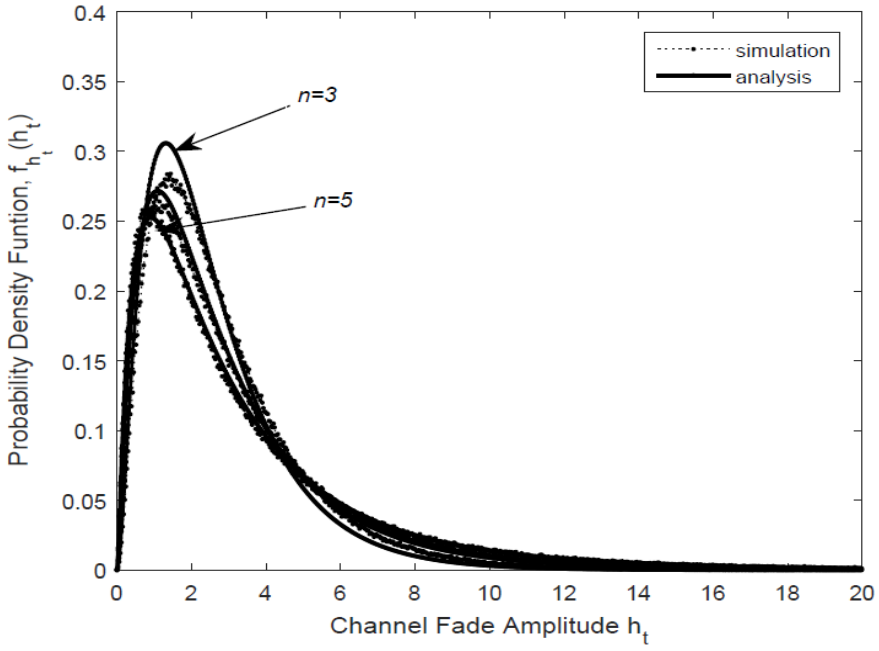

Fig. 4-1. Comparison between analytical results and Monte-Carlo simulation for the PDF formulated by (4.3) $(n = 3; m = 2.256, \Omega = 1.424)$, $(n = 4; m = 2.87, \Omega = 1.351)$, $(n = 5; m = 3.477, \Omega = 1.306)$, $\sigma^2 = 1, L = 2$ and 10^6 iterations.

where $\alpha_i = Lm_i/n_i$ and $\beta_i = 2Lm_i/\Omega_i(L\bar{\gamma}_i)^{1/n_i}$. However, eq.(4.2) is novel and has not been derived yet for the MRC scheme with *n**Rayleigh fading. In addition, by introducing a change of variables in the expression for the PDF $f_{\gamma_{ti}}(\gamma_t)$ of γ_{ti}, $f_{\gamma_{ti}}(\gamma_t) = f_{h_t}(\sqrt{2^n{\sigma_i}^2\gamma_t/\bar{\gamma}_i})/2\sqrt{\gamma_t\bar{\gamma}_i/2^n{\sigma_i}^2}$, the channel fading amplitude h_t is distributed according to

$$f_{h_{ti}}(h_t) \approx \frac{2\left(\frac{2Lm_i}{\Omega_i}\right)^{Lm_i} {h_t}^{2\alpha_i-1}}{n_i\Gamma(Lm_i)(L{\sigma_i}^2)^{\alpha_i}} \exp\left(-\frac{2Lm_i}{\Omega_i}\left(\frac{h_t}{L\sigma_i}\right)^{\frac{2}{n_i}}\right). \tag{4.3}$$

For a double check, the PDF in (4.3) is validated by Monte-Carlo simulation, as observed in Fig. 4-1, the approximate PDF has high accuracy as the cascading order *n* increases. The larger the value of *n* is, the higher accuracy will be [15].

For nonregenerative relaying that is employed in analog systems, the relay amplifies the incoming signal and forwards it to the next relay without decoding. In this case, the end-to-end SNR, γ_{eq}, at the destination can be upper-bounded by [91]

$$\gamma_{eq} = \left(\sum_{i=1}^{N} \frac{1}{\gamma_{ti}} \right)^{-1} \quad . \tag{4.4}$$

Since (4.4) is related to the harmonic mean of individual links SNRs, γ_{ti}, we can use the following inequality proposed by [92]

$$\gamma_{eq} \leq \frac{1}{N} \prod_{i=1}^{N} {\gamma_{ti}}^{\frac{1}{N}} \quad . \tag{4.5}$$

From (4.5), the *k*th moment of γ_{eq} over identical fading severity parameters can be evaluated with the help of [13, eq.(3.326.2)], as

$$\mathbf{E}\left(\gamma_{eq}^{k}\right) \leq \frac{N^{-k}}{\prod_{i=1}^{N} \beta_i^{\frac{nk}{N}}} \left[\frac{\Gamma\left(\frac{nk}{N} + Lm\right)}{\Gamma(Lm)} \right]^{N} \quad . \tag{4.6}$$

where $\beta_i = 2Lm/\Omega(L\bar{\gamma}_i)^{1/n}$. By using the *inverse Mellin transform* of $\mathbf{E}\left(\gamma_{eq}^{k}\right)$, defined by the contour integral $f_X(x) = \int_{\mathcal{L}} \frac{1}{j2\pi} \mathbf{E}(X^k) x^{-(k+1)} dk$ [13, Sec.17.41] and with the help of the Meijer's G-function identity in [84, eq.(07.34.02.0001.01)], the upper-bound PDF and the cumulative density function (CDF) of the end-to-end SNR can be expressed as

$$f_{\gamma_{eq}}(\gamma_t) \leq \frac{\gamma_t^{-1} \, G_{0,N}^{N,0}\left((N\gamma_t)^{\frac{N}{n}} \prod_{i=1}^{N} \beta_i \,\middle|\, \begin{matrix} - \\ Lm, \ldots, Lm \end{matrix} \right)}{\Gamma^N(Lm)} \tag{4.7}$$

and

$$F_{\gamma_{eq}}(\gamma_t) \leq \frac{G_{1,N+1}^{N,1}\left((N\gamma_t)^{\frac{N}{n}} \prod_{i=1}^{N} \beta_i \,\middle|\, \begin{matrix} 1 \\ Lm, \ldots, Lm, 0 \end{matrix} \right)}{\Gamma^N(Lm)} \quad . \tag{4.8}$$

respectively, where $G_{p,q}^{m,n}(.)$ is the Meijer's G-function defined in [13, eq.(9.301)]. Note that the inverse Mellin transform approach has the advantage of simplicity in the derivation of both (4.7) and (4.8) rather than using the moment generating function (MGF) approach as in [92].

Special cases: For $N = 1$ with the help of [84, eq.(07.34.03.0228.01)], (4.7) simplifies to (4.2). In addition, for $N = 2$ with the help of [84, eq.(07.34.03.0605.01)], (4.7) reduces to the following case of dual-hop transmission.

$$f_{\gamma_{eq}}(\gamma_t) \leq \frac{2\gamma_t^{-1}\left((2\gamma_t)^{\frac{2}{n}}\prod_{i=1}^{2}\beta_i\right)^{Lm} K_0\left(2(2\gamma_t)^{\frac{2}{n}}\prod_{i=1}^{2}\beta_i\right)}{\Gamma^2(Lm)} \ . \tag{4.9}$$

where $K_0(\cdot)$ is the zeroth-order modified Bessel function of the second kind defined in [13, eq.(9.6.21)].

For regenerative relaying that is employed in digital systems, the relay decodes the received signal and then forwards it to the next hop [91]. In this case, the underlying scheme takes a decision per hop and the equivalent SNR is $\gamma_{eq} = \min\{\gamma_{t1}, \dots, \gamma_{tN}\}$, which leads to derive the approximate CDF of γ_{eq} as follows

$$\begin{aligned} F_{\gamma_{eq}}(\gamma_t) &= \Pr\left(\min_{i\in N}\{\gamma_{ti}\} \leq \gamma_t\right) \\ &= 1 - \Pr(\gamma_{t1} > \gamma_t, \gamma_{t2} > \gamma_t, \dots, \gamma_{tN} > \gamma_t\ ) \end{aligned} \tag{4.10}$$

Using the fact defined in [12, eq.(3.381.1)], (4.10) can be expressed as

$$F_{\gamma_{eq}}(\gamma_t) \approx 1 - \prod_{i=1}^{N}\frac{\Gamma\left(Lm_i,\ \beta_i\gamma_t^{\frac{1}{n}}\right)}{\Gamma(Lm_i)} \ . \tag{4.11}$$

where $\Gamma(.,.)$ represents the upper incomplete gamma function, defined by $\Gamma(\alpha, x) = \int_x^\infty e^{-t}t^{\alpha-1}\,dt$ [13].

4.3 Performance Analysis

4.3.1 Outage Probability

The outage probability of a communication channel can be defined as the probability that the end-to-end SNR γ_{eq} falls below a certain threshold γ_{th}, namely

$$P_{out} = \Pr\left(\gamma_{eq} \leq \gamma_{\text{th}}\right) = F_{\gamma_{eq}}(\gamma_{\text{th}}) \ . \tag{4.12}$$

Using (4.8) and (4.11), lower-bounds for the outage probability can be derived for nonregenerative and regenerative systems respectively. Furthermore, using (4.8) and the asymptotic expression for

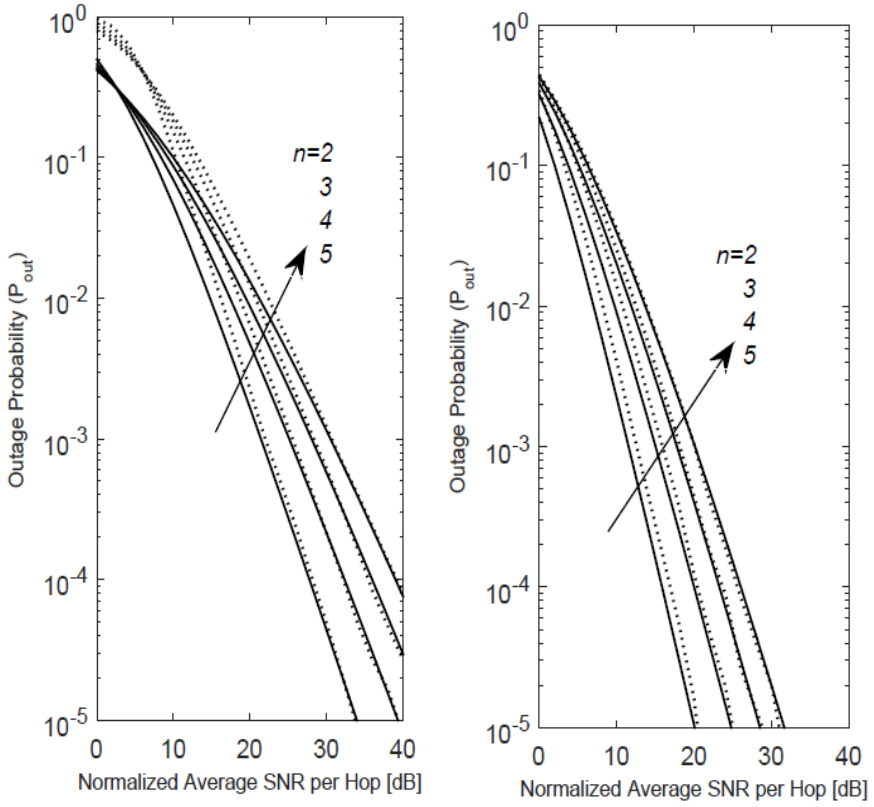

Fig. 4-2. Comparison between analytical results and Monte-Carlo simulation for the outage probability lower-bounds of regenerative and nonregenerative systems with MRC diversity reception over *n**Rayleigh fading channels (Solid lines: analysis, dotted lines: simulation). Left: the left tails of the outage probability of nonregenerative systems ($N = 4, L = 2$). Right: the right tails of the outage probability of regenerative systems ($N = 6, L = 3$).

the Meijer's G-function presented in [84, eq. (07.34.06.0006.01)], we can derive an approximate expression for the outage probability of nonregenerative systems in the high-SNR regime (i.e., when $\bar{\gamma}_i \to \infty$).

On the other hand, assuming that the instantaneous SNRs for all hops are i.i.d random variables (i.e., $\bar{\gamma}_i = \bar{\gamma}$) in (11), we can derive a simple lower-bound expression for the outage probability of regenerative systems in the high-SNR regime using the fact that $\Gamma(\alpha, x) = \Gamma(\alpha) - \sum_{n=0}^{\infty} \frac{(-1)^n x^{\alpha+n}}{n!(\alpha+n)}$ [13], which yields $\Gamma(\alpha, x) = \Gamma(\alpha) - x^{\alpha}/\alpha$ when $x \to 0$, as

$$P_{out} \approx \frac{N\left(\beta \gamma_t^{\frac{1}{n}}\right)^{Lm}}{Lm\Gamma(Lm)} \quad . \tag{4.13}$$

From (4.13), it is noted that the end-to-end outage probability increases as a number of hops increases and it significantly decreases when diversity combining schemes are employed. Fig. 4-2

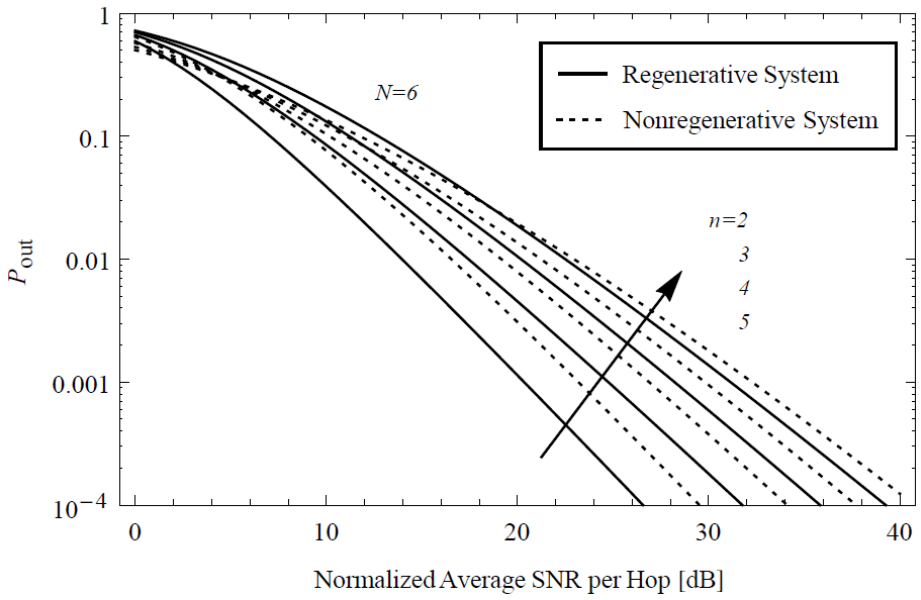

Fig. 4-3. End-to-end outage probability of regenerative and nonregenerative systems with MRC diversity reception over *n**Rayleigh fading channels ($L = 2$).

shows the outage probability achieved by both schemes, which are validated by Monte-Carlo simulation. As clearly observed from Fig. 4-2, lower-bounds for the outage probability-based (4.8) and (4.11) converge to simulation results in the high SNR regime. Additionally, the larger the value of *n* is, the tighter the bounds are obtained.

Fig. 4-3 compares the outage probability of a regenerative system with that of a nonregenerative system over *n**Rayleigh fading channels. It is clear that the regeneration improves the outage performance in the low and high-SNR regimes, and the performance difference between two systems starts decreasing gradually as the cascading order n increases. This means that the decoding error probability for regenerative systems increases as the fading severity parameter n increases. In this case, nonregenerative systems with diversity reception enhance the performance without increasing the complexity of system design.

4.3.2 Amount of Fading

The end-to-end amount of fading (AF) is defined as the ratio of variance to the square average SNR [14].

$$\mathrm{AF} = \frac{\mathrm{var}\left(\gamma_{eq}^2\right)}{\left(\mathbf{E}[\gamma_{eq}]\right)^2}$$

where $\mathrm{var}(.)$ denotes variance. Using (4.6), the following AF lower-bound can be derived

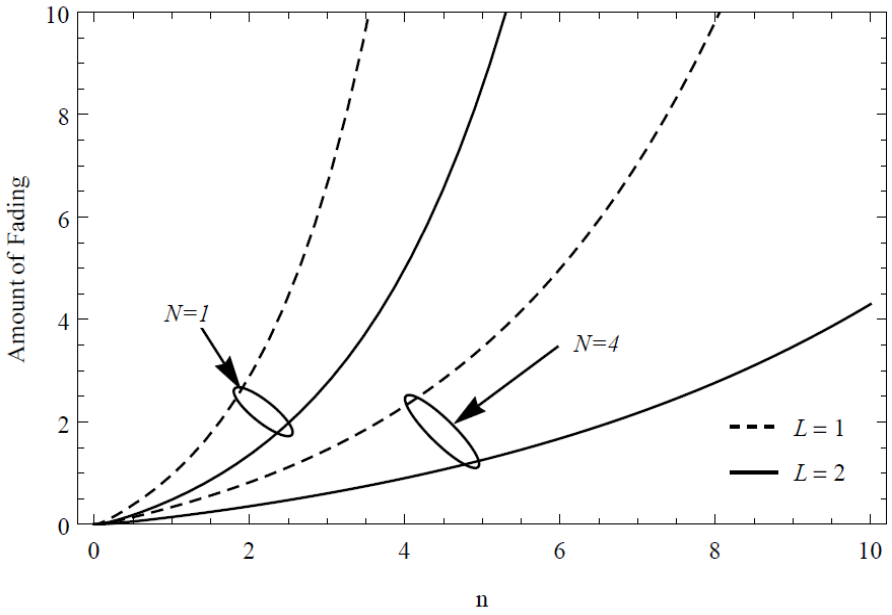

Fig.4-4. Amount of fading of direct and multihop transmission systems with diversity reception over *n**Rayleigh fading channels.

$$\mathrm{AF} \approx \left[\frac{\Gamma(Lm)\Gamma\left(\frac{2n}{N}+Lm\right)}{\Gamma^2\left(\frac{n}{N}+Lm\right)}\right]^N - 1 \tag{4.14}$$

Special case: For $N = 1$ and $L = 1$, AF can be simplified by

$$\mathrm{AF} \approx \frac{(m)_{2n}}{(m)_n^2} - 1 \tag{4.15}$$

where $(x)_n = \Gamma(x+n)/\Gamma(x)$. From (4.15), it is noted that for the classical Rayleigh distribution ($n = 1$), AF ≈ 1.

Fig.4-4 shows the effect of diversity on the performance of both direct and multihop transmission systems. It is interesting to note that: 1) using relays, the amount of fading is reduced compared to the direct transmissio**n**, 2) the overall amount of fading is reduced substantially when diversity reception is employed, and 3) the performance difference between diversity combining systems and no-diversity reception becomes larger as n increases. These results provide new insight into the trade-off between performance and complexity diversity reception over *n**Rayleigh fading channels and assist in the design of such receivers.

4.3.3 Power Optimization

From a practical standpoint, tracking the signal/interference level during the real-time updates of power allocation (PA) among vehicles requires high hardware complexity. This motivates us to investigate optimized power allocation when perfect statistical channel state information (CSI) is available at the source and relay nodes.

To simplify the analysis, we only evaluate the power allocation mode for regenerative systems. In this case, we redefine the instantaneous SNR as $\bar{\gamma}_i = P_i\lambda_i$, where $P_i \triangleq E_{si}/N_o$ is the transmitted signal power per hop with E_{si} denoting the transmitted signal energy. Next, we can optimize the power allocation to minimize the outage probability in (4.12) under a total power constraint ($\sum_{i=1}^{N} P_i \leq P_T$) with the knowledge of channel coefficients λ_i. Consequently, the optimization problem is formulated as follows

$$\min_{P_i} \left(1 - \prod_{i=1}^{N} \frac{\Gamma\left(Lm_i,\ \beta_i \gamma_{th}^{\frac{1}{n_i}} \right)}{\Gamma(Lm_i)} \right)$$

$$\text{subject to } \sum_{i=1}^{N} P_i \leq P_T \text{ and } P_i \geq 0 \tag{4.16}$$

By introducing Lagrange multipliers, the approximate power allocation for the *i*th hop can be expressed as

$$P_i \approx P_T \left[\sum_{k=1}^{N} \frac{n_i \Gamma(Lm_i, X_i)\ X_k^{Lm_k}\ e^{-X_k}}{n_k \Gamma(Lm_k, X_k)\ X_i^{Lm_i}\ e^{-X_i}} \right]^{-1} \tag{4.17}$$

where $X_i = \beta_i \gamma_{th}^{\frac{1}{n_i}}$. From (4.17), we obtain the power allocation for the *l*th diversity branch as $P_l = P_i/L$. For $N = 2$, (4.17) is simplified to

$$P_1 \approx \frac{P_T}{\left[1 + \frac{n_1 \Gamma(Lm_1, X_1)\ X_2^{Lm_2}\ e^{-X_2}}{n_2 \Gamma(Lm_2, X_2)\ X_1^{Lm_1}\ e^{-X_1}} \right]} \tag{4.18}$$

A similar equation can be written in terms of P_2. We note that (4.17) is a transcendental function and it is challenging to derive a closed-form for the transmitted power per hop. Hence, we calculate it numerically using a root-finding algorithm such as the bisection, Newton or successive numeric

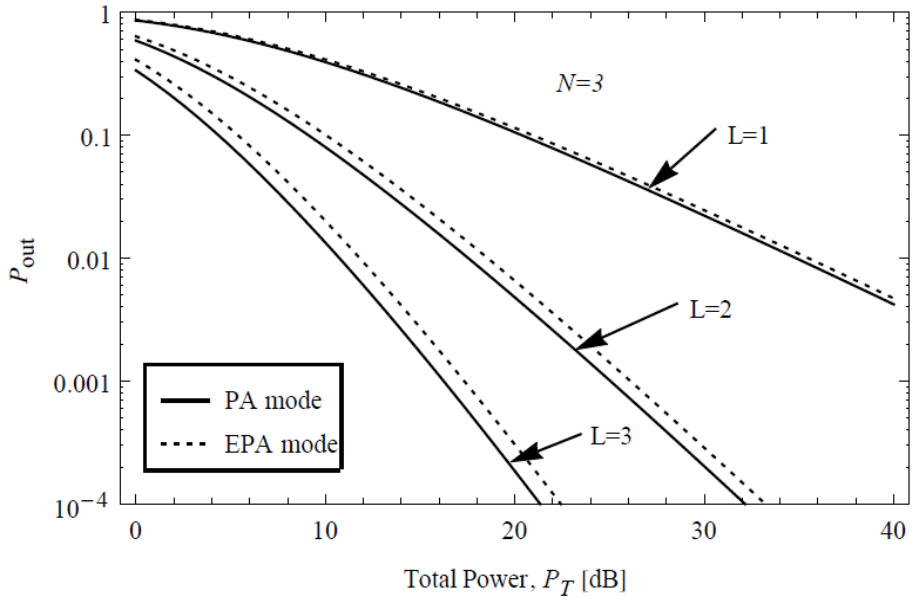

Fig.4-5. Effect of the PA and EPA modes on the outage performance of multihop systems with diversity reception over *n**Rayleigh fading channels

approximation methods.

Asymptotic Analysis: To gain further insight into the performance of regenerative systems over *n**Rayleigh fading channels, we compute an asymptotic solution for (4.17) using the fact that $x^{\alpha}e^{-x} = \Gamma(\alpha+1,x) - \alpha\Gamma(\alpha,x)$ [13, eq.(8.356.2)] and $\Gamma(\alpha+1,x) \leq \alpha\Gamma(\alpha)$ for small values of x, to obtain

$$P_i \approx \frac{m_i}{n_i \sum_{k=1}^{N} \frac{m_k}{n_k}} P_T \tag{4.19}$$

From (4.19), it can be seen that the power allocation for the *i*th hop depends only on the fading severity parameters, regardless of the channels coefficients (λ_i).

Fig.4-5 depicts the minimum outage probability versus the total power consumed to transmit the source's message to the destination node. In this scenario, we assume a three-hop system with/without diversity reception and channel quality set by $\lambda_1 = 1$, $\lambda_2 = 1$ and $\lambda_3 = 10$ for $n_1 = 3, n_2 = 3$ and $n_3 = 2$ respectively. It is clear that the power allocation is more beneficial if diversity reception is used. For instance, at $L = 3$, the power allocation ratio $\rho = P_i/P_T$ is evaluated from (4.17) using the successive approximation algorithm, which turns out to be $\rho \approx 0.429, 0.429, \text{and } 0.142$ for n_1, n_2, and n_3 respectively. It should be noted here that the regenerative systems allocate larger power to the weaker links to reduce the overall outage

probability compared to the equal power allocation (EPA) mode where the total transmitted power splits equally between the nodes ($P_i = P_T/3$). On the other hand, the PA ratio for the case of no-diversity reception, is calculated as $\rho \approx 0.40, 0.40, \text{and } 0.20$ for $n_1, n_2,$ and n_3 respectively. We note that the underlying scheme allocates less power to the first two hops, approaching the EPA mode. As a result, the performance improvement is negligible for the no-diversity reception case.

4.5 Conlusion

In this letter, we analyzed the end-to-end performance of multihop-IVC systems with regenerative and nonregenerative relays. In particular, we investigated the performance of both regenerative and nonregenerative systems with diversity reception over *n**Rayleigh fading channels. We derived new closed-form expressions for the outage probability and the amount of fading. The power optimization problem has also been formulated and solved. Numerical results show that at high cascading order n, nonregenrative systems achieve outage performance close to that of regenerative systems. Finally, we demonstrated that optimizing the transmit power allocation for diversity reception systems can provide a significant performance gain compared to the equal power allocation scenario.

CHAPTER 5

ARTICLE 4: ON THE APPROXIMATE ANALYSIS OF ENERGY DETECTION OVER N*RAYLEIGH FADING CHANNELS THROUGH COOPERATIVE SPECTRUM SENSING

Yahia Alghorani and Samuel Pierre
yahia.alghorani@polymtl.ca; samuel.pierre@polymtl.ca
Mobile Computing and Networking Research Laboratory (LARIM)
Ecole Polytechnique de Montreal
Montreal, Quebec, H3C 3A7, Canada

Sami Muhaidat
sami.muhaidat@uwo.ca
Electrical and Computer Engineering Department
University of Western Ontario
London, Ontario, N6A 5B9, Canada

Georges Kaddoum
Georges.Kaddoum@etsmtl.ca
Department of Electrical Engineering
École de Technologie Supérieure
Montréal, Quebec, H3C1K3 Canada

Accepted for Publication in IEEE Wireless Communications Letters on April 2015

Abstract

In this letter, we consider the problem of energy detection of unknown signals in an intervehicular communication (IVC) system over *n**Rayleigh fading channels (also known as cascaded Rayleigh). Novel tight approximations for the probability of detection are derived for the no-

diversity and the maximum ratio combining (MRC)) diversity schemes. Moreover, we investigate the system performance when cooperative spectrum sensing (CSS) is considered with and without imperfect reporting channels. The analytical results show that the detection reliability is decreased as the fading severity parameter $\boldsymbol{n}$ increases but reliability is substantially improved when CSS employs MRC schemes.

Index Terms: Cognitive radio, energy detection, *n**Rayleigh fading channels, diversity schemes, cooperative spectrum sensing.

5.1 Introduction

Recent studies have reported the importance of using cognitive radio in vehicular networks as a candidate solution for spectrum scarcity, and various techniques have been studied for cooperative spectrum sensing (CSS) as an efficient approach to enhance local spectrum sensing [94, 95]. However, one of the most difficult challenges of implementing spectrum sensing in vehicular networks is the hidden terminal problem which occurs when the CR (secondary user) is hidden in severe multipath fading while the primary user (PU) is operating in the vicinity [18]. Such kinds of problems can cause interference to the licensed users due to the very low SNR environments, which in turn leads to degrade the system performance. Hence, cooperative spectrum sensing has interestingly become a powerful solution to increase the probability of PU detection [19]. In this case, CR users have ability to collect radio environmental information such as power, position, frequency and bandwidth, then report it to fusion center (FC) where the local observations from CR users, are fused to detect the presence of PU. There are several factors play an important role in PU detection process, for instance, the position of CR user as a relay, whether it is located nearby or far away from the PU. By assuming the CR user is nearby the PU, the signal can be detected reliably with short sensing duration, which in turn makes the whole sensing time short at the FC. In addition, the number of cooperative partners is also another factor. By increasing the number of CR users, the probability of detecting the PU can be improved significantly but it makes the whole sensing time long [96].

It has been demonstrated recently that the so-called *n**Rayleigh fading channel model, which involves the product of two or more independent Rayleigh distributed random variables, provides an accurate statistical description of the intervehicular communications (IVC) channels [10]. In

[28, 29], experimental results in different vehicular communication environments have shown that in vehicular networks, several small-scale fading processes are multiplied together, leading to a worse-than Rayleigh fading. Unfortunately, most of the studies in the literature discussed cooperative spectrum sensing with energy detection over classical Rayleigh fading channels, which is limited to fixed-to-mobile cellular radio channels (see, e.g, [73, 74] and reference therein). There are very few studies that have discussed the problem of energy detection over *n**Rayleigh distribution, which is presented as an accurate statistical propagation model for mobile-to-mobile scenario. For instance, in [76], the detection probability over double Rayleigh fading channels (i.e., $n = 2$) has been investigated with and without receive diversity reception such as selection combining (SC) and switch and stay combining (SSC). The results have shown that the energy detection over double Rayleigh fading is worse than that of Rayleigh channels, and is improved by diversity systems.

In this letter, we analyze the energy detection over *n**Rayleigh fading channels (i.e, $n > 2$) when CSS scheme is employed in IVC system with and without maximum ratio combining (MRC) diversity reception, which to the best of our knowledge, has not been studied yet. Specifically, each local detector (CR user) makes a local binary decision, depending on whether the CR user decides H_0 (PU is absent) or H_1 (PU is present). All local decisions are then reported to a common receiver-enabled CR (i.e., a moving vehicle with a data fusion center), where they are combined to make a final decision about the presence or the absence of the PU. Through this approach, we analyze the spectrum sensing performance under various detection constraints, in cases of perfect reporting channels (where the reporting channel is free of error) and imperfect reporting channels (where the reporting channels between the CR users and the common receiver suffer from severe fading). Accordingly, approximate closed-form expressions of the average detection probability for both the no-diversity and diversity reception cases $\overline{P_{dl}^{n}}$ are presented, and the receiver operating characteristic (ROC) curves (probability of missed detection $Q_m = 1 - Q_d$ versus probability of false alarm Q_f) are obtained for different values of the fading severity parameter n.

The rest of this letter is organized as follows: in Section 5.2, the performance of local spectrum sensing over *n**Rayleigh fading channels is introduced. Section 5.3 studies the impact of diversity reception on *n**Rayleigh fading channels. In Section 5.4, cooperative spectrum sensing is

investigated. In Section 5.5, the numerical evaluation of cooperative spectrum sensing with and without imperfect reporting channels is presented. Finally, conclusions are given in Section 5.6.

5.2 Local Spectrum Sensing with No-Diversity

We consider a vehicular network composed of M CR users each equipped with a single pair of transmit and receive antennas. Each CR user performs its spectrum sensing independently to decide between the following two hypotheses

$$x_i(t) = \begin{cases} w_i(t), & : H_0 \\ h_i(t)s(t) + w_i(t), & : H_1 \end{cases} \tag{5.1}$$

where $x_i(t)$ is the signal received by the *i*th CR user in time slot t, $s(t)$ is the PU transmitted signal, $w_i(t)$ is the additive white Gaussian noise (AWGN) with zero mean and variance $(N_o W)$-denoted by one-sided noise and signal bandwidth, and $h_i(t)$ is a product of n independent circularly complex Gaussian random variables of the sensing channel between the PU and the *i*th CR user, which is defined as $h_i \triangleq \prod_{j=1}^{n} h_{i,j}$ with zero mean and channel variance of (η_i), for $i = 1, \dots, M$. Hence, $|h_i|$ follows *n**Rayleigh distribution. We assume the received signal undergoes slow fading (i.e., the symbol period of the detected signal is smaller than the coherence time of the channel), which can be justified for rush-hour traffic. At each CR user, the received signal is filtered, squared and integrated over a time interval T, and the energy of output signal measured by $y_i \triangleq \frac{2}{N_o}\int_0^T |x_i(t)|^2 dt$ [97]. Therefore, y_i acts as a test statistic and follows a central chi-square distribution with $2TW$ degrees of freedom under H_0 and a non-central chi-square distribution with $2TW$ degrees of freedom under H_1.

In order to find an approximate expression for the average probability of detection over n*Rayleigh fading channels $\overline{P_{di}^{n}}$, we need to recall the probabilities of false alarm and detection for a non-fading AWGN channel, which are given respectively by [97]

$$P_{fi} = P\{y_i > \lambda_i | H_0\} = \frac{\Gamma(u, \lambda_i/2)}{\Gamma(u)}, \tag{5.2}$$

$$P_{di} = P\{y_i > \lambda_i | H_1\} = Q_u\left(\sqrt{2\gamma_i}, \sqrt{\lambda_i}\right). \quad (5.3)$$

where $u = TW$, λ_i and $\gamma_i = |h_i|^2 E_s/N_o W$ are the energy detection threshold and the instantaneous signal-to-noise ratio (SNR) at the *i*th CR user respectively. E_s is the transmission energy per symbol, $\Gamma(.)$ is the gamma function defined by $\Gamma(\alpha) = \Gamma(\alpha, 0)$ [13], $\Gamma(.,.)$ represents the upper incomplete gamma function, defined by $\Gamma(\alpha, x) = \int_x^\infty e^{-t} t^{\alpha-1}\, dt$ [13], and $Q_u(.,.)$ is the generalized Marcum-Q function defined as $Q_u(a,b) = \int_b^\infty \frac{x^u}{a^{u-1}} e^{-\frac{x^2+a^2}{2}} I_{u-1}(ax)dx$ [98], where $I_{u-1}(.)$ is the modified Bessel function of the first kind and order $u-1$.

The generalized Marcum Q-function can be expressed by an infinite series representation as [99, eq. (29)]. To converge more quickly, by having a finite series, an asymptotic solution for the generalized Marcum Q-function has been introduced in [100, eq.(6)] for arbitrary values of its order u, which is given in a finite series representation and leads us to rewrite (5.3) in an approximate expression as

$$P_{di} \approx \sum_{l=0}^{k} \frac{\Gamma(k+l)k^{1-2l}\Gamma\left(u+l, \frac{\lambda_i}{2}\right)\gamma_i^l}{\Gamma(l+1)\Gamma(k-l+1)\Gamma(u+l)e^{\gamma_i}}. \quad (5.4)$$

Since $k = \infty$ is exact, it's worthwhile to mention that k-value selection in (5.4) is related to the involved parameters (i.e., u, λ_i, γ_i). Thus, the accuracy of (5.4) depends on the value of k and improves when k increases [100].

Under *n**Rayleigh distribution [12] with the help of [14, eq.(2.3)], the exact probability density function (PDF) of instantaneous SNR γ_i at the *i*th CR user is given by

$$f_{\gamma_i}(\gamma_i) = (\bar{\gamma}_i \gamma_i)^{-\frac{1}{2}} G_{0,n_i}^{n_i,0}\left(\frac{\gamma_i}{\bar{\gamma}_i}\middle| \overline{\frac{1}{2}, \ldots, \frac{1}{2}}\right). \quad (5.5)$$

where $G_{p,q}^{m,n}(.)$ is the Meijer-G function defined in [13, eq.(9.301)], and $\bar{\gamma}_i = \mathbf{E}(|h_i|^2)E_s/N_o W$ is the average SNR of γ_i, where $\mathbf{E}(.)$ is the statistical expectation operator. By averaging (5.4)

over (5.5) and using the fact defined in [85, eq.(07.34.21.0088.01)], the average probability of detection for the *i*th CR user over *n**Rayleigh fading channels can be obtained as

$$\overline{P_{di}^{n}} \approx \sum_{l=0}^{k} \frac{\Gamma(k+l)k^{1-2l}\Gamma\left(u+l,\frac{\lambda_i}{2}\right)}{\Gamma(l+1)\Gamma(k-l+1)\Gamma(u+l)} \sqrt{2^{1-n_i}}\, \bar{\gamma}_i^{-\frac{1}{2}} G_{1,n_i}^{n_i,1}\left(\frac{2^{1-n_i}}{\bar{\gamma}_i}\middle| \begin{matrix} \frac{1}{2}-l \\ \frac{1}{2},\ldots,\frac{1}{2} \end{matrix}\right). \tag{5.6}$$

However, a new accurate approximation for the PDF of *n**Rayleigh distribution has been proposed in [15], which is derived based-on a transformed Nakagami-*m* distribution as

$$f_{\gamma_i}(\gamma_i) \approx \frac{{\beta_i}^{m_i}{\gamma_i}^{\alpha_i-1}}{n_i\Gamma(m_i)} \mathrm{e}^{-\beta_i{\gamma_i}^{\frac{1}{n_i}}}, \quad \gamma_i \geq 0 \tag{5.7}$$

where $\alpha_i = m_i/n_i$ and $\beta_i = 2\,m_i/\Omega_{\mathrm{i}}\overline{\gamma_i}^{1/n_i}$. The fading severity parameters $(m_i, \Omega_{\mathrm{i}})$ are given by [15]

$$m_i = 0.6102n_i + 0.4263, \quad \Omega_{\mathrm{i}} = 0.8808{n_i}^{-0.9661} + 1.12$$

It's important to mention that the novel approximation for the PDF in (5.7) has been examined in [15], by comparing it to the exact PDF derived in (5.5). The results have shown that the new approximation has high accuracy in most cases considered. Furthermore, the approximate PDF is easy to calculate and to manipulate compared to the exact PDF as noticed later for deriving the PDF of the SNR at the output of MRC scheme.

By averaging (5.4) over (5.7) and using the fact that $\exp(-x) = G_{0,1}^{1,0}\left(x\middle|\begin{matrix}-\\0\end{matrix}\right), \forall x$ [85], the approximate closed-form expression for the average probability of detection for the *i*th CR user can be found as

$$\overline{P_{di}^{n}} \approx \sum_{l=0}^{k} \frac{\Gamma(k+l)k^{1-2l}\Gamma\left(u+l,\frac{\lambda_i}{2}\right)}{\sqrt{n_i}\Gamma(m_i)\Gamma(l+1)\Gamma(k-l+1)\Gamma(u+l)}$$

$$\times \frac{{\beta_i}^{m_i}}{(2\pi)^{\frac{n_i-1}{2}}} G_{1,n_i}^{n_i,1}\left(\left(\frac{\beta_i}{n_i}\right)^{n_i}\middle| \begin{matrix} 1-(\alpha_i+l) \\ 0,\ldots,\frac{n_i-1}{n_i} \end{matrix}\right). \tag{5.8}$$

The Meijer-G function in (5.8) can be evaluated much faster than that of (5.6) using the common

mathematical software packages such as MATHEMATICA or MAPLE. This is due to the fact that (5.8) is built based on a simple PDF compared to (5.6) which requires high computational complexity of the PDF in (5.5).

5.3 Local Spectrum Sensing with Diversity Reception

In this section, we derive an approximate expression for the average probability of detection when the MRC diversity reception is employed at each CR user. In such a scenario, the diversity scheme is employed to combat the severe fading due to *n**Rayleigh fading channels. We consider *L* diversity branches which are independent and identically distributed (i.i.d), and are subject to *n**Rayleigh fading. The instantaneous SNR of the combiner output for *i*th CR user is given by $\gamma_{ti} = \sum_{r=1}^{L} \gamma_{i,r}$ [14].

For a non-fading AWGN channel, the probabilities of false alarm and detection at the output of MRC are the same as (5.2) and (5.3), respectively. The PDF of γ_{ti} for the *i*th CR user over i.i.d *n**Rayleigh fading random variables can be derived by normalizing (5.7) to the PDF of the SNR at the MRC output with Nakagami fading [93, eq.(7)], to be finally expressed as

$$f_{\gamma_{ti}}(\gamma_{ti}) \approx \frac{(L\beta_i)^{Lm_i} {\gamma_{ti}}^{L\alpha_i - 1}}{n_i \Gamma(Lm_i) L^{L\alpha_i}} \exp\left(-\frac{L\beta_i}{L^{1/n_i}} {\gamma_{ti}}^{\frac{1}{n_i}}\right). \tag{5.9}$$

The PDF of γ_{ti} is quite similar to that in (5.7) by replacing m_i by Lm_i and $\overline{\gamma_i}$ by $L\overline{\gamma_i}$. However, eq.(5.9) is novel and has not been derived yet for the MRC scheme with *n**Rayleigh fading. Similarly, the average detection probability for the MRC diversity scheme at the *i*th CR user, can be evaluated by averaging P_{di} over (5.9).

$$\overline{P_{di}^{n}} \approx \sum_{l=0}^{k} \frac{\Gamma(k+l) k^{1-2l} \Gamma\left(u+l, \frac{\lambda_i}{2}\right)}{\sqrt{n_i}\,\Gamma(Lm_i)\Gamma(l+1)\Gamma(k-l+1)\Gamma(u+l)}$$

$$\times \frac{(L\beta_i)^{Lm_i}}{(2\pi)^{\frac{n_i-1}{2}}} G_{1,n_i}^{n_i,1}\left(\left(\frac{L\beta_i}{n_i}\right)^{n_i} \middle| \begin{matrix} 1-(L\alpha_i+l) \\ 0, \dots, \frac{n_i-1}{n_i} \end{matrix}\right). \tag{5.10}$$

5.4 Cooperative Spectrum Sensing

In cooperative spectrum sensing, each CR user sends its binary decision $D_i \in \{0,1\}$, to fusion center (FC). At the FC, all the local decisions are combined according to the OR fusion rule which gives better performance than other rules [101]. Consequently, the global decision is made to infer the presence or the absence of PU after M symbol periods. In this case, we assume the instantaneous SNRs at the CR users, are independent, but not necessarily identically (i.n.i.d) distributed random variables. In addition, all CR users use different decision thresholds λ_i, for $i = 1,,..,M$. Hence, the global probabilities of false and miss through an error-free channel, are given respectively by [102]

$$Q_f = 1 - \prod_{i=1}^{M}\left(1 - P_{fi}\right), \quad Q_m = \prod_{i=1}^{M} \overline{P_{mi}^{n}} \ . \tag{5.11}$$

where $\overline{P_{mi}^{n}} = 1 - \overline{P_{di}^{n}}$ is the average probability of missed detection of the local spectrum sensing of the *i*th CR user.

On the other hand, in case of imperfect reporting channels between *i*th CR user and the FC, the global probabilities of false alarm and miss are given respectively by [103]

$$Q_f = 1 - \prod_{i=1}^{M}\left[\left(1 - P_{fi}\right)(1 - P_{ei}) + P_{fi}\,P_{ei}\right], \tag{5.12}$$

$$Q_m = \prod_{i=1}^{M}\left[\overline{P_{mi}^{n}}(1 - P_{ei}) + \left(1 - \overline{P_{mi}^{n}}\right)P_{ei}\right] . \tag{5.13}$$

where P_{ei} is the probability of reporting error between the *i*th CR user and the common receiver.

5.5 Numerical Results

In this section, we analyze the performance of cooperative spectrum sensing with and without diversity reception over *n**Rayleigh fading channels. The performance analysis has been implemented under various channel constraints.

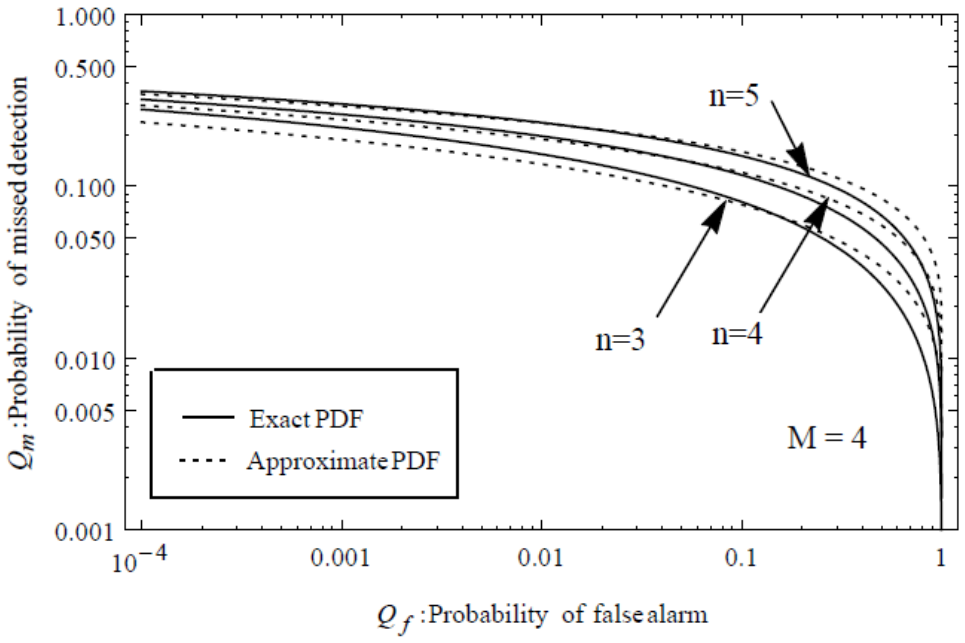

Fig.5-1. Comparison of complementary ROC curves for cooperative spectrum sensing-based the exact PDF and approximate PDF in (5.7) with different n values and perfect reporting channels ($\bar{\gamma} = 10\text{dB},\ u = 5, (n = 3;\ m = 2.25,\ \Omega = 1.42), (n = 4;\ m = 2.86,\ \Omega = 1.35), (n = 5;\ m = 3.47,\ \Omega = 1.30)$).

Fig.5-1 shows the cooperative spectrum sensing performance without diversity reception over n*Rayleigh fading channels. The figure compares the performance results-based the exact PDF (5.5) with that of the approximate PDF (5.7) under perfect reporting channels. In this case, we set $k = 500$ and the accuracy of analysis improves as the value of k increases. As observed from Fig.5-1, the detection performance-based the approximate PDF is closely fits the analytical results-based the exact PDF. The larger the value of n is, the higher accuracy will be [15]. Furthermore, we can see that, increasing n would result in missing the presence of the primary user, which leads to increase the interference to licensed users. Therefore, CSS is more attractive in practical scenarios as n increases.

Fig.5-2 shows the effect of MRC diversity scheme on the cooperative spectrum sensing performance over n*Rayleigh fading channels. In this scenario, we analyze the system performance under imperfect reporting channels. As clearly observed from this figure, MRC scheme has a positive impact on the probability of missed detection Q_m compared to the no-diversity system. In particular, there is an obvious diversity gain, about one order of magnitude for all values of n, and this gain starts to decrease as n increases. Further, when the false alarm probability reaches to a threshold (i. e, $Q_f \geq MP_e$) [103], the probability of missed detection Q_m

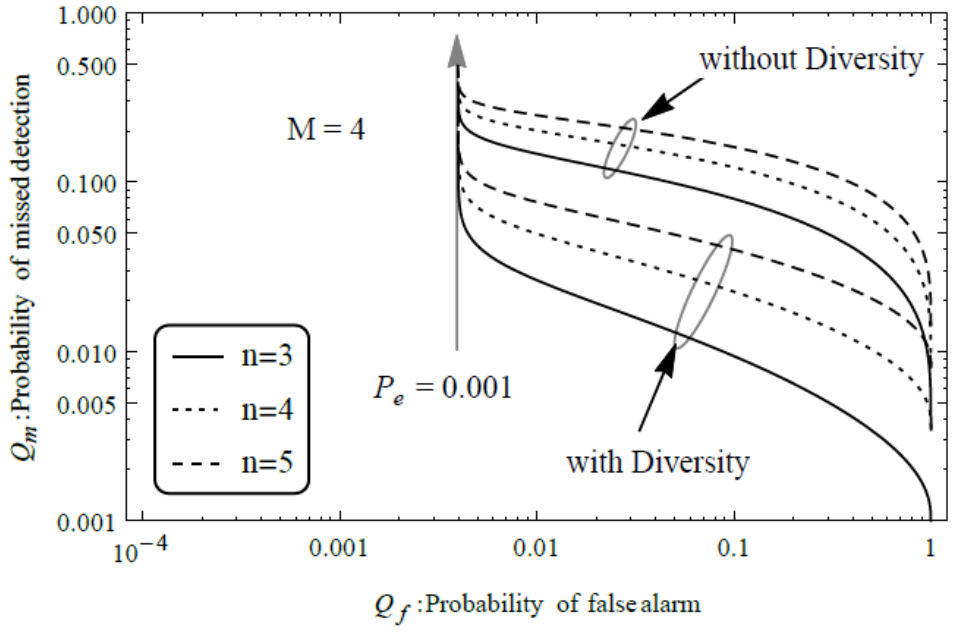

Fig.5-2. Complementary ROC curves for cooperative spectrum sensing with MRC diversity reception over *n**Rayleigh fading and imperfect reporting channels ($L = 3,\ \bar{\gamma} =$ 10dB, $u = 5$).

tends to one, which leads to deteriorate the detection performance. In general, MRC diversity scheme can bring additional gain to CSS when the probability of false alarm Q_f is considered, in such a way that CSS keeps the Q_f minimal rather than increasing the number of cooperative users, which results in increasing the probability of false alarm and low spectrum utilization as observed in [103].

5.6 Conlcusion

In this letter, we have studied the performance of an energy detector over *n**Rayleigh fading channels. Approximate expressions of the average detection probability are derived for both the no-diversity and receive diversity schemes. The performance of cooperative spectrum sensing has been further investigated with and without imperfect reporting channels. The results indicate that the probability of detection deteriorates when the fading severity parameter n increases. Finally, we have demonstrated that the underlying CSS scheme with diversity reception improves the sensing diversity order but this improvement is limited under imperfect reporting channels.

CHAPTER 6

ARTICLE 5: ON THE PERFORMANCE OF REDUCED-COMPLEXITY TRANSMIT/RECEIVE-DIVERSITY SYSTEMS OVER MIMO-V2V CHANNEL MODEL

Yahia Alghorani and Samuel Pierre
yahia.alghorani@polymtl.ca; samuel.pierre@polymtl.ca
Mobile Computing and Networking Research Laboratory (LARIM)
Ecole Polytechnique de Montreal
Montreal, Quebec, H3C 3A7, Canada

Sami Muhaidat
sami.muhaidat@uwo.ca
Electrical and Computer Engineering Department
University of Western Ontario
London, Ontario, N6A 5B9, Canada

Georges Kaddoum
Georges.Kaddoum@etsmtl.ca
Department of Electrical Engineering
École de Technologie Supérieure
Montréal, Quebec, H3C1K3 Canada

Naofal Al-Dhahir
aldhahir@utdallas.edu
Department of Electrical Engineering
University of Texas at Dallas
Richardson, TX 75083 USA

Submitted to IEEE Transactions on Vehicular Technology, December 2014

Abstract

In this paper, we investigate the performance of multiple-input multiple-output techniques in a vehicle-to-vehicle (V2V) communication system. We consider both transmit antenna selection with maximal-ratio combining and transmit antenna selection with selection combining. The channel propagation model between two vehicles is represented as *n**Rayleigh distribution, which has been shown to be a realistic model for V2V communication scenarios. We derive tight analytical expressions for the outage probability and amount of fading of the post-processing signal-to-noise ratio. Furthermore, we derive closed-form expressions for the symbol error probability. Numerical results show that the underlying schemes offer a maximum diversity order of $(m\, n_T\, n_R\, /n)$, where m and n are the fading severity parameters respectively, and n_T, n_R are the number of transmit and receive antennas respectively.

Index Terms: Antenna selection, TAS, MRC, diversity, MIMO, *n**Rayleigh fading channels, V2V communications.

6.1 Introduction

Vehicle-to-vehicle (V2V) communication systems have received considerable attention in recent years due to the urgent need to develop a new road safety strategy. Such systems are expected to resolve many transportation problems and reduce fatalities and serious injuries caused by road collisions. Future developments are expected in this field by using multiple antennas (MIMO) at transmit and receive ends to enhance channel capacity and diversity (reliability) [4],[5], since multiple antenna elements can easily be placed on the large vehicle surface [6]. To exploit the maximum transmit and receive diversity of MIMO systems, transmit antenna selection with maximal-ratio combining (TAS/MRC) scheme was proposed by [17], as a prospective solution to provide a power efficient and low computational complexity, while maintaining the full diversity gain as conventional MIMO systems [104],[105]. The main advantage of TAS/MRC scheme is to reduce hardware cost due to RF chains required to transmit antennas [106]. By selecting only one transmit antenna that provides the highest post-processing signal-to-noise ratio (SNR), the feedback overhead of channel state information (CSI) at the transmitter is effectively minimized compared to conventional MIMO systems. In this case, a single RF chain can be used at the transmit

side regardless of the number of transmit antennas. To further reduce the number of expensive RF chains at the receive side, the transmit antenna selection with selection combining (TAS/SC) is implemented to select a single transmit and receive antenna, in which a single RF chain is used at both terminals.

The performance analysis of TAS/MRC scheme has been extensively studied in the literature (see, e.g., [50],[51] and the references therein), most of these works were focused on classical Rayleigh or Nakagami distributions, which is limited to fixed-to-mobile cellular radio channels. Therefore, *n**Rayleigh distribution was proposed as an accurate statistical keyhole propagation model for mobile-to-mobile scenario where both the transmitter and receiver are in motion and typically use the same antenna height, resulting in two or more independent Rayleigh fading processes generated by independent groups of scatterers around the two mobile terminals [10]. Specifically, *n**Rayleigh fading channel is defined as a product of *n* independent identically distributed complex Gaussian random variables connected via narrow pipes and its probability density function (PDF) is given in [12]. On the receiver side, the received amplitude is evaluated as a product of Rayleigh random variables. For the case of double-Rayleigh fading channel model ($n = 2$), the distribution function was considered in [107]. The recent studies have proved that *n**Rayleigh fading is an appropriate keyhole channel model for V2V communication [28].

There are some contributions that have considered MIMO systems over the keyhole channels. However, all reported results mainly focused on double-Rayleigh/Nakagami fading channels. For instance, in [59], the authors analyzed the average symbol error rate (SER) for MIMO-orthogonal space-time block codes (STBCs) scheme in the presence of keyhole channels which are characterized by double Nakagami-*m* fading channels. The results showed that the keyhole channels significantly degrade the SER for MIMO-STBC scheme. The maximum special diversity gain was obtained for keyhole MIMO-STBC channels in [108]. The authors in [60] investigated the outage capacity distribution of spatially correlated keyhole MIMO channels with perfect knowledge of the CSI at the receiver and with/or without CSI at the transmitter. The measurements showed that if the number of antennas is small, the outage capacity decreases with correlation. On the other hand, if the number of antennas is large, the keyhole channel is equivalent to Rayleigh fading channels. In [61], the exact and approximate closed-form expressions were determined for the level crossing rate and the average fade duration of double Nakagami-MIMO channels. In [62], the authors investigated the performance of MIMO-STBC systems over generalized-*K* fading

channels. In this work, exact analytical expressions were derived for the outage probability, the symbol error probability and average channel capacity. In [109], closed-form expressions for the ergodic mutual information over uncorrelated keyhole MIMO channels were derived. In [110], the authors investigated the outage capacity of multi-keyhole MIMO channel model, taking into account the impact of correlation and the number of keyholes/antennas on the system performance. The results showed that if the number of keyhole channels and/or the number of antennas is large, there is an equivalent Rayleigh fading channels, in which the outage capacity of both channels is asymptotically equal. In [71], the authors investigated the maximum diversity order for a maximum ratio combining (MRC) scheme over double-Rayleigh fading channels and demonstrated that the maximum diversity order is equal to the number of receive antennas. In [111], the outage and error probabilities were calculated for dual selection combining scheme over cascaded Nakagami fading channels.

To the best of our knowledge, MIMO systems with antenna selection approaches such as TAS/MRC and TAS/SC schemes over *n**Rayleigh fading channels have not been studied yet. Thus, in this paper, we investigate the performance of MIMO-V2V networks-based the best antenna selection approach, considering *n**Rayleigh fading channel assumption.

Contributions: The main contributions of this paper are summarized as follows:

1. We derive new approximate closed-form expressions of the outage probability for both TAS/MRC and TAS/SC schemes over independent and identically distributed (i.i.d) *n**Rayleigh random variables.
2. We derive new closed-from expressions of the moment generating function (MGF) for both TAS/MRC and TAS/SC schemes, which are required to compute the symbol error probability of *M*-ary phase shift keying (*M*-PSK) modulation.
3. We calculate the approximate amount of fading for the underlying schemes over *n**Rayleigh fading.
4. We demonstrate the maximum achievable diversity order for *n**Rayleigh fading channels is equivalent to $(d \approx m\, n_T\, n_R\, /n)$, which deteriorates by increasing the fading severity parameter n.

The rest of this paper is organized as follows. Section 6.2 describes the system and channel model of TAS/MRC over *n**Rayleigh fading channels. In Section 6.3, we derive the approximate closed-form expressions for the outage probability, the amount of fading, and the symbol error rate. In

Section 6.4, numerical evaluation of our derived expressions is presented. Finally, concluding remarks are presented in Section 6.5.

6.2 System Model

We consider a MIMO-V2V communication system equipped with n_T transmit and n_R receive antennas and signaling over a product of *n* independent circularly complex Gaussian random variables, each having a channel coefficient between the *i*-th transmit antenna and *j*-th receive antenna equivalent to $h_{ij} \triangleq \prod_{k=1}^{n} h_{ij,k}$ with zero mean and channel variance ${\sigma_{ij}}^2$ for $i = 1, 2, \dots, n_T$, and $j = 1, 2, \dots, n_R$. Therefore, $|h_{ij}|$ follows a *n**Rayleigh distribution. The input-output relation for such a system is characterized by the $n_R \times n_T$ channel transfer matrix **H** consisting of h_{ij} channel coefficients and rank $r \leq \min(n_T, n_R)$. We further assume that all underlying channels are quasi-static, which can be justified for V2V communications scenarios in rush-hour traffic, as well as the channel matrix **H** is known at both the transmitter and the receiver. Let the $(n_T \times 1)$ symbols transmitted vector at the time instant t be $\boldsymbol{x} = [x_1, \quad x_2 \cdots, \quad x_{n_T}]^T$, and the $(n_R \times 1)$ received signal vector is $\mathbf{y} = [y_1, \quad y_2 \cdots, \quad y_{n_R}]^T$, where the superscript denoted by $(.)^T$, is the transpose operator. By writing the received signal in vector form, we have

$$\mathbf{y} = \sqrt{P}\mathbf{H}\mathbf{x} + \mathbf{w} \tag{6.1}$$

where *P* is the total transmit power of the signal, and $\mathbf{w} = [w_1, \quad w_2 \cdots, \quad w_{n_R}]^T$ is a circularly symmetric complex-Additive Gaussian noise (AWGN) vector with zero mean and variance N_o, denoted as $w_j \sim \mathcal{CN}(0, N_o)$.i.i.d.

6.2.1 TAS/MRC scheme

In this approach, a single antenna out of n_T transmit antennas is selected to maximize the post-processing SNR $\left(\gamma_p = \|\mathbf{H}^{\max}\|^2 (P/N_o)\right)$ at the maximal-ratio combining output, where the received signal vector can be expressed as

$$\mathbf{y} = \sqrt{P}\mathbf{H}^{\max} x + \mathbf{w} \tag{6.2}$$

where x is the transmit symbol, the squared channel vector norm is defined as $\|\mathbf{H}^{\max}\|^2 = \underset{i\in n_T}{\text{argmax}}\{\|\mathbf{H}_i\|^2 = \sum_{j=1}^{n_R}|h_{ij}|^2\}$, where $\mathbf{H}_i$ is the $(n_R \times 1)$ complex channel vector with n independent Rayleigh random variables. Further, the instantaneous SNR at the receiver-MRC can be expressed as $\gamma_i = \sum_{j=1}^{n_R}|h_{ij}|^2\,(P/N_o)$. Now, we can sort the RVs γ_i which follow n*Rayleigh distribution in a descending order denoted as $\gamma_{n_T} \geq \cdots \gamma_i \geq \cdots \geq \gamma_1$, such that a transmit antenna harmonious with the n_T-th order statistics is selected for the transmission, where $\gamma_{n_T} = \gamma_p$. By assuming $\{h_{ij}\}$ are i.i.d random variables with zero mean and variance σ^2, and using the approximate PDF for n*Rayleigh distribution given as [15]

$$f_X(x) \approx \frac{\beta^m}{n\Gamma(m)} x^{\alpha-1} e^{-\beta x^{1/n}}, \qquad x \geq 0 \tag{6.3}$$

where $\alpha = m/n$ and $\beta = 2\,m/\Omega\bar{x}^{1/n}$, the approximate PDF of instantaneous SNR γ at the receiver-MRC can be deduced from [93, eq.(7)], to be found as

$$f_\gamma(\gamma) \approx \frac{\beta_{MRC}^{mn_R}}{n\Gamma(mn_R)} \gamma^{\alpha_{MRC}-1} \exp\left(-\beta_{MRC}\gamma^{1/n}\right) \tag{6.4}$$

where $\alpha_{MRC} = mn_R/n$, $\beta_{MRC} = 2mn_R/\Omega(n_R\bar{\gamma})^{1/n}$, and $\bar{\gamma} = P\sigma^2/N_o$, m and Ω are the fading severity parameters of n*Rayleigh fading channels given by [15].

$$m = 0.6102n + 0.4263, \quad \Omega = 0.8808n^{-0.9661} + 1.12$$

It is important to mention that the novel approximation for the PDF in (6.1) has been examined in [15], by comparing it to the exact PDF derived in [12, eq.(8)]. The results have shown that the new approximation has high accuracy in most cases considered. In addition, the approximate PDF is easy to calculate and to manipulate compared to the exact PDF. Moreover, in Fig.6-1, Monte-carlo simulation is performed to show the accuracy of (4). From Fig.6-1, the approximate PDF is very close to simulation results. The larger the value of n is, the higher accuracy will be.

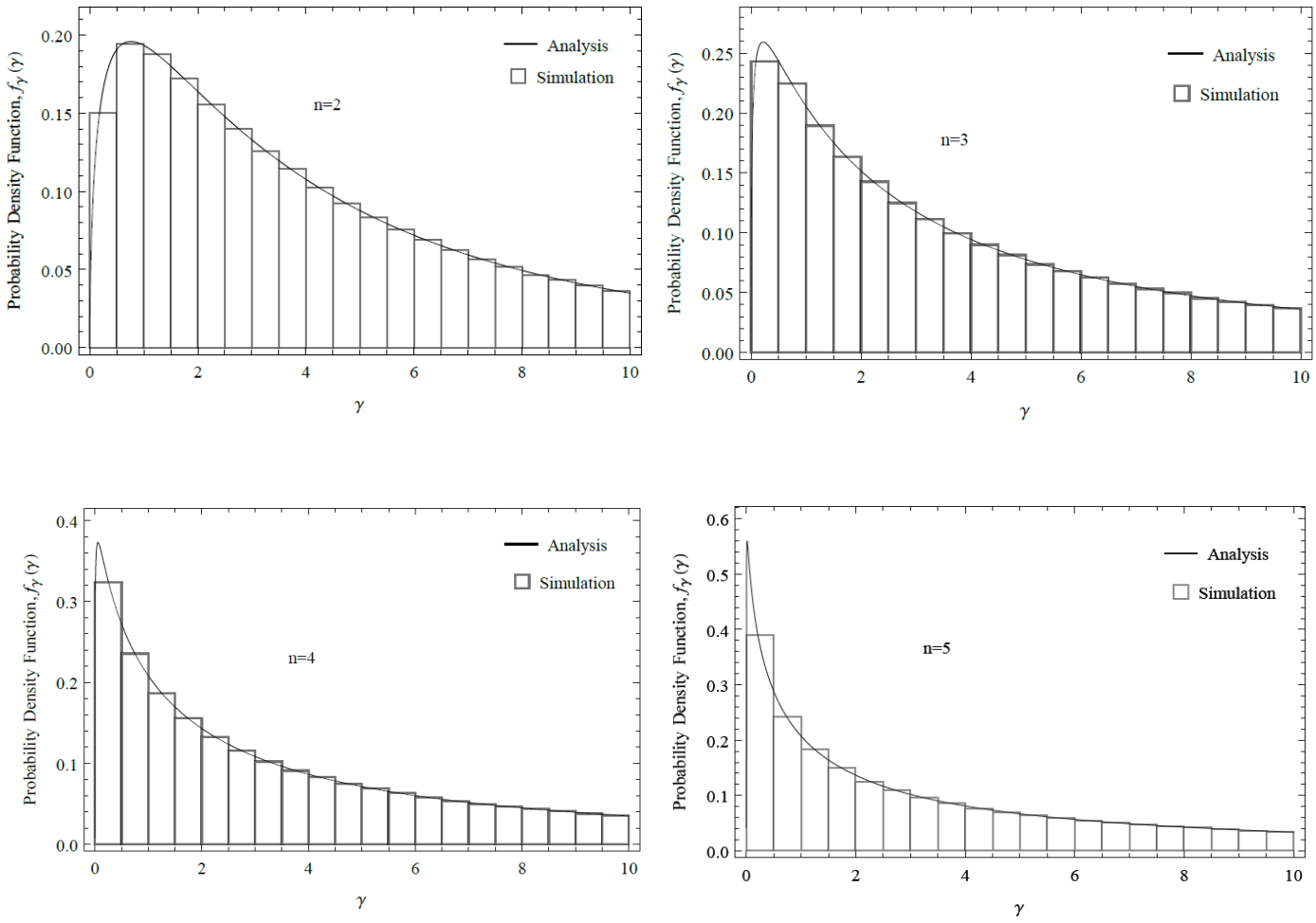

Fig.6-1. Comparison between analytical results and Monte-Carlo simulation for the PDF formulated by (6.4) ($n_R = 2$ and 10^6 iterations)

From (6.4), we can find the approximate cumulative density function (CDF) of instantaneous SNR γ with the help of fact that $\int_0^u x^{v-1}\exp(-\mu x)\,dx = \mu^{-v}\gamma(v,\mu u)$ [13, eq.(3.381.1)], to be

$$F_\gamma(\gamma) \approx \frac{\gamma\left(mn_R, \beta_{MRC}\gamma^{1/n}\right)}{\Gamma(mn_R)} \tag{6.5}$$

where $\gamma(\alpha,x) = \int_0^x e^{-t}t^{\alpha-1}\,dt$ is the lower incomplete gamma function, defined in [80]. Consequently, the approximate CDF of the post-processing SNR γ_p which is equivalent to the CDF of the largest of order statistics γ_{n_T}, can be derived using [112, Sec. 2.1], as

$$F_{\gamma_p}(\gamma) \approx \left[1 - \frac{\Gamma\left(mn_R, \beta_{MRC}\gamma^{1/n}\right)}{\Gamma(mn_R)}\right]^{n_T} \tag{6.6}$$

where $\Gamma(\alpha, x) = \int_x^{\infty} e^{-t} t^{\alpha-1}\, dt$ is the upper incomplete gamma function, defined in [24]. Now, the approximate PDF of γ_p can be easily obtained from (6.6) as

$$f_{\gamma_p}(\gamma) \approx \frac{n_T\, \beta_{MRC}^{mn_R}}{n\Gamma(mn_R)} \gamma^{\alpha_{MRC}-1} \exp\left(-\beta_{MRC}\gamma^{1/n}\right)$$

$$\times \left[1 - \frac{\Gamma\left(mn_R, \beta_{MRC}\gamma^{1/n}\right)}{\Gamma(mn_R)}\right]^{n_T-1} \tag{6.7}$$

6.2.2 TAS/SC scheme

In this approach, a single antenna out of n_T antennas at the transmitter and a single antenna out of n_R antennas at the receiver are jointly selected to maximize the post-processing SNR $\left(\gamma_p = |h^{\max}|^2 (P/N_o)\right)$ at the receiver terminal, where the received signal can be expressed as

$$\mathrm{y} = \sqrt{P} h^{\max} x + \mathrm{w} \tag{6.8}$$

where the squared magnitude of the best channel coefficient between two terminals is $|h^{\max}|^2 = \underset{i \in n_T, j \in n_R}{\operatorname{argmax}} \left\{\left|h_{ij}\right|^2\right\}$. The instantaneous SNR between the *i*-th transmit antenna and *j*-th receive antenna can be expressed as $\gamma_{ij} = \left|h_{ij}\right|^2 P/N_o$. In this case, the RVs γ_{ij} re-arranged in a descending order denoted as $\gamma_{n_T n_R} \geq \cdots \gamma_{ij} \geq \cdots \geq \gamma_{11}$, in which a single pair of antennas corresponding to the $n_T\, n_R$ -th order statistics is selected for transmission and reception. Hence, the approximate CDF of the post-processing SNR γ_p can be found as

$$F_{\gamma_p}(\gamma) \approx \left[1 - \frac{\Gamma\left(m, \beta_{SC}\gamma^{1/n}\right)}{\Gamma(m)}\right]^{N} \tag{6.9}$$

where $\beta_{SC} = 2\, m/\Omega\, \bar{\gamma}^{1/n}$, $N = n_T\, n_R$. The approximate PDF of γ_p can be consequently

determined as

$$f_{\gamma_p}(\gamma) \approx \frac{N\beta_{SC}^{m}}{n\Gamma(m)}\gamma^{\alpha_{SC}-1}\exp\left(-\beta_{SC}\gamma^{1/n}\right)$$

$$\times\left[1-\frac{\Gamma\left(m,\beta_{SC}\gamma^{1/n}\right)}{\Gamma(m)}\right]^{N-1} \tag{6.10}$$

where $\alpha_{SC} = m/n$

6.3 Performance Analysis

6.3.1 Outage Probability

The outage probability ($P_{out} \triangleq F_{\gamma_p}(\gamma_o)$) of a communication channel can be defined as the probability of the post-processing SNR γ_p falls below a certain threshold ($\gamma_o = 2^R - 1$), namely

$$P_{out} = \Pr\left(\gamma_p \le \gamma_o\right)$$

TAS/MRC scheme

From (6.6), the approximate closed-form expression of the outage probability for TAS/MRC scheme can be expressed as

$$P_{out} \approx \left[1-\frac{\Gamma\left(mn_R\,,\beta_{MRC}{\gamma_o}^{1/n}\right)}{\Gamma(mn_R)}\right]^{n_T} \tag{6.11}$$

To compute the maximum achievable diversity order, we need to find an asymptotic expression for the outage probability at the high SNR regime (i.e., when $\bar{\gamma} \to \infty$), using the fact that $\Gamma(\alpha, x) = \Gamma(\alpha) - \sum_{n=0}^{\infty}\frac{(-1)^n x^{\alpha+n}}{n!(\alpha+n)}$ [13, eq.(8.354.2)], which leads to $\Gamma(\alpha, x) = \Gamma(\alpha) - x^{\alpha}/\alpha$ when $x \to 0$. Thus, we can rewrite (6.11) in an asymptotic form as

$$P_{out} \approx \left(\frac{(2mn_R/\Omega)^{mn_R}}{mn_R\,\Gamma(mn_R)}\right)^{n_T}\left(\frac{\gamma_o}{n_R\,\bar{\gamma}}\right)^{\frac{mN}{n}} + \mathcal{O}\left(\left(\frac{\gamma_o}{n_R\,\bar{\gamma}}\right)^{\frac{mN}{n}+1}\right) \tag{6.12}$$

Table 6.1: Coding Gain for TAS/MRC and TAS/SC Schemes with Antenna Configuration: $n_T = 2,\ n_R = 2$

System Model	Coding Gain (CG)			
	$n = 2$	$n = 3$	$n = 4$	$n = 5$
TAS/MRC	1.7018	0.8860	0.4301	0.2008
TAS/SC	1.4667	0.8809	0.4771	0.2433

Table 6.2: Coding Gain for TAS/MRC and TAS/SC Schemes with Antenna Configuration $n_T = 2,\ n_R = 3$

System Model	Coding Gain (CG)			
	$n = 2$	$n = 3$	$n = 4$	$n = 5$
TAS/MRC	2.0219	0.9969	0.4646	0.2101
TAS/SC	1.4667	0.8809	0.4771	0.2433

Subsequently, from (6.12), the achievable diversity order can be easily deduced as $d \approx mN/n$, with a coding gain equivalent to

$$\mathrm{CG} = \left[\frac{\left(mn_R\,\Gamma(mn_R)\right)^{1/mn_R}}{mn_R\,/\Omega\,{n_R}^{1/n}}\right]^n \tag{6.13}$$

Note that the coding gain in (6.13) depends only on the fading severity parameters and the number of receive antennas regardless the number of transmit antennas.

TAS/SC scheme

From (6.9), the approximate closed-form expression of the outage probability for TAS/SC scheme can be expressed as

$$P_{out} \approx \left[1 - \frac{\Gamma\left(m, \beta_{SC}{\gamma_o}^{1/n}\right)}{\Gamma(m)}\right]^N \tag{6.14}$$

As a result, at the high SNR values, (6.14) can be rewritten in an asymptotic form as

$$P_{out} \approx \left(\frac{(2m/\Omega)^m}{m\Gamma(m)}\right)^N \left(\frac{\gamma_o}{\bar{\gamma}}\right)^{\frac{mN}{n}} + \mathcal{O}\left(\left(\frac{\gamma_o}{\bar{\gamma}}\right)^{\frac{mN}{n}+1}\right) \tag{6.15}$$

Notice that from (6.12) and (6.15), both TAS/MRC and TAS/SC schemes offer the same diversity order of $d \approx mN/n$, but TAS/SC scheme provides a coding gain equal to

$$\mathrm{CG} = \left[\frac{\left(m\Gamma(m)\right)^{1/m}}{2m/\Omega}\right]^n \tag{6.16}$$

Note that the coding gain in (6.16) depends only on the fading severity parameters which assumed to be fixed during the whole transmission time regardless the number of transmit and receive antennas.

Table 6.1 and 6.2 compares the coding gain of TAS/MRC scheme and TAS/SC under different antenna configurations. As it is noticed from Table 6.1, the coding gain of TAS/MRC scheme outperforms that of TAS/SC when $n = 2$ and 3, and gradually decreased when *n* increases, which leads to increase the outage probability of TAS/MRC compared to TAS/SC. In Table 6.2, we study the impact of receive antennas on the coding gain when $n_T = 2,\ n_R = 4$. As observed, TAS/MRC has better coding gain when $n = 2, 3$, and 4 (due to the better error performance when n_R increases). This means that TAS/MRC scheme works quite well compared to TAS/SC when the number of receive antennas is large.

Some special cases for the outage probability and diversity order of MIMO-V2V channel modeling are summarized in Table 6.3.

6.3.2 Average Symbol Error Rate

In this subsection, we derive the approximate average SER for both TAS/MRC and TAS/SC schemes-based the MGF approach.

TAS/MRC Scheme

To derive the average SER for the considered scheme, we find a closed-form expression for the MGF of post-processing SNR $\phi_{\gamma_p}(s)$, which is given by $\phi_{\gamma_p}(s) = s\mathcal{L}\left\{F_{\gamma_p}(\gamma); s\right\}$, where $\mathcal{L}(.;.)$

denotes the Laplace Transform. Using (6.6) and the fact defined in [13, eq.(8.354.1)], the MGF of post-processing SNR can be expressed as

$$\phi_{\gamma_p}(s) \approx \sum_{k_i=0}^{\infty} \dots \sum_{k_M=0}^{\infty} \left(\beta_{MRC} s^{-\frac{1}{n}}\right)^{\sum_{i=1}^{n_T}(mn_R+k_i)} \times \prod_{i=1}^{n_T} \frac{(-1)^{k_i}}{k_i!\,(mn_R+k_i)} \Gamma\left(1+\sum\nolimits_{i=1}^{n_T} \frac{mn_R+k_i}{n}\right) \tag{6.17}$$

Although the expression of the MGF in (6.17) enables a numerical evaluation of the symbol error probability, but it may not be a practical solution due to the problem of truncation of infinite series; thus to have further insight into the SER performance over cascaded Rayleigh fading channels, we use the bounds for the incomplete gamma function given in [84, eq.(4.1)], in this case, (6.6) can be further simplified to

$$F_{\gamma_p}(\gamma) \approx \left[\frac{\beta_{MRC}^{mn_R}\,\gamma^{\alpha_{MRC}}}{mn_R\,\Gamma(mn_R)} e^{-\frac{mn_R}{mn_R+1}\beta_{MRC}\gamma^{\frac{1}{n}}}\right]^{n_T} \tag{6.18}$$

Now, using the fact that $e^{-x} = G_{0,1}^{1,0}\left(x\middle|\begin{matrix}-\\0\end{matrix}\right)$, $\forall x$ and the useful identity defined in [85, eq.(07.34.21.0088.01)], the MGF lower-bound can be derived as

$$\phi_{\gamma_p}(s) \approx \frac{\sqrt{n}\beta_{MRC}^{mN} s^{-(\frac{mN}{n}+1)}}{(2\pi)^{\frac{n-1}{n}}\left(mn_R\,\Gamma(mn_R)\right)^{n_T}} \times G_{1,n}^{n,1}\left(s^{-1}\left(\frac{mN\beta_{MRC}}{n(mn_R+1)}\right)^{n}\middle|\begin{matrix}-\frac{mN}{n}\\0,..,\frac{n-1}{n}\end{matrix}\right) \tag{6.19}$$

where $G_{p,q}^{m,n}(\cdot)$ is the Meijer-G function defined in [13, eq. (9.301)].

Table 6.3: Approximate Outage Probability over MIMO-V2V Channel Model

System Model	Channel capacity C(bps/Hz)	Approximate P_{out}	Diversity gain
SISO	$C = \log_2\left(1 + \frac{P}{N_o}\lvert h_{11}\rvert^2\right)$	$P_{out} \approx 1 - \frac{\Gamma\left(m, \frac{2m}{\Omega}\left(\frac{\gamma_o}{\bar{\gamma}}\right)^{1/n}\right)}{\Gamma(m)}$	$d = \frac{m}{n}$
MISO	$C = \log_2\left(1 + \frac{P}{n_T N_o}\lVert\mathbf{H}\rVert_F^2\right)$ where $\lVert\mathbf{H}\rVert_F^2 = \sum_{i=1}^{n_T}\lvert h_{i1}\rvert^2$	$P_{out} \approx 1 - \frac{\Gamma\left(mn_T, \frac{2mn_T}{\Omega}\left(\frac{\gamma_o}{\bar{\gamma}}\right)^{1/n}\right)}{\Gamma(mn_T)}$	$d = \frac{mn_T}{n}$
SIMO-MRC	$C = \log_2\left(1 + \frac{P}{N_o}\lVert\mathbf{H}\rVert_F^2\right)$ where $\lVert\mathbf{H}\rVert_F^2 = \sum_{j=1}^{n_R}\lvert h_{1j}\rvert^2$	$P_{out} \approx 1 - \frac{\Gamma\left(mn_R, \frac{2mn_R}{\Omega}\left(\frac{\gamma_o}{n_R\bar{\gamma}}\right)^{1/n}\right)}{\Gamma(mn_R)}$	$d = \frac{mn_R}{n}$
SIMO-SC	$C = \log_2\left(1 + \frac{P}{N_o}\lvert h_1^{\max}\rvert^2\right)$ where $\lvert h_1^{\max}\rvert^2 = \max_{j\in n_R}\lvert h_{1j}\rvert^2$	$P_{out} \approx \left[1 - \frac{\Gamma\left(m, \frac{2m}{\Omega}\left(\frac{\gamma_o}{\bar{\gamma}}\right)^{1/n}\right)}{\Gamma(m)}\right]^{n_R}$	$d = \frac{mn_R}{n}$

Average SER of M-PSK: The approximate average SER of *M*-PSK modulation can be calculated using [14]

$$P_e = \frac{1}{\pi}\int_0^{\pi-\frac{\pi}{M}} \Phi_{\gamma_p}\left(\frac{g_{PSK}}{\sin^2\theta}\right) d\theta \tag{6.20}$$

where $g_{PSK} = \sin^2(\pi/M)$. By substituting (6.19) into (6.20), and assuming $\theta = \pi/2$, we can upper-bound the SER as $P(e) \leq \frac{M-1}{M}\phi_{\gamma_p}(g_{PSK})$.

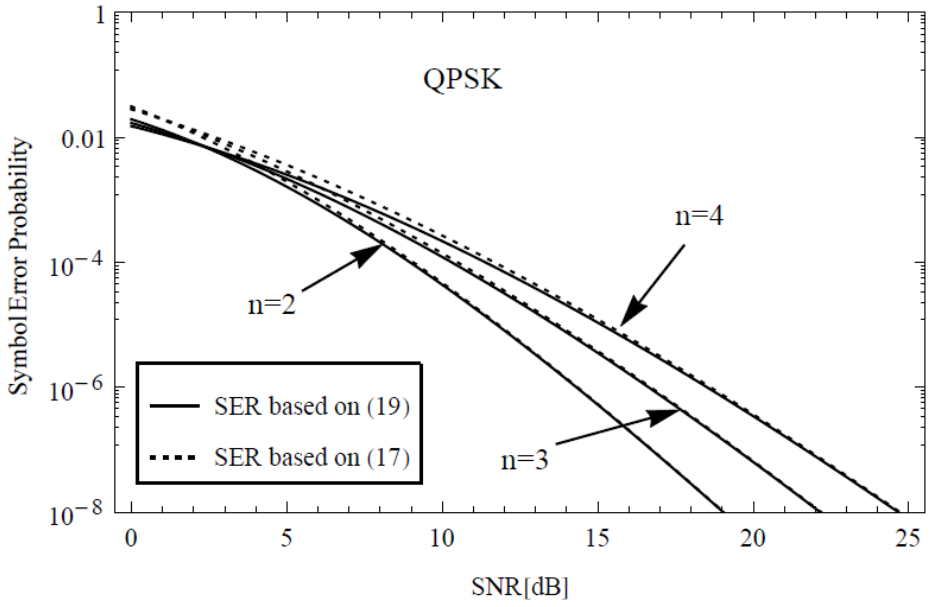

Fig.6-2. SER of TAS/MRC for QPSK modulation type over *n**Rayleigh fading channels (antenna configuration: $n_T = 2,\ n_R = 3$)

Asymptotic Analysis: To get an asymptotic form for the MGF of γ_p at the high SNR values where ($\bar{\gamma} \gg 0$), we apply the zeroth-order Taylor approximation to (6.18) (where $e^{-x} \approx 1$ for x is sufficiently small), and after some algebraic manipulations, the SER of binary phase shift keying (BPSK) modulation can be obtained in a simple compact form as

$$P_e \leq \frac{1}{2}\left[\frac{\left(2\,mn_R/\Omega\bar{\gamma}^{1/n}\right)^{mn_R}}{mn_R\,\Gamma(mn_R)}\right]^{n_T}\Gamma\left(1+\frac{mN}{n}\right) \tag{6.21}$$

Notice that the diversity order can also be deduced from (6.20) as $d = mN/n$. Fig.6-2 shows the average SER for quadrature phase shift keying (QPSK) modulation over *n**Rayleigh fading channels, and compares the analytical results (i.e., (6.17)) with the proposed bound counterpart (6.19). Fig.6-1. demonstrates that the SER improves as n decreases, since the diversity gain ($d \approx mN/n$) increases as n decreases. Moreover, the slopes of the analytical SER performance curves match very well with the lower bound curves over all SNR values and the tightness is improved in the high SNR regime, which confirms that our proposed bound is tight. Moreover, the lower the value of n is, the tighter the proposed bound will be.

TAS/SC scheme

In this scheme, the upper-bound SER can be found by taking the Laplace transform of eq.(6.9). Following similar steps for the MGF derivation of TAS/MRC scheme, the MGF lower-bound for TAS/SC scheme can be expressed as

$$\phi_{\gamma_p}(s) \approx \frac{\sqrt{n}\beta_{SC}^{mN} s^{-(\frac{mN}{n}+1)}}{(2\pi)^{\frac{n-1}{n}}\left(m\Gamma(m)\right)^N} \times G_{1,n}^{n,1}\left(s^{-1}\left(\frac{mN\beta_{SC}}{n(m+1)}\right)^n \middle| \begin{matrix} -\frac{mN}{n} \\ 0,..,\frac{n-1}{n} \end{matrix} \right) \quad (6.22)$$

By substituting (6.22) into (6.20), and assuming $\theta = \pi/2$, we can upper-bound the SER as $P(e) \leq \frac{M-1}{M}\phi_{\gamma_p}(g_{PSK})$.

Asymptotic Analysis: Here, we analyze the asymptotic SER at the high SNR regime. By referring to eq.(6.9) and following similar steps of TAS/MRC scheme, the SER of BPSK modulation can be obtained as

$$P_e \leq \frac{1}{2}\left[\frac{\left(2\,m/\Omega\bar{\gamma}^{1/n}\right)^m}{m\Gamma(m)}\right]^N \Gamma\left(1+\frac{mN}{n}\right) \quad (6.23)$$

Notice that the diversity order of TAS/SC scheme can also be extracted from (6.23) as $d = mN/n$.

6.3.3 Amount of Fading

In this subsection, we introduce approximate closed-form expressions of the amount of fading (AF) for both TAS/MRC and TAS/SC schemes over *n**Rayleigh fading channels. In order to evaluate the severity of fading at the receiver, we derive the approximate *l*-th moment of γ_p, $\mathbf{E}[\gamma_p^l]$, which is used to calculate the fading figure defined by [14]

$$\mathrm{AF} = \frac{\mathrm{var}(\gamma_p^2)}{\left(\mathbf{E}[\gamma_p^2]\right)^2}$$

where $\mathbf{E}[.]$ and $\mathrm{var}(.)$, denote respectively the statistical average and the variance.

TAS/MRC scheme

In this approach, the approximate *l*-th moment of γ_p can be derived from (6.6) with the help of fact in [13, eq.(3.326.2)] and the bounds for the incomplete gamma function given in [84, eq.(4.1)], to be finally expressed as

$$\mathbf{E}\left[\gamma_p^l\right] \approx \frac{n_T \beta_{MRC}^{mn_R}}{\Gamma(mn_R)} \left[\frac{\beta_{MRC}^{mn_R}}{mn_R\,\Gamma(mn_R)}\right]^{n_T-1} \times \frac{\Gamma(mN+nl)}{\left[\beta_{MRC}\left(1+\frac{mn_R(n_T-1)}{mn_R+1}\right)\right]^{mN+nl}} \tag{6.24}$$

By determining the first and the second moment of γ_p, we can calculate the AF lower bound of the considered scheme.

Special Case: For the SIMO-MRC channel model, (6.24) can be rewritten in a simple compact form as

$$\mathbf{E}\left[\gamma_p^l\right] \approx \frac{\Gamma(mn_R+nl)}{\Gamma(mn_R)\beta_{MRC}^{nl}}$$

yielding to

$$\text{AF} \approx \frac{\Gamma(mn_R)\Gamma(mn_R+2n)}{\Gamma^2(mn_R+n)} - 1 \tag{6.25}$$

TAS/SC scheme

In this approach, the approximate *l*-th moment of γ_p can be derived from (6.9) as

$$\mathbf{E}\left[\gamma_p^l\right] \approx \frac{N\beta_{SC}^m}{\Gamma(m)} \left[\frac{\beta_{SC}^m}{m\Gamma(m)}\right]^{N-1} \frac{\Gamma(mN+nl)}{\left[\beta_{SC}\left(1+\frac{m(N-1)}{m+1}\right)\right]^{mN+nl}} \tag{6.26}$$

By computing the first two moments, we can calculate the approximate AF of the underlying scheme.

Special Case: For the SISO channel model, eq.(6.26) can be rewritten in a simple compact form as

$$\mathbf{E}\left[\gamma_p^l\right] \approx \frac{\Gamma(nl+m)}{\Gamma(m)\beta_{SC}^{nl}}$$

yielding to

$$\mathrm{AF} \approx \frac{\Gamma(m)\Gamma(m+2n)}{\Gamma^2(m+n)} - 1 \tag{6.27}$$

In this case, for the classical Rayleigh distribution $(n = 1)$, the corresponding AF is equivalent to $\mathrm{AF} \approx 1$. As observed from (6.25) and (6.27), the fading figure over *n**Rayleigh is more severe than that of classical Nakagami-m fading with $\mathrm{AF} = 1/m$ and Rice model with $\mathrm{AF} = (1+2K)/(1+K)^2$. In addition, TAS/MRC scheme outperforms TAS/SC in reducing the amplitude of fading at the receiver, the more the number of receive antennas, the less the amount of fading is achieved.

6.4 Numerical Results

In this section, we present numerical results of the approximate outage probability and the symbol error probability for both TAS/MRC and TAS/SC schemes over *n**Rayleigh fading channels.

Fig.6-3 compares the performance of the outage probability of TAS/MRC and TAS/SC schemes with antenna configuration $n_T = 2,\ n_R = 3$. We assume the fading severity parameters, n, takes the values $n = 2, 3, 4$ and 5. In general, as observed from Fig.6-3, the outage performance of both schemes deteriorates by increasing the fading severity parameter n, confirming our observations that the diversity order $(d \approx m\,N/n)$ decreases when n increases. In addition, TAS/MRC scheme outperforms TAS/SC scheme for $n = 2$ and their performance are matched for $n = 3$, but the performance of TAS/SC scheme surpasses TAS/MRC in the cases of $n = 4$ and 5; therefore, the outage performance for $n \geq 4$ can be improved when TAS/SC is employed. This is due to the fact that TAS/SC achieves better coding gain for $n \geq 4$.

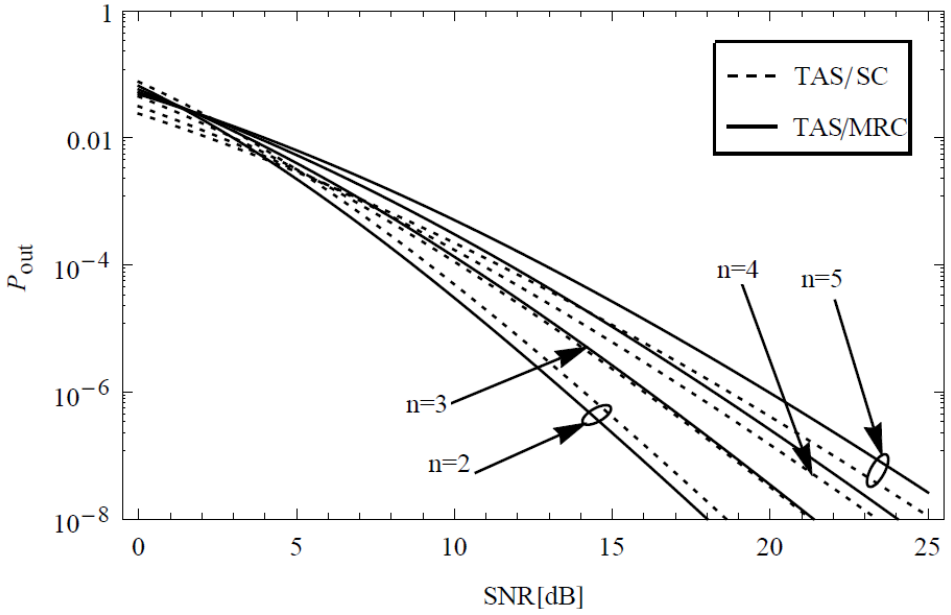

Fig.6-3. Outage probability of TAS/MRC and TAS/SC schemes over *n**Rayleigh fading channels (antenna configuration: $n_T = 2,\ n_R = 3$)

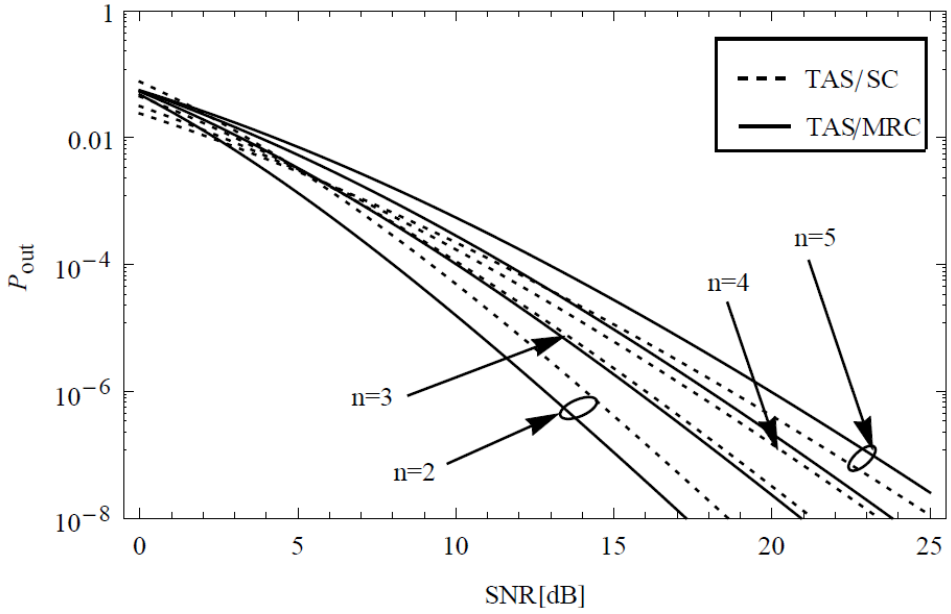

Fig.6-4. Outage probability of TAS/MRC and TAS/SC schemes over *n**Rayleigh fading channels (antenna configuration: $n_T = 3,\ n_R = 2$)

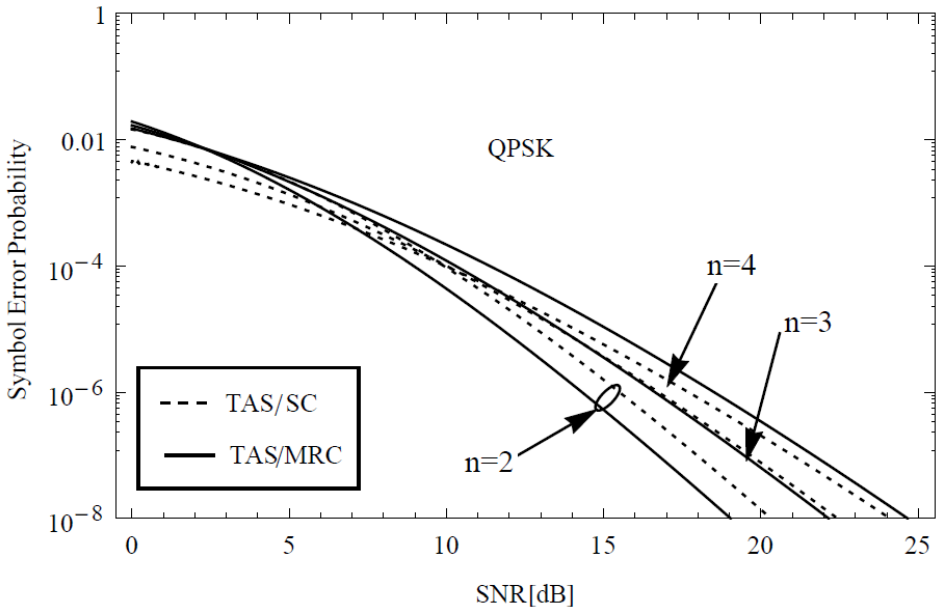

Fig.6-5. SER of TAS/MRC and TAS/SC schemes for QPSK modulation over n*Rayleigh fading channels (antenna configuration: $n_T = 2,\ n_R = 3$)

In Fig.6-4, both schemes are equipped with $n_T = 3,\ n_R = 2$. It's noted from the figure that by increasing the number of transmit antennas, the SNR gap between both schemes decreases for $n = 2$, compared to the case of $n_T = 2,\ n_R = 3$. On the other hand, TAS/SC scheme has shown to provide better performance for $n \geq 3$, which implies that the increase in the number of transmit antennas corresponds to the performance enhancement of TAS/SC scheme over TAS/MRC scheme.

In Fig.6-5, we analyze the upper-bound SER for both TAS/MRC and TAS/SC schemes over QPSK modulation. Specifically, Fig.6-5 shows the average SER of TAS/MRC scheme (6.19) for QPSK modulation against the average SER of TAS/SC scheme (6.22). Generally, the diversity order of both schemes decreases when n increases. Further, the performance of TAS/MRC scheme is better than that of TAS/SC scheme for $n = 2$ and 3, and less for $n = 4$ (due to the performance of TAS/MRC is limited as n increases).

6.5 Conclusion

In this paper, we have examined the performance of reduced-complexity systems-based transmit and receive diversity over *n**Rayleigh fading channels. In particular, the performance of TAS/MRC and TAS/SC schemes have been investigated over *n**Rayleigh distribution. Novel closed-form expressions have been derived for the outage probability, the symbol error probability, and the amount of fading. Our diversity order analysis shows that the maximum diversity order of $(m\, n_T\, n_R\, /n)$ is achieved for both schemes. In addition, our numerical results shows that TAS/MRC offers a better performance than TAS/SC scheme when the number of receive antennas is more than that of transmit antennas, but its performance is limited as n increases. To sum up, our system model can acquire a good cost-performance tradeoff for V2V communications systems when the number of RF chains is limited.

CHAPTER 7 GENERAL DISCUSSION

The work presents in this thesis represents several novel schemes and approaches for intervehicular communications systems over cascaded Rayleigh fading channels. In general, the main contributions of this thesis are threefold. First, we investigated the performance degradation of relay selection and multihop networks in terms of the outage probability, the symbol error rate, the amount of fading, and the average channel capacity. We further investigated the system performance when the power allocation is considered. Second, we considered the problem of energy detection of unknown signals over cascaded Rayleigh fading channels. Novel tight approximation were derived for the probability of detection with/without MRC diversity reception. Furthermore, we studied the probability of detection when CSS approach is considered with/without imperfect reporting channels. Third, we discussed various schemes-based transmit antenna selection approach with both MRC and SC diversity reception. Approximate closed-form expressions were derived for the outage probability, the amount of fading and the symbol error probability.

In particular in Chapter 2 we investigated the performance of IVC systems with DF relay selection approach. We proposed and analyzed new approximate closed-form expressions for the outage probability, the symbol error probability and the average channel capacity over *n**Rayleigh fading channels. From our numerical results, we showed that the outage and error probabilities are increased by increasing the cascading order n and decreased by increasing the number of cooperating nodes between the source and the destination. In other words, the maximum achievable diversity order for *n**Rayleigh fading channels ($d \approx mN/n$) is reduced by increasing the cascading order n and is improved by increasing the number of relays (N). In addition, we showed that the underlying scheme with double Rayleigh fading channels ($n = 2$) has better channel capacity than that of cascading Rayleigh fading channels ($n > 2$) due to the fact that the maximum data rate of communication over n = 2 can be attained with a smaller error probability compared to $n > 2$. This work also proposed a power allocation scheme to optimize the overall transmit power between the source and the best relay when statistical channel state information is available at the source. In particular, we studied the outage performance over highly unbalanced channel links between the source and the selected relay and the destination. We showed that the power allocation mode devotes larger power to the weaker link to reduce the overall outage probability, and the power

allocation ratio converges to 0.5 when $n = 4$, which means that no optimization is required for power when $n \geq 4$. In this case, the EPA mode is used instead of the PA mode to achieve the minimum outage probability.

In Chapter 3, we discussed AF-relay selection in IVC systems. We obtained approximate closed-form expressions for the outage and error probabilities. We showed that the maximum achievable diversity order for the selective AF relaying scheme is equivalent to that of the selective DF relaying in the high SNR regime. Furthermore, we showed that the cooperative diversity systems can play a major role in enhancing the dynamic range of the measurement devices. For example, when the outage probability is assumed at $P_{out} = 10^{-3}$, the required minimum SNR levels for receiving undistorted signal are 12.30, 16.67, 20.36, and 23.77 dB for $n = 1,2,3,4$, respectively. A radio receiver with limited dynamic range will lead to amplitude distortion.

In Chapter 4, we investigated the performance of multihop-IVC systems under *n**Rayleigh distribution, using regenerative and non-regenerative relays with MRC diversity reception to transfer the source message to the destination. In this work, we derived new closed-form expressions for the outage probability and amount of fading. Our numerical results showed that regenerative systems have better outage performance than that of non-regenerative systems as the cascading order *n* decreases and the difference between two system performance starts decreasing gradually as *n* increases. This leads us to the conclusion that nonregenerative systems with diversity reception can enhance the performance without increasing complexity of system design. In addition, from our analysis we showed that the overall amount of fading becomes larger when the diversity reception is employed, which assist in the design of receivers with *n**Rayleigh fading. We further analyzed the power allocation when perfect statistical channel state information is available at the source and regenerative relays. The results showed that optimizing the power for diversity reception systems can provide a significant performance gain in comparison with the EPA mode.

In Chapter 5, we discussed the problem of energy detection of unknown signals for IVC systems over n*Rayleigh fading channels. Particularly, we discussed the hidden terminal problem which occurs when the cognitive radio user is hidden in severe multipath fading while the primary user is operating in the vicinity. In this regard, we invoked the approach of cooperative spectrum sensing with and without MRC diversity reception to enhance local spectrum sensing, as well as we examined the considered scheme under various channel constraints in case of perfect and imperfect

reporting channels. By doing so, we derived accurate approximate closed-from expressions for the probability of detection with and without MRC diversity reception. The numerical results showed that: 1) the detection performance-based the approximate PDF is closely fits the analytical results-based the exact PDF. The larger the value of n is, the higher accuracy will be. 2) Increasing the cascading order n would result in missing the presence of the primary user. 3) CSS is more attractive solution as the cascading order n increases. 4) MRC diversity scheme with imperfect reporting channels has a positive impact on the probability of missed detection compared to the no-diversity systems. 5) MRC scheme can bring additional gain to CSS when the probability of false alarm is considered, in which CSS keeps the false alarm probability minimal rather than increasing the number of cooperative partners, which results in increasing the probability of false alarm.

Finally, Chapter 6 introduced various schemes based on reduced-complexity diversity systems such as TAS/MRC and TAS/SC schemes with n*Rayleigh fading. General analytical expressions were derived for the outage probability, the symbol error rate, and the amount of fading. We performed Monte-Carlo simulation to validate the accuracy of our proposed approximate PDF of the output SNR at MRC receiver. From our analysis, the approximate PDF is very close to simulation results. The larger the value of n is, the higher accuracy will be. In addition, the results showed that the maximum achievable diversity order for both TAS/MRC and TAS/SC schemes is equivalent to $(d \approx m\, n_T\, n_R\, /n)$ which deteriorates by increasing the cascading order n and improves by increasing the number of transmit and/or receive antennas. Further, TAS/MRC offers a better performance gain than TAS/SC scheme when the number of receive antennas is more than that of transmit antennas, but its performance is limited as n increases. We also introduced some special cases for the outage probability and diversity order over MIMO-V2V channel model such as SISO, MISO, SIMO-MRC and SIMO-SC schemes. In this work, tight performance bound for the SER was derived and we showed that the tightness is improved in the high SNR regime. The lower the value of n is, the tighter the proposed bound will be. Moreover, our analysis revealed that TAS/MRC scheme outperforms TAS/SC in reducing the amplitude of fading at the receiver, the more the number of receive antennas, the less the amount of fading is achieved.

CHAPTER 8 CONCLUSION AND FUTURE WORK

In this chapter, we first present the main contributions of this thesis. Then we discuss the limitations of our study and the appropriate solutions for combating these limitations. Finally, we discuss some potential extensions to our work.

8.1 Research Contributions

This thesis has explored several novel schemes and approaches for the use of cooperative and antenna diversity in inter-vehicular communications systems. To the best of our knowledge, cooperative IVC systems with relay and antenna selection over *n**Rayleigh fading channels (i.e., $n \geq 2$) have not been studied yet. Hence, it is the aim of this work to fill this research gap and investigate the performance of cooperative IVC systems in *n**Rayleigh fading. Five schemes have been introduced, demonstrated and optimized analytically. The main contributions to these schemes are summarized as follows:

1. Approximate closed-form expressions for the outage probability for selective DF and AF relaying schemes with *n**Rayleigh fading were derived. Also, we introduced a new lower-bound expression for the MGF which is used to compute the symbol error probability of *M*-PSK modulation. We further derived an asymptotic expression for the average channel capacity for S-DF relaying scheme. Our analysis and numerical results showed that the maximum achievable diversity order of ($d \approx mN/n$) is achieved for both the underlying schemes, and is inversely proportional to the cascading order n. Furthermore, our results confirmed that transmit power allocation optimization is required for IVC systems when the cascading order $n < 4$. However, from our practical standpoint, this will be an attractive solution for design engineers when the PA mode is taking place over cascaded Rayleigh fading channels.

2. For the scheme-based multihop transmission with a regenerative and non-regenerative relay, we derived a new approximate closed-form expression for the outage probability over n*Rayleigh fading channels. Our analysis showed that a non-regenerative system can improve the outage performance close to that of a regenerative system when the cascading order n is high. Also, the multihop scheme with diversity combining systems can substantially reduce the overall amount of fading over cascaded Rayleigh fading channels

compared to no-diversity reception. Furthermore, optimizing the power for MRC diversity reception can provide a significant performance gain in comparison with the EPA mode.

3. In order to solve the hidden terminal problem due to *n**Rayleigh fading channels, we employed CSS scheme with MRC diversity reception to overcome such kind of problems. In this scenario, we analyzed the energy detection over *n**Rayleigh fading channels (i.e,$n > 2$) when CSS is employed with/without MRC diversity combining, which to the best of our knowledge, has not been studied before. We also investigated the system performance when CSS is considered with/without imperfect reporting channels. In this context, we derived novel tight approximations for the probability of detection for the no-diversity and MRC diversity schemes. We showed that the detection probability of primary user signal deteriorates as the cascading order *n* increases. By using MRC systems for energy detection, the sensing diversity order is improved effectively but this improvement is limited under imperfect reporting channels.
4. The new schemes being developed for MIMO-VTV channel modeling acquired a good cost-performance tradeoff for V2V communications when the number of RF chains is limited. In this study, we considered both transmit antenna selection with MRC and transmit antenna selection with SC over *n**Rayleigh fading channels. We derived tight analytical expressions for the outage probability and amount of fading of the post-processing SNR. Moreover, we derived closed-form expressions for the SER of *M*-PSK modulation. Our numerical results showed that both TAS/MRC and TAS/SC schemes achieve the same diversity order of $(d \approx m\, n_T\, n_R\, /n)$. By increasing the number of receive antennas, TAS/MRC can achieve a better outage performance than TAS/SC scheme but the performance improvement is limited by increasing the cascading order *n*.

8.2 Research Limitations

In this section, we present our research limitations as follows:

1. The significant limitation of the S-DF relaying scheme lies in deriving a closed-form expression for the MGF of effective SNR received by the destination. Since the fading parameter *m* is a real-valued parameter, it is challenging to derive a closed-form expression for the MGF with a finite sum representation. Therefore, using the bounds for the lower

incomplete gamma function given by the CDF of instantaneous SNR, we simplified our derivation for the MGF and obtained a compact expression for the SER accordingly.

2. Derivation of less cumbersome expression for the average channel capacity is also another limitation for the S-DF relaying scheme since the fading parameter *m* takes real values. Hence, for simplicity we derived the average channel capacity for the underlying scheme in the high SNR regime.

3. For the selective AF relaying scheme under *n**Rayleigh distribution, derivation of the outage probability based on the effective end-to-end instantaneous SNR does not lend itself well to a closed-form solution. Therefore, we upper-bounded the effective received SNR to find a simple closed-form expression for the outage probability. In addition, finding a closed-form expression for the SER based on the total harmonic SNR is highly complex due to the Meijer G-function given by the CDF. For this reason, we invoked the outage probability lower-bound to evaluate the SER over *n**Rayleigh random variables.

4. Evaluating the power allocation mode for multihop-IVC systems with non-regenerative relays is also considered a challenge since the outage probability lower bound is expressed by Meijer G-function. Thus, in this study we just analyzed the outage behavior for regenerative systems over *n**Rayleigh fading channels.

5. With respect to analysis of the energy detection over *n**Rayleigh fading channels, we used an asymptotic solution for the generalized Marqum-Q function which was given in a finite series representation. Unfortunately, this solution depends on the truncation of infinite series after *k* terms and the accuracy of detection probability improves when *k* increases.

6. Evaluating the SER for TAS/MRC scheme may not be a practical solution due to the truncation of infinite series given in the MGF of post-processing SNR. Thus, to have further insight into the performance of TAS/MRC scheme, we upper-bounded the CDF of post-processing SNR, which in its turn leads to simplify the analysis of SER.

8.3 Direction for Future Work

There are several directions for future research which are summarized as follows:

1. Cooperative IVC systems with multiple sources

In Chapter 2 and 3, we focused on cooperative communications scenario where each user acts as the source at any instant time while the other users serve as relays. In multiuser systems [2], multiple sources share the same set of relays to transfer their messages to multiple destinations. In this case, all sources may access the cooperative channel simultaneously, and therefore it is important to devise new algorithm to properly allocate radio resources at the relays. By using Round-Robin scheduler as one of the simplest Time Division Multiple Access (TDMA) strategies, the sources take turns in accessing the relays to achieve high diversity gain over *n**Rayleigh fading channels. Another TDMA scheduling scheme can be employed in this scenario, which is called 'opportunistic scheduler' where the scheme dynamically select the best source that has the highest SNR at its destination to transmit in each time slot. In this study, one can investigate the outage probability and diversity order achieved by both schemes.

2. MIMO-V2V schemes with multihop transmission

The work in Chapter 4 investigated the performance of multihop-IVC systems with MRC diversity reception over *n**Rayleigh fading channels. Future work can increase the complexity of transmitters and receivers to examine the effect of MIMO systems on the performance of multihop-IVC in terms of the outage and error probabilities, and the ergodic capacity. In this context, it is expected to obtain high diversity order compared to MRC diversity schemes. In addition, it is recommended to analyze the waterfilling power allocation among transmit antennas under the assumption of full CSI to improve the long-term system throughput. In this scenario, one can also distribute the power between the source and relays to minimize the end-to-end outage probability.

3. Analytic solution to a Marqum-Q function over *nRayleigh fading channels**

In Chapter 5, we used an asymptotic solution for the generalized Marqum-Q function to evaluate the average probability of detection over *n**Rayleigh fading channels. However, this solution depends on the truncation of infinite series after *k* terms to reach the required level of accuracy. Thus, the future work in this area should be dedicated to derive another tractable analytic solution for the integral which involves the generalized Marqum-Q function in combination with an exponential function given in [113], which allows to find another accurate closed-form expression for the energy detection over *n**Rayleigh fading channels.

4. Effect of outdated CSI on Dual-Hop AF-MIMO systems with antenna selection

In this thesis, we investigated the performance of both TAS/MRC and TAS/SC schemes (point-to-point link scenario) over *n**Rayleigh fading channels. Since various wireless communications applications use the cooperative diversity concept to extend system coverage and/or improve spectral efficiency, our results can be extended to dual-hop AF-MIMO systems with antenna selection scenario, taking into consideration the imperfect CSI occurred between the source and destination. However, in practice, the CSI used for antenna pair selection at the source and relay can be imperfect due to the effect of feedback delay and channel estimation error, which in its turn leads to severe performance degradation. In this regard, it is recommended to investigate the impact of outdated CSI on the performance of both TAS/MRC and TAS/SC scheme.

5. MIMO-V2V Testbed: Implementation and Measurements

Another open research area is to validate our analysis by real measurements, and to provide a dedicated environment for experimental research in the field of intelligent transportation systems that can offer a significant enhancement in safety and operational efficiency. Therefore, it is interesting to develop a real-time testbed measurements that enable the rapid prototyping of MIMO-V2V schemes based on the field programmable gate arrays (FPGAs) development boards to process larger data with a few clock cycle. Cascaded Rayleigh scattering measurements should be performed in cities and highway scenarios under varying distances and velocities. In addition, different antenna deployment mechanisms can be implemented at a carrier frequency of 5.9 GHz and the radio link quality can be analyzed in terms of the BER and outage probability.

REFERENCES

[1] U. Lee, R. Cheung, M. Gerla, "*Emerging Vehicular Applications Vehicular Networks: From Theory to Practice"*, CRC Press, Taylor & Francis Group, 2009.

[2] Y.-W. P. Hong, W.-J. Huang, and C.-C. J. Kuo, *Cooperative Communications and Networking: Technologies and System Design*. New York, USA: Springer, 2010.

[3] K. J. R. Liu, A. K. Sadek, W. Su, and A. Kwasinski, *Cooperative Communications and Networking*. Cambridge University Press, 2009.

[4] A. Lozano, F. R. Farrokhi, and R. A. Valenzuela, "Lifting the Limits on High-Speed Wireless Data Access Using Antenna Arrays," *IEEE Commun. Mag*., vol. 39, pp. 156–62., Sept. 2001.

[5] R. D. Murch and K. B. Letaief, "*Antenna Systems for Broadband Wireless Access*," IEEE Commun. Mag., vol.40, pp. 76–83A, Apr. 2002.

[6] C.-X. Wang, X. Cheng, and D. I. Laurenson, "Vehicle-to-Vehicle Channel Modeling and Measurements: Recent Advances and Future Challenges," *IEEE Commun. Mag*., vol. 47, no. 11, pp. 96–103. Nov. 2009.

[7] I.F. Akyildiz, W.-Y. Lee, M.C. Vuran, and S. Mohanty, "A Survey on Spectrum Management in Cognitive Radio Networks," *IEEE Comm. Magazine*, vol. 46, no. 4, pp. 40-48, Apr. 2008.

[8] J. N. Laneman, D. N. C. Tse, and G. W. Wornell, "Cooperative diversity in wireless networks: Efficient protocols and outage behavior*," IEEE Trans. Inf. Theory,* vol. 51, no. 12, pp. 3062–3080, Dec. 2004.

[9] A. F. Molisch,"*Wireless Communications*", 2nd edition, Chicester, U.K, IEEE Press - Wiley, 2011.

[10] I. Z. Kovacs, "*Radio channel characterisation for private mobile radio systems: Mobile-to-mobile radio link investigations*," Ph.D.dissertation, Aalborg Univ., Aalborg, Denmark, Sep. 2002.

[11] J.Salo, "*Statistical analysis of the wireless propagation channel and its mutual information*", Doctoral thesis, Helsinki University of Technology, Espoo, Finland, Jul.2006.

[12] J. Salo, H. E. Sallabi, and P. Vainikainen, “The distribution of the product of independent Rayleigh random variables,” *IEEE Trans. Antennas Propagat.*, vol. 54, no. 2, pp. 639–643, Feb. 2006.

[13] I. S. Gradshteyn and I. M. Ryzhik, *Table of Integrals, Series and Products*, 7th ed. New York: Elsevier, 2007.

[14] M. K. Simon and M.-S. Alouini, *Digital Communication Over Fading Channels*, 2nd ed. New York: Wiley, 2004.

[15] H. Lu, Y. Chen, and N. Cao, “Accurate approximation to the PDF of the product of independent Rayleigh random variables,” *IEEE Antennas Wireless Propag. Lett.*, vol. 10, pp. 1019–1022, Oct. 2011.

[16] M. Seyfi, S. Muhaidat, J. Liang, and M. Uysal, "Relay Selection in Dual- Hop Vehicular Networks," *IEEE Signal Processing Letters*, vol.18, no.2, pp.134,137, Feb. 2011.

[17] S. Thoen, L. Van der Perre, B. Gyselinckx, and M. Engels, “Performance analysis of combined transmit-SC/receive-MRC,” *IEEE Trans. Commun.*, vol. 49, pp. 5–8, Jan. 2001.

[18] D. Cabric, S. M. Mishra, and R. W. Brodersen, “Implementation issues in spectrum sensing for cognitive radios,” *in Proc. 38th Asilomar Conf. Signals, Syst., Computers*, Nov. 2004, vol. 1, pp. 772-776.

[19] A. Ghasemi and E. S. Sousa, “Collaborative spectrum sensing for opportunistic access in fading environments,” in *Proc. IEEE Dyspan*, Nov. 2005, pp. 131-136.

[20] I. Lee, H. Lee, H. Choi, “Exact outage probability of relay selection in decode-and-forward based cooperative multicast systems,” *IEEE Commun. Lett.*, vol. 17, no. 3, pp. 483–486, Mar. 2013.

[21] A. Ikhlef., D. S Michalopoulos, R. Schober, "Max-Max Relay Selection for Relays with Buffers," *Wireless Communications, IEEE Trans on Wireless Comm*, vol.11, no.3, pp.1124,1135, Mar. 2012

[22] S. Ikki and S. Aissa, “Multihop wireless relaying systems in the presence of co-channel interferences: performance analysis and design optimization,” *IEEE Trans. Veh. Technol.*, vol 61, no. 2, Feb. 2012.

[23] K. S. Hwang, Y. C. Ko, and M. S. Alouimi, "Performance Analysis of Two-Way Amply and Forward Relaying with Adaptive Modulation over Multiple Relay Network," *IEEE Transactions on Communications*, vol. 59, no. 2, pp. 402-406. Feb. 2011.

[24] J. B. Andersen and I. Z. Kovács, "Power distributions revisited," presented at the *COST273 3rd Management Committee Meeting*, Guildford, U.K., Jan. 17–18, 2002

[25] J. B. Andersen, "Statistical distributions in mobile communications using multiple scattering," presented at the *27th URSI General Assembly*, Maastricht, Netherlands, Aug. 2002.

[26] I. Z. Kovács, P. Eggers, K. Olesen, and L. Petersen, "Investigations of outdoor-to-indoor mobile-to-mobile radio communication channels," in *Proc. IEEE 56th Vehicular Technology Conf.*, vol. 1, 2002, pp. 430–434.

[27] A. Zajic and G. Stuber, "A new simulation model for mobile-to-mobile Rayleigh fading channels," in *Proc. IEEE Wireless Commun. Netw. Conf.*, vol. 3, pp. 1266-1270, Las Vegas, NV, Apr. 2006.

[28] D. W. Matolak and J. Frolik, "Worse-than-Rayleigh fading: Experimental results and theoretical models," *IEEE Commun. Mag.*, vol. 49, no. 4, pp. 140-146, Apr. 2011.

[29] I. Sen and D. Matolak, "Vehicle-vehicle channel models for the 5-GHz band," *IEEE Trans. Intell. Transp. Syst.*, vol. 9, no. 2, Jun. 2008.

[30] Y. Chen, G. K. Karagiannidis, H. Lu, and N. Cao, "New analytical framework for the products of independent RVs with wireless applications," *in Proc. IEEE Wireless Communications and Networking Conference (IEEE WCNC)*, pp. 103-108, Paris, France 2012.

[31] G. Karagiannidis, N. Sagias, and P. Mathiopoulos, "N*Nakagami: *A novel stochastic model for cascaded fading channels*," *IEEE Trans. Commun.*, vol. 55, pp. 1453–1458, 2007.

[32] N. Sagias and G. Tombras, "*On the cascaded weibull fading channel model*," J. Franklin Inst., vol. 344, pp. 1–11, 2007.

[33] I. Trigui, A. Laourine, S. Affes, and A. Stephenne, "On the performance of cascaded Generalized K fading channels," in *IEEE GLOBECOM*, 2009, pp. 1–5.

[34] H. Ilhan; M. Uysal; I. Altunbas, "Cooperative Diversity for Intervehicular Communication: Performance Analysis and Optimization," *Vehicular Technology, IEEE Transactions on* , vol.58, no.7, pp.3301,3310, Sept. 2009.

[35] A. S. Akki and F. Haber, "A statistical model for mobile-to-mobile land communication channel," *IEEE Trans. on Veh. Tech*., vol. 35, pp. 2–10, Feb. 1986.

[36] H. Ilhan, "Performance analysis of two-way AF relaying systems over cascaded Nakagami-m fading channels," *IEEE Signal Process. Lett.*, vol. 19, no. 6, pp. 332–335, June 2012.

[37] M. F. Feteiha and M. Uysal ,"Cooperative Transmission for Broadband Vehicular Networks over Doubly-Selective Fading Channels," *J. IET Commun*., no 16, pp 1-9, Nov. 2012.

[38] H. Ilhan, I. Altunbas, and M. Uysal, "Novel distributed space-time trellis codes for relay systems over cascaded Rayleigh fading," *IEEE Commun. Lett*., vol. 14, pp. 1140–1142, Nov. 2010.

[39] C. S. Zhang, J. H. Ge, J. Li and Y. Hu, "Performance analysis for mobilerelay-based M2M two-way AF relaying in N*Nakagami-m fading,"*Electronics Lett.*, vol. 49, no. 5, Feb. 2013.

[40] F. Gong, J. Ge, and N. Zhang, "SER analysis of the mobile-relay-based M2M communication over double Nakagami-m fading channels," *IEEE Commun. Lett*., vol. 15, no. 1, pp. 34–36, Jan. 2011.

[41] B. Talha and M. Patzold, ''BEP analysis of M-ary PSK modulation schemes over double Rice fading channels with EGC,'' *in Proc. 2nd Workshop Scenarios for Network Evaluation Studies (SCENES 2010),* San Francisco, CA, pp. 624–629, Nov. 2010.

[42] H. Ilhan., I. Altunbas, & M. Uysal. "Moment generating function-based performance evaluation of amplify-and forward relaying in N*Nakagami fading channels". *IET Communications*, 5, 253–263, Feb. 2011.

[43] S. Bharadwaj, N. B. Mehta, "Accurate Performance Analysis of Single and Opportunistic AF Relay Cooperation with Imperfect Cascaded Channel Estimates," *IEEE Transactions on Communications*, vol.61, no.5, pp.1764,1775, May. 2013.

[44] Z. Hadzi-Velkov, N. Zlatanov, and G. K. Karagiannidis, "On the second order statistics of the multihop Rayleigh fading channel*," accepted for publication in IEEE Trans. Commun*., 2008.

[45] G. Rafiq, B. Hogstad, M. Pätzold, "Statistical properties of the capacity of double Nakagami-m channels", *in Proc IEEE 5th Int Symposium on Wireless Pervasive Computing, (ISWPC 2010),* Modena, Italy, pp. 39–44, May. 2010.

[46] N. Hajri, N. Youssef, M. Patzold. "A study on the statistical properties of double Hoyt fading channels*". IEEE ISWCS;* Sept. 2009.

[47] C. S. Patel, G. L. Stuber, and T. G. Pratt, "Simulation of Rayleigh faded mobile-to-mobile communication channels," *IEEE Trans. on Commun*., vol. 53, pp. 1876–1884, Nov. 2005.

[48] Z. Ding and K. K. Leung, "Cross-layer routing using cooperative transmission in vehicular ad-hoc networks," *IEEE J. Sel. Areas Commun.*, vol. 29, no. 3, pp. 571–581, Mar. 2011.

[49] P. L. Yeoh, M. E. adn N. Yang, D. B. da Costa, and T. Q. Duong, "Unified analysis of transmit antenna selection in MIMO multirelay networks," *IEEE Transactions on Vehicular Technology*, vol. 62, no. 2, pp. 933–939, Feb. 2013.

[50] V. Blagojevic and P. Ivanis, "Ergodic capacity for TAS/MRC spectrum sharing cognitive radio," *IEEE Commun. Lett*., vol. 16, no. 3, pp. 321–323, Mar. 2012.

[51] J. Karedal et al., "A Geometry-based Stochastic MIMO Model for Vehicle-to-Vehicle Communications," *IEEE Trans. Wireless Commun*., vol. 8, no. 7, pp. 3646–57, July. 2009.

[52] O. Renaudin, V.-M. Kolmonen, P. Vainikainen, and C. Oestges, "Nonstationary narrowband MIMO inter-vehicle channel characterization in the 5-GHz band," *IEEE Trans. Veh. Technol.*, vol. 59, no. 4, pp. 2007- 2015, May. 2010.

[53] T. Abbas, J. Karedal, and F. Tufvesson, "Measurement-based analysis: The effect of complementary antennas and diversity on vehicleto-vehicle communication", *IEEE Antennas and Wireless Propagation Letters,* vol.12, no.1, pp.309–312, 2013.

[54] A. Paier, J. Karedal, N. Czink, C. Dumard, T. Zemen, F. Tufvesson, A. Molisch, and C. F. Mecklenbra¨uker, "Characterization of vehicle-to vehicle radio channels from measurements at 5.2 GHz", *Wireless Personal Commun*., vol. 50, pp. 19–29, 2009.

[55] A. G. Zajic et al., "Wideband MIMO mobile-to-mobile Channels: Geometry-Based Statistical Modeling with Experimental Verification*", IEEE Trans. Vehic. Tech*., vol.58, no. 2, pp. 517–34, Feb. 2009.

[56] M. Patzold, B. O Hogstad, and N. Youssef, "Modeling, analysis, and simulation of MIMO mobile-to-mobile fading channels", *IEEE Trans. Wireless Commun.*, vol. 7, no. 2, pp. 510-520, Feb. 2008.

[57] Q. Wu, D. W. Matolak, and I. Sen, "5-GHz-band vehicle-to-vehicle channels: models for multiple values of channel bandwidth" *IEEE Trans. Veh. Technol*., vol. 59, no. 5, pp. 2620–2625, June. 2010.

[58] H. Shin and J. H. Lee, "Performance analysis of space—time block codes over keyhole Nakagami- fading channels*," IEEE Trans. Veh. Technol*., vol. 53, no. 2, pp. 351–362, Mar. 2004.

[59] G. Levin and S. Loyka, "On the outage capacity distribution of correlated keyhole MIMO channels*," IEEE Trans. Inform. Theory*, vol. 54, no. 7, pp. 3232-3245, July. 2008.

[60] N. Zlatanov, Z. Hadzi-Velkov, and G. Karagiannidis, "Level crossing rate and average fade duration of the double nakagami-m random process and application in mimo keyhole fading channels," *IEEE Communications Letters*, vol. 12, no. 11, pp. 822–824, Nov. 2008.

[61] J. Xue, C. Zhong and T. Ratnarajah, "Performance Analysis of Orthogonal STBC in Generalized-K Fading MIMO Channels," *IEEE Trans on Vehicular Technology*, vol. 61, no. 3, pp. 1473-1479, Mar. 2012.

[62] M. Matthaiou, D. Chatzidiamantis, K. Karagiannidis, and A. Nossek, "On the capacity of generalized-*K* fading MIMO channels," *IEEE Trans. Signal Process*., vol. 58, no. 11, pp. 5939–5944, Nov. 2010.

[63] K. Peppas and A. Maras, "Performance evaluation of space-time block codes over keyhole Weibull fading channels," *Wireless Personal Commun.*, vol. 46, pp. 385–395, Jan. 2008.

[64] P. Loskot and N. C. Beaulieu. "Performance Analysis of Coded MIMO-OFDM Systems Over Generalized Ricean Fading Channels*". In Proc. Canadian Conference on Electrical and Computer Engineering CCECE '06*, pages 1634–1639, 2006.

[65] A.Z. Ghanavati, U. Pareek, S. Muhaidat, D. Lee. “On the Performance of Imperfect Channel Estimation for Vehiclar Ad-Hoc Networks”. *In Proceedings 72nd IEEE Vehicular Technology Conference Fall (VTC 2010-Fall)*, 6-9 September 2010, Ottawa, Canada.

[66] J. Salo, H. M. El-Sallabi, and P. Vainikainen, “Impact of double- Rayleigh fading on system performance,” in *Proc. International Symposium on Wireless Pervasive Computing 2006, ISWPC’06*, Jan. 2006.

[67] W. Wongtrairat, P. Supnithi, and S. Tantaratana, “Performance of M-PSK modulation in double Rician fading channels with MRC diversity,” *Proc. 5th International Conference on Electrical Engineering/Electronics, Computer, Telecommunications and Information Technology 2008*, Krabi, Thailand, vol. 1, pp. 321–324, May. 2008.

[68] P. M. Shankar. "Diversity in cascaded N*Nakagami channels." Annals of telecommunications-annales des télécommunications 68.7-8 (2013): 477-483.

[69] M. Uysal, “Diversity analysis of space-time coding in cascaded Rayleigh fading channels," *IEEE Commun. Lett*, vol. 10, no. 3, pp. 165-167, Mar. 2006.

[70] M. Uysal, “Maximum achievable diversity order for cascaded Rayleigh fading channels," *Electronics Lett*., vol. 41, no. 23, pp. 1289-1290, Nov. 2005.

[71] C. Zhu, J. Mietzner, and R. Schober, “On the performance of noncoherent transmission schemes with equal-gain combining in generalized K-fading,” *IEEE Trans. Wireless Commun.*, vol. 9, no. 4, pp. 1337–1349, Apr. 2010.

[72] S. Atapattu, C. Tellambura, and H. Jiang, “Energy detection based cooperative spectrum sensing in cognitive radio networks,” *IEEE Trans. Wireless Commun.*, vol. 10, no. 4, pp. 1232–1241, Apr. 2011.

[73] A. Singh, M. R. Bhatnagar, and R. K. Mallik, “Cooperative spectrum sensing in multiple antenna based cognitive radio network using an improved energy detector,” *IEEE Commun. Lett*., vol. 16, no. 1, pp. 64–67, Jan. 2012.

[74] X. Jiang, and et al, “On hybrid overlay-underlay dynamic spectrum access: Double-threshold energy detection and Markov model,” *IEEE Trans. Veh. Technol.*, vol. 62, no. 8, pp. 4078–4083, 2013.

[75] Q. Li; H. Hu, "Analysis of energy detection over double-Rayleigh fading channel," *Communication Technology (ICCT), 2012 IEEE 14th International Conference on* , vol., no., pp.61-66, Nov. 2012

[76] A. Bletsas, A. Khisti, D. P. Reed, and A. Lippman, “A simple cooperative diversity method based on network path selection,” *IEEE J. Select. Areas Commun.*, vol. 24, no. 3, pp. 659–672, Mar. 2006.

[77] H. Ilhan, I. Altunbas, and M. Uysal, “Cooperative diversity for relay assisted inter-vehicular communication,” in *Proc. IEEE VTC—Spring*, Singapore, pp. 605–609, May 2008.

[78] S. Ikki and M. H. Ahmed, “Performance analysis of adaptive decodeand-forward cooperative diversity networks with best-relay selection,” *IEEE Trans. Commun.*, vol. 58, no. 1, pp. 68–72, Jan. 2010.

[79] N. C. Beaulieu and J. Hu, “A closed-form expression for the outage probability of decode-and-forward relaying in dissimilar Rayleigh fading channels," *IEEE Commun. Lett.*, vol. 10, no. 12, pp. 813-815, Dec. 2006.

[80] M. Abramowitz and I. A. Stegun, *Handbook of Mathematical Functions with Formulas, Graphs, and Mathematical Tables*, 9th ed. New York: Dover, 1970.

[81] R. U. Nabar, H. Bolcskei, and F. W. Kneubuhler, “Fading relay channels: Performance limits and space-time signal design,” *IEEE J. Sel. Areas Commun.*, vol. 22, no. 6, pp. 1099–1109, Aug. 2004.

[82] R. U. Nabar, H. Bolcskei, and F. W. Kneubuhler, “Fading relay channels: Performance limits and space-time signal design,” *IEEE J. Sel. Areas Commun.*, vol. 22, no. 6, pp. 1099–1109, Aug. 2004.

[83] E. Neuman, Inequalities and Bounds for the Incomplete Gamma Function, *Results. Math.* 63 (2013), 1209–1214.

[84] The Wolfram Functions Site. [Online] http://functions.wolfram.com/

[85] F.W.J. Olver, D.W. Lozier, R.F. Boisvert, C.W. Clark (Eds.), NIST Handbook of Mathematical Functions, Cambridge Univeristy Press, 2010.

[86] T. K. Moon and W. C. Stirling, *Mathematical Methods and Algorithms for Signal Processing*. Upper Saddle River, New Jersey: Prentice Hall Publishers, 2000.

[87] P. A. Anghel and M. Kaveh, “Exact symbol error probability of a cooperative network in a Rayleigh-fading environment,” *IEEE Trans. Wireless Commun.*, vol. 3, pp. 1416-1421, Sept. 2004.

[88] M. Hasna and M.-S. Alouini, “Harmonic mean and end-to-end performance of transmission systems with relays,” *IEEE Trans. Commun.*,vol. 52, no. 1, pp. 130–135, Jan. 2004.

[89] A. Papoulis, Probability, Random Variables, and Stochastic Processes, 3rd ed. New York: McGraw-Hill, 1991.

[90] M. O. Hasna and M. S. Alouini, “Outage probability of multihop transmission over Nakagami fading channels,” *IEEE Commun. Lett*., vol. 7, no. 5, pp. 216–218, May 2003.

[91] G. K. Karagiannidis, T. A. Tsiftsis, and R. K. Mallik, “Bounds of multihop relayed communications in Nakagami-m fading,” *IEEE Trans. Commun.*,vol. 54, no. 1, pp. 18–22, Jan. 2006.

[92] E. K. Al-Hussaini and A. A. M. Al-Bassiouni, “Performance of MRC diversity systems for the detection of signals with Nakagami fading,” *IEEE Trans. Commun*., vol. COM-33, pp. 1315–1319, Dec. 1985.

[93] M. Di Felice, R. Doost-Mohammady, K. Chowdhury, and L. Bononi, “Smart radios for smart vehicles: Cognitive vehicular networks,” *IEEE Veh. Technol. Mag*., vol. 7, no. 2, pp. 26–33, Jun. 2012.

[94] Y. Sun, K. Chowdhury, "Enabling emergency communication through a cognitive radio vehicular network," *Communications Mag, IEEE*, vol.52, no.10, pp.68-75, Oct. 2014.

[95] K. B. Letaief and W. Zhang, “Cooperative communications for cognitive radio networks,” *Proc. IEEE*, vol. 97, no. 5, pp. 1–16, May 2009.

[96] F. F. Digham, M. S. Alouini, and M. K. Simon, “On the energy detection of unknown signals over fading channels,” *IEEE Trans. Commun.*, vol. 55, no. 1, pp. 21–24, Jan. 2007.

[97] A. H. Nuttall, “Some integrals involving the QM-function,” Naval Underwater Systems Center (NUSC) technical report, May 1974.

[98] V. M. Kapinas, S. K. Mihos, and G. K. Karagiannidis, "On the monotonicity of the generalized Marcum and Nuttall Q-functions," *IEEE Trans. Inf. Theory*, vol. 55, no. 8, pp. 3701–3710, Aug. 2009.

[99] P. C. Sofotasios, S. Freear, "Novel expressions for the Marcum and one dimensional Q−functions," *Proceedings of* 7th *ISWCS,* York, UK, Sep. 2010, pp. 736-740.

[100] A. Ghasemi and E. S. Sousa, "Opportunistic spectrum access in fading channels through collaborative sensing," *J. Commun.*, vol. 2, no. 2, pp. 71–82, Mar. 2007.no. 2, pp. 71–82, Mar. 2007.

[101] P. K. Varshney, *Distributed Detection and Data Fusion*. NewYork: Springer-Verlag, 1997.

[102] W. Zhang and K. B. Letaief, "Cooperative spectrum sensing with transmit and relay diversity in cognitive networks," *IEEE Trans. Wireless Commun*., vol. 7, no. 12, pp. 4761–4766, Dec. 2008.

[103] A. F. Molisch, M. Z. Win, and J. H. Winters, "Reduced-complexity transmit/receive diversity systems," *IEEE Trans. Signal Process*, vol. 51, no. 11, pp. 2729–2738, Nov. 2003.

[104] Z. Chen, J. Yuan, and B. Vucetic, "Analysis of transmit antenna selection/maximal-ratio combining in Rayleigh fading channels," *IEEE Trans. Veh. Technol*., vol. 54, no. 4, pp. 1312–1321, Jul. 2005.

[105] A. F. Molisch and M. Z. Win, "MIMO systems with antenna selection," *IEEE Micro. Mag*., vol. 5, no. 1, pp. 46–56, Mar. 2004.

[106] V. Erceg, S. Fortune, J. Ling, A. Rustako, and R. Valenzuela, "Comparisons of computer-based propagation prediction tool with experimental data collected in urban microcellular environments," *IEEE J. Sel. Areas Commun.*, vol. 15, pp. 677–684, 1997.

[107] Y. Gong and K. Letaief, "On the error probability of orthogonal space time block codes over keyhole MIMO channel," *IEEE Trans. Wireless Commun.*, vol. 6, pp. 3402–3409, Sep. 2007.

[108] C. Zhong, S. Jin, K. K. Wong, and M. R. McKay, "Ergodic mutual information analysis for multi-keyhole MIMO channels," *IEEE Trans. Wireless Commun*. vol. 10, no. 6, pp. 1754–1763, June 2011.

[109] G. Levin and S. Loyka, “From multi-keyhole to measure of correlation and power imbalance in MIMO channels: Outage capacity analysis,” *IEEE Trans. Inf. Theory*, vol. 57, no. 6, pp. 3515–3529, Jun. 2011.

[110] P. M. Shankar “Performance of N*Nakagami cascaded fading channels in dual selection combining diversity,” in *IEEE 7th Wireless Communications and Mobile Computing Conf. (IWCMC’11*), Istanbul, Turkey, pp. 1539–1544, Jul. 2011.

[111] H. A. David, *Order Statistics*. New York: Wiley, 1970.

[112] P. C. Sofotasios, M. Valkama, T. A. Tsiftsis, Yu. A. Brychkov, S. Freear, G. K. Karagiannidis, “Analytic solutions to a Marcum Q−function-based integral and application in energy detection of unknown signals over multipath fading channels,” *in Proc. of 9th CROWNCOM* ’14, pp. 260−265, Oulu, Finland, 2-4 June, 2014.

[113] D. Chizhik, G. Foschini, M. Gans, and R. Valenzuela, “Keyholes, correlations and capacities of multielement transmit and receive antennas,” *IEEE Trans. Wireless Commun.*, vol. 1, pp. 361–368, Apr. 2002.

[114] Erdélyi, Arthur, Wilhelm Magnus, Fritz Oberhettinger, Francesco G. Tricomi, and Harry Bateman. *Higher transcendental functions*. Vol. 1. McGraw-Hill: New York, 1953.

[115] M.O. Hasna and M.-S. Alouini, “Performance analysis of two-hop relayed transmission over Rayleigh fading channels,” in *Proc. IEEE Vehicular Technology Conf. (VTC’02)*, Vancouver, BC, Canada, Sept. 2002, pp. 1992–1996.

[116] D. Gesbert, H. Bölcskei, D. A. Gore, and A. J. Paulraj, “Outdoor MIMO wireless channels: Models and performance prediction,” *IEEE Trans. Commun.*, vol. 50, no. 12, pp. 1926–1934, Dec. 2002.

[117] H, Yun, et al. "Partial relay selection for a roadside-based two-way amplify-and-forward relaying system in mixed Nakagami-m and ‘double’ Nakagami-m fading." *IET Communications*, vol.8, no.5 pp571-577, Mar 2014.

[118] C. S. Patel, “*Wireless channel modeling, simulation and estimation*," Ph.D. thesis, Georgia Institute of Technology, May 2006.

[119] R. Bansal,: *Engineering Electromagnetics*, Taylor & Francis, Boca Raton, FL, 2006, pp. 185–346.

[120] E. Hossain and V. K. Bhargava, *Cognitive Wireless Communication Networks*, (edited volume). Springer, 2007.

APPENDIX A – PROOF OF PROPOSITION: PDF AND CDF OF THE HARMONIC MEAN OF TWO GAMMA RVS FUNCTIONS

In this appendix, we prove the proposition for both the PDF and CDF of the harmonic mean of two gamma RVs as given in (3.6) and (3.7) respectively. Following [88], by assuming two i.i.d RVs(Y_1, Y_2), where $Y_1 = X_1^{\frac{1}{n}}$ and $Y_2 = X_2^{\frac{1}{n}}$ are distributed as $Y_i \sim \mathcal{G}(n\alpha, \beta), i = 1,2$. Note that the PDF of RV X is given by $f_X(x) = \frac{\beta^{n\alpha}}{n\Gamma(n\alpha)} x^{\alpha-1} e^{-\beta x^{1/n}}$, therefore, using [89, Sec.5.2], the RV Y follows a gamma distribution with the PDF given by

$$f_Y(y) = \frac{\beta^{n\alpha}}{\Gamma(n\alpha)} y^{n\alpha-1} e^{-\beta y} \qquad (A-1)$$

To find the PDF of the harmonic mean of Y_1 and Y_2, and the desire to get closer to a simple derivation, we need to define the following two new RVs as

$$\begin{aligned} Z &= 2Y_1Y_2 \\ W &= Y_1 + Y_2 \end{aligned} \qquad (A-2)$$

As a result, the joint PDF of Z and W, $f_{Z,W}(z,w)$ can be derived by taking the Jacobian transformation of (A-2), to be written as

$$\begin{aligned} f_{Z,W}(z,w) &= \frac{f_{Y_1}(y) f_{Y_2}(y)}{|\mathrm{J}(Y_1, Y_2)|} \\ &= \frac{(\beta^{n\alpha}/\Gamma(n\alpha))^2}{2\sqrt{w^2 - 2z}} \left(\frac{z}{2}\right)^{n\alpha-1} e^{-\beta w} \end{aligned} \qquad (A-3)$$

By assuming, $Y = Z/W$, where $Y = X^{\frac{1}{n}}$ is the harmonic mean of the two RVs (Y_1, Y_2), the PDF of Y can be derived with the help of [89, Sec. 6.2] as follows

$$f_Y(y) = \left(\frac{\beta^{n\alpha}}{\Gamma(n\alpha)}\right)^2 \left(\frac{y}{2}\right)^{n\alpha-1} \int_{2y}^{\infty} w^{n\alpha-\frac{1}{2}} (w-2y)^{-\frac{1}{2}} e^{-\beta w}\, dw \qquad (A-4)$$

Finally, the above integral can be obtained with the help of [13, eq. (3.383.4)] to be

expressed as

$$f_Y(y) = \left[\left(\frac{\beta^{n\alpha}}{\Gamma(n\alpha)}\right)^2 \left(\frac{y}{2}\right)^{n\alpha-1}\right] \beta^{-\left(\frac{n\alpha+1}{2}\right)} (2y)^{\frac{n\alpha-1}{2}} \Gamma\left(\frac{1}{2}\right) e^{-\beta y} W_{\frac{n\alpha}{2},-\frac{n\alpha}{2}}(2\beta y) \qquad (A-5)$$

where $W_{k,\lambda}(.)$ is the Whittaker function [13, eq.(9.222)]. Now, using the relationship between the Whittaker function and the confluent hypergeometric function given in [80, eq. (13.1.33)], eq. (A-5) can be reduced to

$$f_Y(y) = \frac{\sqrt{\pi}\beta^{n\alpha}}{\Gamma^2(n\alpha)} \left(\frac{y}{2}\right)^{n\alpha-1} e^{-2\beta y} U\left(\frac{1}{2} - n\alpha, 1 - n\alpha, 2\beta y\right) \qquad (A-6)$$

which agrees with eq.(3.6) and coincides the proof. Moreover, we can rewrite the PDF given by (A-5) in terms of the Meijer-G function using the relationship between the Whittaker function with the Meijer-G function as [114, eq. (5.6.6)]

$$f_Y(y) = \frac{\sqrt{\pi}\beta}{2^{2(n\alpha-1)}\Gamma^2(n\alpha)} G_{1,2}^{2,0}\left(2\beta y \middle| \begin{matrix} n\alpha - \frac{1}{2} \\ n\alpha - 1, 2n\alpha - 1 \end{matrix}\right) \qquad (A-7)$$

Using the [13, eq. (7.811.2)], the CDF of Y can be extracted as

$$F_Y(y) = \frac{\sqrt{\pi}\beta\ \ y}{2^{2(n\alpha-1)}\Gamma^2(n\alpha)} G_{2,3}^{2,1}\left(2\beta y \middle| \begin{matrix} 0, n\alpha - \frac{1}{2} \\ n\alpha - 1, 2n\alpha - 1, -1 \end{matrix}\right) \qquad (A-8)$$

which agrees with eq.(3.7) and coincides the proof.

APPENDIX B – USEFUL IDENTITY

In this appendix, we present a useful identity as defined in [84] that helps to find the Laplace transform of equations (2.23), (3.19), and (6.18).

$$\int_0^\infty x^{\alpha-1}\exp(-\sigma x)\, G_{p,q}^{m,n}\left(\omega x^{\frac{l}{k}}\middle|\begin{matrix}a_1, a_2, \dots, a_p\\ b_1, b_2, \dots, b_q\end{matrix}\right) dx$$

$$= \frac{k^{\mu} l^{\alpha-\frac{1}{2}} \sigma^{-\alpha}}{(2\pi)^{\frac{l-1}{2}+(k-1)c}}\; G_{kp+l,kq}^{km,kn+l}\left(\frac{\omega^k l^l}{\sigma^l k^{k(q-p)}}\middle|\begin{matrix}\Delta(l,\alpha), \Delta\big(k,(a_p)\big)\\ \Delta\big(k,(b_q)\big)\end{matrix}\right), \mathrm{k} \in \mathbb{N}^+, l \in \mathbb{N}^+$$

where

$\Delta(l,\alpha) = \frac{1-\alpha}{l}, \dots, \frac{l-\alpha}{l}$

$\Delta\big(k,(a_p)\big) = \frac{a_1}{k}, .., \frac{k+a_n-1}{k}, \frac{a_{n+1}}{k}, .., \frac{k+a_p-1}{k}$

$\Delta\big(k,(b_q)\big) = \frac{b_1}{k}, .., \frac{k+b_m-1}{k}, \frac{b_{m+1}}{k}, .., \frac{k+b_q-1}{k}$

$\mu = \sum_{j=1}^{q} b_j - \sum_{j=1}^{p} a_j + \frac{p-q}{2} + 1,\ c = m + n - \frac{p+q}{2}$